Fluorination of Polylactides as a Path to Enhanced Hemocompatibility

Razieh Khalifehzadeh

A dissertation

submitted in partial fulfillment of the

requirements for the degree of

Doctor of Philosophy

University of Washington

2018

Reading Committee:

Buddy D. Ratner, Chair

Shaoyi Jiang

Elizabeth Nance

Program Authorized to Offer Degree:

Chemical Engineering
&
Nanotechnology and Molecular Engineering

University of Washington

Abstract

Fluorination of Polylactides as a Path to Enhanced Hemocompatibility

Razieh Khalifehzadeh

Chair of the Supervisory Committee:
Professor Buddy D. Ratner
Departments of Chemical Engineering and Bioengineering

Polymers derived from lactic acid have been extensively used for various biomedical applications such as sutures and implants due to their biocompatibility and biodegradability. The ability to modify the physiochemical properties of these polymers is a key to expand their application spectrum. Poly(lactic acid) (PLA) has been the predominant polymer for making bioresorbable vascular scaffolds; the first generation of fully bioresorbable stents made from PLA was recently approved by FDA to treat coronary artery disease. Although these bioresorbable stents are claimed to have long-term advantages such as vasomotion restoration and potential recovery of the endothelial function, they have shown higher rates of early thrombosis when compared with permanent metallic stents. Surface-induced thrombosis by biomaterials still remains a significant clinical concern for many types of blood-contacting

medical devices. In particular, protein adsorption and platelet adhesion are important events due to their ability to trigger the coagulation cascade and initiate thrombosis.

To resolve this clinical challenge, we developed a novel method for fluorinating PLA with trifluoromethyl functional groups using either surface or bulk modification techniques. Fluoropolymer medical devices such as expanded polytetrafluoroethylene vascular grafts have been generally used as blood-contacting materials in clinics, due to their increased thromboresistance and reduced platelet adhesion and activation. Fluorocarbon modification has been shown to decrease platelet adhesion and activation despite the presence of fibrinogen on the biomaterials surfaces.

This is the first report of PLA fluorination, which would allow a PLA-based cardiovascular stent with greater blood compatibility. Relevant parameters associated with hemocompatibility including protein adsorption, platelet adhesion, and morphology were evaluated. We found that fluorinated PLA adsorbs and retains a higher ratio of albumin/fibrinogen and, relative to other materials tested here, exhibits a lower number of adherent platelets and a reduced degree of activation. Such promising characteristics pave the way for fabrication of a new generation of fluorinated PLA stents with improved hemocompatibility, alongside tunable degradability and drug release capabilities.

TABLE OF CONTENTS

ACKNOWLEDGEMENTS

I would like to take this opportunity and gratefully acknowledge the many people who have been instrumental in my journey through graduate school and towards the completion of this thesis. First, I would like to thank my advisor, Prof. Buddy Ratner, for providing me the opportunity to join his research group at the University of Washington and for his support and guidance thought out this project. Secondly, I want to say thank you to my dissertation committee members Prof. Shaoyi Jiang, Prof. Elizabeth Nance and Prof. Christine Luscombe for your feedback, advice and career insight. I also would like to thank Dr. Esmaeel Naeemi for all his dedication to this project and for the countless hours of discussions, training and above all teaching me the beauty of organic chemistry.

My sincere gratitude also goes to the many people who have contributed time, effort and scientific feedback during the completion of this project. These include (although not exclusively) the following people: Winston Ciridon for his extraordinary commitment in training me various experimental techniques and helping me to troubleshoot and prepare samples for this study. Sharon A. Creason, Ratner group lab manager, for helping me pushing forward and going above and beyond her duties for supporting group members. The progress of this project had noticeably increased since the time she joined our research group. Dr. Tom Horbett, Dr. Felix Simonovsky, Dr. Rajan Paranji, Dr. Floyd Karp, Dr. Dan Graham, Gerry Hammer, Nancy Cooper, Marvin Mecwan, Samuel Herschbein, Dr. Alex Chen, Dr. Maria Jeanette Stein, Dr. Jean-Rene Ella, Dr. Ruying Chen and the rest of the Ratner group members that provide the valuable comments, technical assistance and helpful discussions along the way.

I also would like to thank Prof. François Baneyx, Prof. Daniel T. Schwartz, Prof. John Berg and Prof. James Davis in chemical engineering department for providing invaluable insight and guidance and helping to navigate my roller coaster journey in grad school.

Finally, I would like to express my sincere appreciation to my family for their deep love and tireless support though all of my tribulations and triumphs. Their encouragement, sacrifice, devotion and patience helped me to make it through my dissertation odyssey. Thank you for everything.

DEDICATION

To my parents, for all their love and support.

Chapter 1

Introduction

A coronary stent is a small mesh tube placed in the closed artery to keep the vessel open after treatment for coronary artery disease (atherosclerosis) Figure 1. This condition is a result of a build-up plaque on the walls of the arteries which over time narrows the artery lumen and reduces blood supply to the heart. According to the American Heart Association, currently 560-700,000 stents are implanted per year which is about more than 70% of interventional procedures (Figure 2) [1]. The stent manufacturing market is estimated to be $2.4 billion in 2019.

In patients who received metallic coronary stents, adverse events such as late stent failure might occur with the passage of time [2]. This failure may be related in part to the presence of a rigid metal scaffold in the vessel wall that accelerates hyperplasia around the stent and prevents physiologic vasomotion around the stent [3]. Bioresorbable vascular scaffolds (BVS), in which their composition allows gradual breakdown over time, are an emerging and novel treatment for improving long-term coronary stent outcomes [4].

Poly(lactic acid) (PLA) has been the most commonly used material for BVS. This polymer is fully resorbable and it degrades through a bulk erosion process by hydrolysis of ester bonds, with resulting lactic acid monomers and oligomers being metabolized into CO_2 and water [5]. So far, the everolimus-eluting Absorb bioresorbable vascular scaffold system (Abbott Vascular) and the novolimus-eluting DESolve bioresorbable coronary scaffold system (Elixir Medical) are two

such devices that have received prerequisite qualifications for clinical use in Europe (2011 and 2013, respectively). A recent article in The New England Journal of Medicine [6] reported the results of a clinical trial for the Absorb GT1 scaffold that led to device approval in the United States. (ClinicalTrials.gov number, NCT01751906). Figure 3 [7] shows the rate of stent thrombosis in randomized trials in patients treated with the bioresorbable vascular scaffold (blue bars) versus metallic stents, including Xience (red bars). The probable stent thrombosis for bioresorbable scaffolds was about twice as likely for Xience stent.

Although the trial was conducted to a high standard, the issue of increased thrombosis associated with BVS should be taken into consideration. Surface-induced thrombosis by biomaterials still remains a significant clinical concern for many types of blood-contacting medical devices [8]. In particular, protein adsorption and platelet adhesion are important events due to their ability to trigger the coagulation cascade and initiate thrombosis [9].

To address PLA stent thrombogenicity, we modified the surface of PLA resorbable stent polymer with a perfluoro compound. Fluoropolymers have been extensively used in blood contacting applications due to a long clinical history, demonstrations of reduced thrombogenicity and mild response upon implantation (Figure 4) [10-16]. Fluorocarbon modification has been shown to decrease platelet adhesion despite the presence of fibrinogen (Fg) on the biomaterials surfaces [17]. In addition, hydrophobic stent fluoropolymers that have shown good clinical performance exhibit high albumin adsorption and albumin tight binding [18]. A well-known example, expanded polytetrafluoroethylene vascular graft, has been considered as clinical standard for blood vessel replacements down to 5 mm diameter.

The aim of chapter two is to develop a robust strategy to modify the surfaces of PLA with perfuloro compound and evaluate the blood compatibility parameters. Surface analysis was

performed to ensure high-quality surfaces. Also, relevant blood compatibility parameters including protein adsorption, platelet adhesion and platelet morphology, were evaluated.

The aim of chapter three is to provides a process for synthesis and characterizations of trifluoromethyl-functionalized poly(lactic acid). Our strategy involves substitution of hydrogen or methyl group of the glycolide/lactide repeat unit with trifluoromethyl functional group. Applying established polymerization methods such as ring-opening polymerization (ROP) generated CF_3-functionalized poly(lactic acid). The structure of polymer backbone remains unchanged and due to its analogy to poly(lactide), we believe that such substituted polymers, retain their hydrolysis characteristics, which is a key factor determining their degradability in biological environments.

Polymers derived from lactic/glycolic acid have been extensively used for various biomedical applications such as sutures and implants due to their biocompatibility and biodegradability [19-24]. The ability of modifying the physiochemical properties (e.g., degradability, hydrophobicity/philicity) of these polymers is a key to expand their application spectrum. Conventional approaches usually involve copolymerization and block copolymer preparations [25-27]. Alternatively, modifications may be introduced using well-designed lactic/glycolic acid derivatives as monomers for preparing polylactides/glycolides [28-31]. Various functional groups including alkyl [32-37], allyl [38], hydroxy [39], carboxylic acid [40, 41], amine [40] , polyethylene glycol (PEG) [42] and alkenyl [43, 44] have been reported. However, to our knowledge, the halogen- and particularly fluorine-substituted lactide monomer/polymer has not been reported in the literature so far. The introduction of fluorine and fluorine-containing substituents can affect the properties of organic compound. Fluorine is the most electronegative element and its size, lipophilicity and electrostatic interactions can significantly affect chemical

outcome. For example, the trifluoromethyl (CF_3) group serves as an important component of many active pharmaceutical drugs [45-52]. Fluoropolymers demonstrate excellent inertness to various biological environments as well as hydrophobicity and lipophilicity [53]. They have been used in various biomedical applications such as vascular graft, bypass graft, [54-56], in vivo oxygen transport (blood substitutes) and drug delivery [57]. In this chapter, a novel synthesis method for bulk fluorination of PLA is offered. Also, relevant biological assays including cytotoxicity and protein adsorption is presented.

Figures

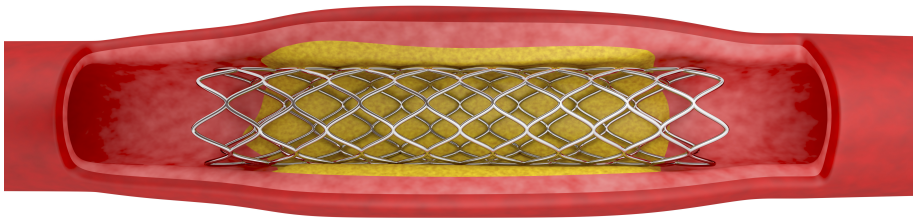

Figure 1. Schematic of a coronary stent expanded inside the blocked artery. Expanded stent prevents a previously blocked artery from re-closing.

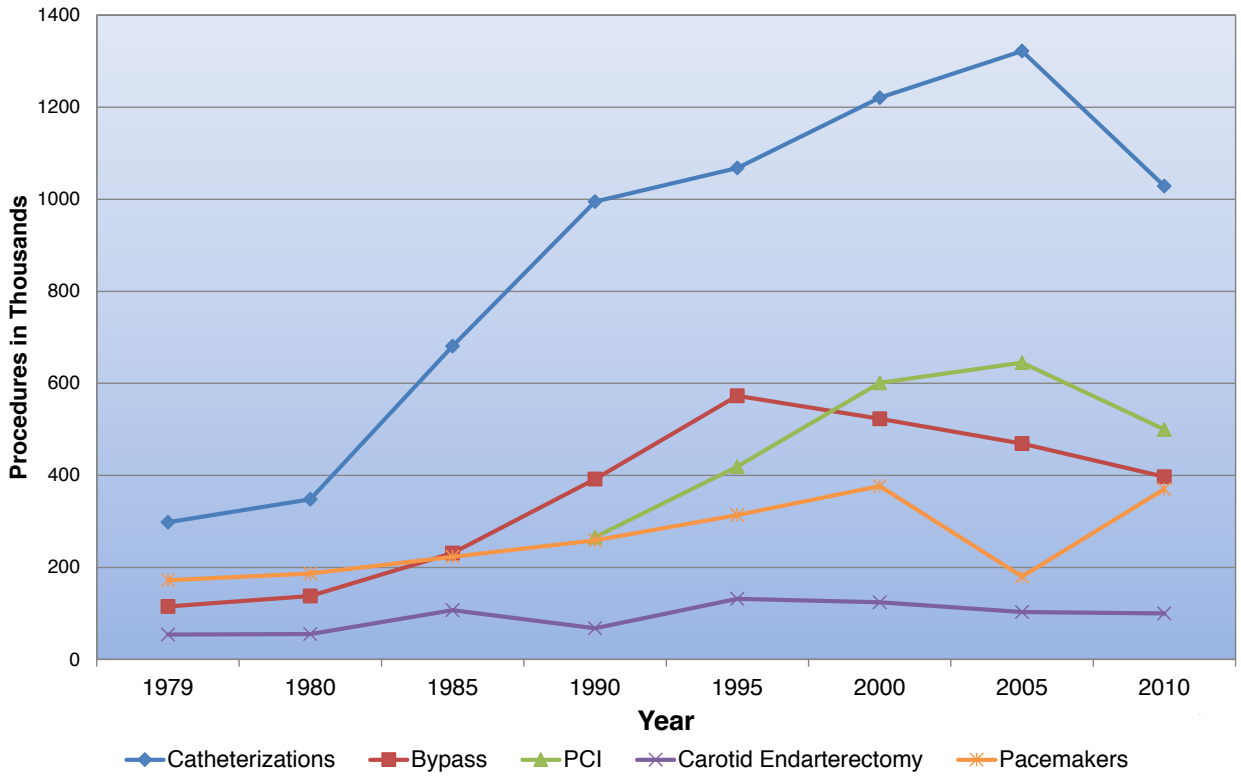

Figure 2. Trends in cardiovascular procedures:1979-2010, United States. PCI stands for percutaneous coronary intervention which is a procedure for placing stent in narrowed artery [1].

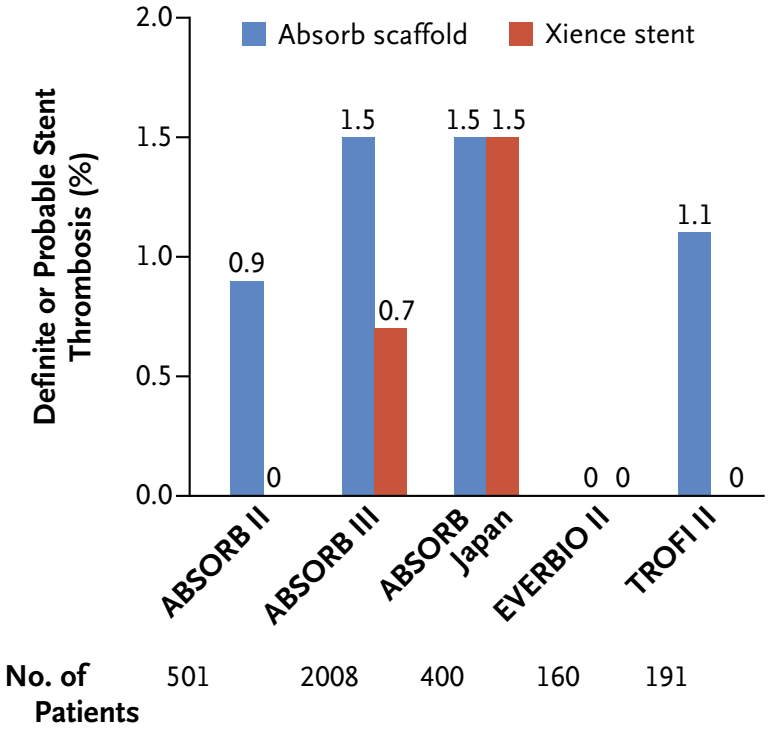

Figure 3. Thrombosis comparison between bioresorbable (blue bars) and metallic (Xience, red bars) stents [7].

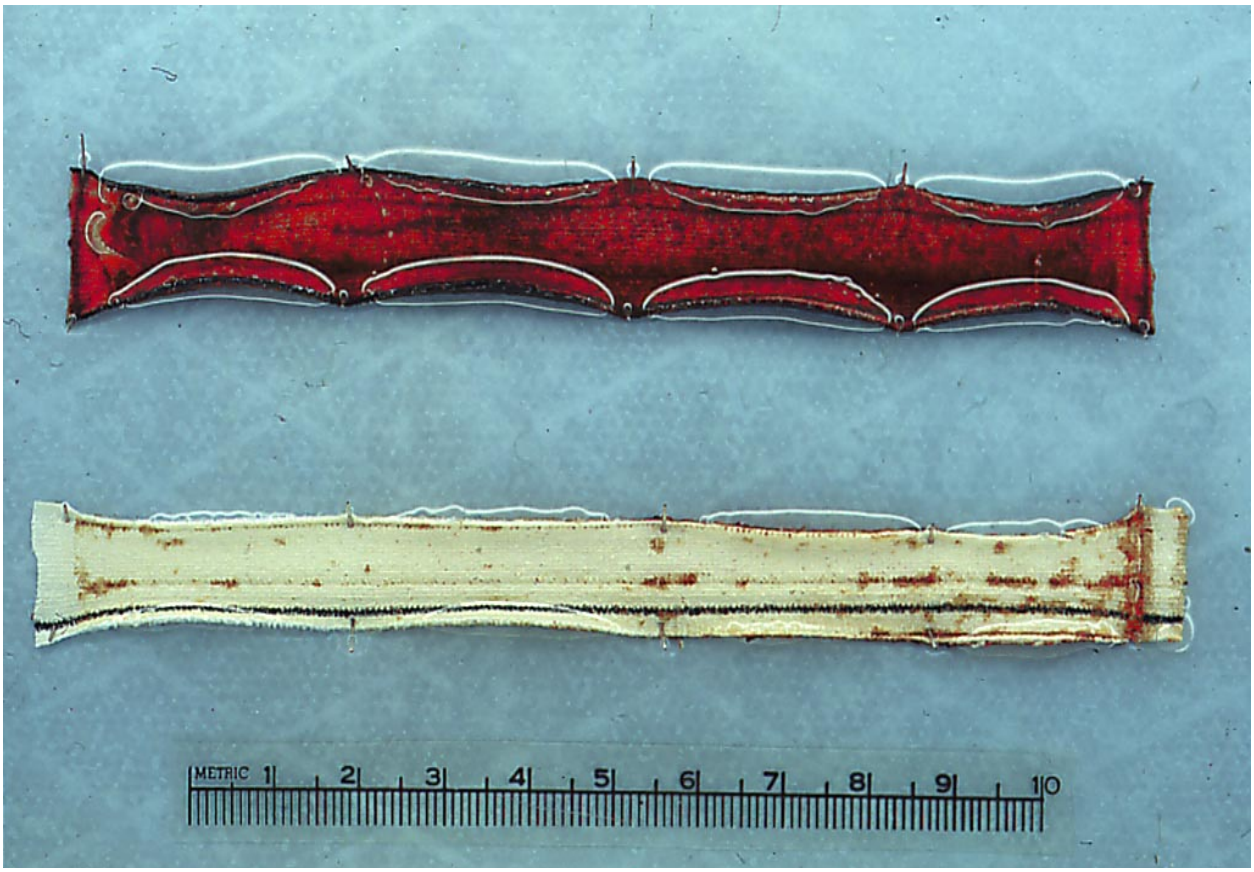

Figure 4. Comparison between tetrafluoroethylene glow discharge treatment on blood compatibility of small diameter Dacron vascular graft. Top: Untreated Dacron. Bottom: Fluorinated Dacron [10].

Chapter 2

Surface Fluorination of Polylactides

Abstract

Bioresorbable vascular scaffolds (BVS) have garnered considerable attention after their efficacy was demonstrated in clinical applications. Poly(lactic acid) (PLA) has been the predominant polymer used for making bioresorbable stents. The United States Food and Drug Administration (FDA) approved the first fully absorbable stent manufactured from PLA to treat coronary artery disease in 2016. Although BVS have long-term advantages, they are associated with higher rates of early thrombosis compared with polymer-coated and drug eluting permanent metallic stents. To address this issue, we modified the surface of PLA with a perfluoro compound facilitated by surface activation using radio frequency (RF) plasma. Fluoropolymers have been extensively used in blood contacting materials, such as blood vessel replacements due to their reduced thrombogenicity and reduced platelet reactivity. The compositions of plasma-treated surfaces were determined by electron spectroscopy for chemical analysis (ESCA). Also, contact angle measurements, cell cytotoxicity and the degradation profile of the treated polymers are presented. Finally, relevant blood compatibility parameters, including plasma protein adsorption, platelet adhesion and morphology, were evaluated. We hypothesized that tight binding of adsorbed albumin by fluoropolymers enhances its potential for blood-contacting applications.

1. Materials and Methods

1.1.Buffer solutions

The protein adsorption buffer used in this study contained 0.01 M sodium citrate, 0.01M sodium phosphate, 0.12 M sodium chloride, and 0.02 % sodium azide, and is referred to as CPBSz. CPBSzI is CPBSz to which 10 mM NaI was added. All salts were reagent grade and purchased from Sigma-Aldrich (St. Louis, MO) and used without further purification. A sodium dodecyl sulfate (SDS) solution, composed of 2% SDS, was used to elute the adsorbed proteins. SDS (electrophoresis purity) was obtained from BioRad (Richmond, CA).

Platelet suspension buffer without calcium or magnesium (PSB) contained 137 mM NaCl, 5.5 mM dextrose, 4mg/ml bovine serum albumin (BSA), 0.4 mM sodium phosphate monobasic, 2.7 mM KCl and 10 mM HEPES and was sterile filtered. Immediately before use, 0.1 U/ml apyrase (Sigma-Aldrich, St. Louis, MO) was added to this buffer. To prepare platelet suspension buffer with Ca^{2+}/Mg^{2+} ions (PSB-complete), 2.5 mM $CaCl_2$ and 1.0 mM $MgCl_2$ was added to the PSB buffer. All the buffers were at pH 7.4.

1.2. Polymer pellets and samples preparation

PLA polymer pellets were processed using a procedure analogous to that used for making KBr discs for infrared spectroscopy. Approximately, 60 mg of the polymer was placed in an assembled mold and evacuated for 2 minutes followed by applying about 9 bar pressure for 3 min. The pressure and vacuum were then removed and pellet disks were taken out of the mold. The disks formed from compressed PLA pellets were 13 mm in diameter and ~0.4 mm thickness. These were then cut into 8 mm discs using an 8 mm punch.

316 stainless steel (SS) sheets were cut into 7 mm^2 coupons and cleaned by sonicating for 10 minutes in hexane, dichloromethane, acetone and methanol (repeated twice). 316 SS samples

were then air dried and stored in a desiccator.

Prior to cell adhesion studies, samples were sterilized by soaking in 70% ethanol for 2 h and then washed twice with PBS.

1.3. Polymer surface activation and modification

1.3.1. Ammonia-plasma treatment of PLA

We applied an approach similar to that described by Petersen et al. [58, 59] to activate the PLA surface with primary amine functionalities. The surface treatment process (Figure 1) was performed in a radio-frequency glow discharge plasma reactor (frequency 13.56 MHz, Diener Electronic GmbH & Co. KG, Ebhausen, Germany) with two capacitively-coupled electrodes (Figure 2), described in detail elsewhere [17]. The compressed polymer pellet disks were placed on a glass rack and ammonia gas was introduced into the reactor at a controlled flow rate of 1.4 sccm. We used 40 W RF power for 2 min for all PLA samples. Under the same experimental conditions, the samples were flipped over so both sides of the PLA pellet disks were activated with primary amine groups ($-NH_2$).

1.3.2. Immobilization of 1,1,1-trifluoro-3-isocyanatopropane (TFICP)

The immobilization of TFICP to the amino-activated PLA surfaces was performed using the chemical reaction between the isocyanate functional group in TFICP and the primary amine groups introduced to the PLA surface (Figure 1). All the reagents were transferred into a glovebox and the reaction was performed in a water and oxygen-free environment to avoid the

undesirable side reaction of isocyanate groups with ambient moisture. Amino-activated PLA pellet disks were placed into glass vials and filled with 1ml of 10% (v/v) of TFICP solution in dry hexane. After 2 h incubation at room temperature, the reaction mixture was removed and samples were rinsed three times with copious amount of Milli-Q water (Millipore, Milli-Q water with at least 18MΩ.cm resistivity) and dried in a desiccator overnight. We used hexane as a diluent since it does not swell or solubilize the PLA [60].

1.4. Surface characterization of modified PLA

The chemical composition of the treated PLA samples was determined by electron spectroscopy for chemical analysis (ESCA) at the National ESCA and Surface Analysis Center for Biomedical Problems (NESAC/BIO, University of Washington, Seattle). Spectra were collected using a Surface Science SSX-100 spectrometer (Surface Science Instrument, Mountain View, CA) equipped with a monochromatic Al Kα x-ray source. The samples were analyzed at a 55° take-off angle probing the topmost 50-80 Å of the surface. Compositional survey scans (0-1000 eV) and high-resolution C1s scans were acquired at an analyzer pass energy of 150 eV with an x-ray spot size of approximately 1000 μm. High-resolution scans were then obtained at a pass energy of 50 eV and resolved into individual Gaussian peaks using a least-squares algorithm in the Service Physics SSI software. Peaks were identified and integrated to calculate the atomic percentage using the peak areas under the elemental curves and linear background function. Each peak was referenced to the C_{1S} hydrocarbon peak at 285 eV to account for binding energy shifts. Samples were presoaked in ultrapure water for 2 hours prior to ESCA analysis.

1.5. Contact angle goniometry

Advancing contact angles on the sample surfaces were measured by a Ramé-Hart contact angle goniometer by the sessile drop technique using ultrapure water as the probe liquid [61, 62]. Samples, at least 13 mm in size, were placed on top of the sample platform and five droplets were added to obtain the advancing contact angle curve. At least three samples were measured for each group studied.

1.6. Degradation studies

Degradation studies were carried out by transferring polymer pellet disks into glass vials filled with 10 ml of carbonate buffer (100 mM, pH 10.2). Samples were placed on a shaker at 37 °C. At pre-determined times, polymer pellet disks were collected, rinsed with Milli-Q water and dried to a constant weight prior to determination of mass loss. Weight loss (%) was evaluated by gravimetric analysis and calculated by:

$$\text{Weight loss } (\%) = [(W_0 - W_t)/W_0] \times 100$$

W_0 is the initial weight and W_t is the residual weight of the dry polymer pellet disks at time t.

1.7.Cell culture

The mouse embryonic fibroblast cells (NIH-3T3) were purchased from American Type Culture Collection (ATCC, Manassas, VA, USA). Cells were cultured in Dulbecco's Modified Eagle's Medium (DMEM), supplemented with 10% fetal bovine serum (FBS). Cells were plated into cell culture flasks and maintained according to ATCC-suggested procedures.

1.8. *In vitro* cytotoxicity assessment

To evaluate cytotoxicity, samples were incubated in the DMEM culture medium supplemented with 10% FBS at 37 °C for 24 hours to extract soluble substances. Latex and tissue culture polystyrene (TCPS) were used as the positive and negative controls, respectively. Cell viability was determined using the 3-(4,5-dimethylthiazol-2-yl)-2,5-diphenyltetrazolium bromide (MTT) colorimetric method. This method is based on the reduction of the MTT (Sigma; St. Louis, MO) into formazan crystals by viable cells. NIH-3T3 cells were seeded into the 24-well tissue culture plate at an initial density of 50,000 cells per well and incubated for 24 h. The cell culture medium was then removed and replaced with the same amount of the extracting medium from samples and incubated for an additional 24 hours. The metabolic activity of the cells was measured by addition of 50 µl of MTT (5 mg/ml solution in PBS) to each well. The cells were incubated for an additional 2.5 h. After removing the MTT solution, 0.5 ml dimethyl sulfoxide was added to each well and incubated for 30 min to dissolve the formazen crystals. A 200 μl aliquot from each well was transferred into a 96-well plate and the optical density of each well was measured at 570nm using a microplate reader (tunable VERSAmax microplate reader, Molecular Devices; Sunnyvale, CA).

1.9. Live/dead assay

To evaluate cell viability/cytotoxicity at various time points, we used a live/dead cell staining assay kit (Molecular Probes, Inc). NIH-3T3 mouse fibroblast cells were seeded in 24-well plates (10000 cells/well) and allowed to adhere overnight. Then culture media was removed and cells

were treated with the sample eluents, which were prepared by incubating samples in the DMEM supplemented with 10% FBS at 37 °C for 24 hours. At the end of each time point culture media was removed and cells were prepared for microscopy following manufacturing protocol. Briefly, after aspirating cells and washing with PBS, we added 200 μl of a staining solution consisting of 2 μM ethidium homodimer (EthD-1) and 4 μM calcein AM for 20 min. The staining solution was then removed and replaced with phenol red-free DMEM for imaging. Cell attachment and morphology were examined on a Nikon TE200 inverted microscope using rhodamine and FITC filters to visualize EthD-1-stained (dead) and calcein AM-stained (live) cells, respectively. Images were acquired in pseudocolored, greyscale, and combined using ImageJ software.

1.10. Protein radiolabeling

We used the iodine monochloride (ICl) method developed by Helmkamp et al. [63] and modified by Horbett [64] to radiolabel human fibrinogen (Fg, FIB 3 2642P, Enzyme research, South Bend, IN) and human albumin (Alb, A8763, Sigma, St. Louis, MO). An ICl stock solution consisted of 0.02 M ICI, 2.0 M NaCl, 0.02 M KC1, and 1.0 M HC1.

In this method, radioactive ("hot") $Na^{125}I$ iodide (Perkin Elmer, Waltham, MA) is mixed with nonradioactive ("cold") iodine monochloride. Hot ICl is formed by rapid iodide-iodine exchange. The iodine is substituted in the tyrosine residues (Figure 3) of the protein [65]. The degree of substitution can be tuned by adjusting the stoichiometry, i.e. the ICl to protein ratio. We used a 3:1 ICl to protein molar ratio for labeling Fg and a 2:1 ICl/protein molar ratio for labeling Alb.

At the end of the reaction, the unbound ^{125}I is separated from the radiolabeled protein by transferring the reaction mixture to a disposable size-exclusion chromatography column (#732-

2010 EconoPac 10DG, BioRad, Hercules, CA). Typically, two passes through the desalting columns are required to sufficiently remove the free iodine. Radiolabeled Alb and Fg were aliquoted and stored at -80˚C and used within two weeks.

1.11. Protein adsorption and retention

Protein adsorption was performed by incubating samples with radiolabeled protein for 2 h at physiological temperature (37 °C). A standard protein concentration equivalent to 1% plasma concentration was used for each individual protein adsorption experiment. This corresponded to a concentration of 0.3 mg/ml for Alb and 0.03 mg/ml for Fg.

Prior to protein adsorption, samples were placed into 1.5 ml polystyrene cups and equilibrated by submersion in 0.75 ml of degassed cPBSzI (pH 7.4) for one hour at room temperature. cPBSzI is the cPBSz buffer to which 10 mM NaI was added. The buffers used for adsorption studies are prepared the day before and adjusted to pH 7.4 with sodium hydroxide. Approximately, 1 L cPBSzI was vacuum degassed for 2 hours prior to use as a protein diluent or equilibrant. The citrate is added both as a buffer compound and a calcium chelator to inhibit the calcium-dependent proteases, which are common to blood and blood products. Shortly before use, a 2x concentration stock protein solution (0.6 mg/ml Alb or 0.06 mg/ml Fg) and 2 % citrated pooled plasma solution were made and enough ^{125}I-labeled protein was added to the unlabeled protein solution to obtain a minimum of a 2:1 signal-to-noise ratio (~50 cpm/ng). Since the specific activity of the ^{125}I protein was high, only a small quantity of that was required to add to unlabeled protein solutions. Thus, the initial protein concentrations did not change significantly.

Protein adsorption experiments were initiated by mixing 0.75 ml of the 2x concentration stock

solution to the samples soaking in cPBSzI to yield a final protein concentration consistent with 1% plasma solution. At the end of the 2 h adsorption time, samples were rinsed three times with 1 ml fresh cPBSzI buffer and then transferred to counting tubes. The radioactivity is measured after a one minute count with a Cobra II gamma counter (Packard Instruments). The amount of adsorbed protein was calculated from the retained radioactivity after correcting for the background, the specific activity of the stock protein solution, radioactivity decay and the exposed surface area of both sides the sample.

Protein retention was measured by storing samples for 24 h with 1 ml of 2% sodium dodecyl sulfate (SDS). Samples were then removed from the counting tubes and carefully rinsed with fresh cPBSzI three times and transferred into new gamma counter tubes for measuring the specific activity of the retained proteins.

1.12. Platelet rich plasma preparation and platelet adhesion

Human blood was collected from healthy donors by trained phlebotomists at the University of Washington Medical Center, under a protocol approved by the UW Human Subjects Institutional Review Board. Blood was drawn by venipuncture into vacutainers containing ACD anticoagulant (1:9 v/v). The blood was transferred to 50ml polyethylene conical tubes and centrifuged at 180g for 20 minutes at room temperature. Platelet rich plasma (PRP) was harvested by careful removal of the upper platelet rich layer and centrifuged again at 1500g for 15 minutes. Then plasma was removed and platelets were resuspended in an appropriate volume of PSB to render 10^8 platelets/ml. Immediately before platelet adhesion experiments, Ca^{2+} and Mg^{2+} were added into PSB to make a final concentration of 2.5 mM $CaCl_2$ and 1.0 mM $MgCl_2$.

Samples were sterilized in 70% ethanol as previously described and preadsorbed with 1% human plasma for 1.5 h. They were then rinsed twice to remove loosely adsorbed protein and incubated with PRP for 2 h at 37 °C. After platelet adhesion, samples were rinsed with sterile PBS buffer with at least five times the original solution volume to remove non-adherent or loosely bound platelets.

1.13. Evaluation of number and morphology of adherent platelets

Scanning electron microscopy (SEM) was used to observe the morphology and number of adherent platelets. At the end of *in vitro* platelet adhesion experiments, samples were fixed at room temperature for 2 h with Karnovsky's fixative (Electron Microscopy Sciences, Hatfield, PA) prepared in 0.1M cacodylate buffer. Samples were then washed with cacodylate buffer and post-fixed for 30 minutes with 1% osmium tetroxide (Electron Microscopy Sciences, Hatfield, PA) in cacodylate buffer followed by dehydration using a graded series of ethanol solutions: 50%, 70%, 80%, 90%, and 100% ethanol each for 15 minutes. Samples were then critical point dried, sputter-coated with gold and analyzed by SEM (FEI Sirion XL30) at an accelerating voltage of 5kV. At least three images were randomly selected for each material and platelet activation was categorized as (I) round or discoid, (II) dendritic, (III) partially spread and (IV) fully spread [66] .

1.14. Statistical analysis

Significant differences amongst sample groups were assessed by one-way analysis of variance (ANOVA) and the means compared using Bonferroni’s posthoc correction with α=0.05, unless

otherwise noted. Protein adsorption and platelet adhesion data are reported with their standard error of mean.

2. Results and Discussion

2.1. Surface characterization

A compositional survey scan of the PLA substrate is shown in Figure 4, indicating that only carbon (C) and oxygen (O) are present in the surface zone with no additional elements detected. The spectrum of a PLA disc after ammonia-plasma surface activation is also shown in Figure 4. We observed that, in addition to C and O peaks, a nitrogen (N) peak is also present in the spectrum, which is attributed to the ammonia-plasma activation process. Also, compared to the untreated PLA, there is a decrease in O and no significant changes in C in the sample surface elemental compositions.

C (1s) high resolution XPS spectra (HRXPS) of untreated PLA, amino-activated PLA and TFICP immobilized PLA are presented in Figure 5. After spectral resolution into individual Gaussian peaks, we can see that both spectral envelops are comprised of three primary C peaks: (1) a 285.0 eV peak corresponding to carbon with one, two or three bonds to hydrogen (CH, CH_2, CH_3, hydrocarbons), (2) a 286.9 eV peak corresponding to carbon with one bond to oxygen (C-O) and (3) a 289.1 eV peak corresponding to carbons with three bonds to oxygen (O=C–O, esters). The TFICP immobilized PLA spectrum shows decreased C-O and O=C–O peak amplitudes in the backbone of the polymer, resulting from this modification.

The XPS survey spectrum of the TFICP immobilized PLA is also shown in Figure 4. In addition to C, O and N peaks, an F (1s) peak is also present in the spectrum indicating the successful immobilization of TFICP on these surfaces. The chemical compositions of untreated PLA,

amino-activated PLA and TFICP immobilized PLA are shown in Figure 6. The untreated PLA films have about 62% atomic % carbon and 38% oxygen and a C/O ratio of 1.6 (theory: 60% C, 40% O, C/O = 1.5) with no other detectable elements. Also, the % carbon did not significantly change during the surface treatment process while the oxygen was noticeably reduced from its initial value on untreated PLA. The % oxygen remained in the same range during subsequent chemical reaction with TFICP.

2.2.Contact angles

Contact angle analysis provides insights into the wettability of a surface by measuring the force balance of surface interaction versus self-attraction of a liquid droplet at an interface. Water contact angle using the sessile drop method [62] has been used to measure the change of wettability of various surface treatments on the PLA pellet disks. Higher contact angle reflects increased surface hydrophobicity. Water static contact angles are presented in Figure 7 and were compared to the water contact angle on the smooth polytetrafluoroethylene (PTFE) sheet. We observed significant differences in contact angle values between the amino-activated and TFICP immobilized PLA. As expected, smooth PTFE sheet was most hydrophobic with a contact angle 102±1.8° whereas, the contact angle of the amino-activated PLA was much reduced at 36±6.2°. The contact angle of the TFICP immobilized PLA increased to 85± 2.5° compared to untreated PLA (contact angle: 70±1.3°) as expected for fluorine addition to the surface. The surface characteristic of amino-activated PLA dramatically changed from hydrophilic to hydrophobic after immobilization of TFICP. This change in contact angle value has been used to qualitatively monitor the chemical treatment process. Previous studies with perfluoro compounds have

reported reduced surface energy [53, 67]. This surface modification strategy is an efficient method for reducing the surface energy of the PLA surfaces.

2.3. Degradation profile

The degradation profile of the PLA and surface modified PLA at 37 °C in carbonate buffer (100 mM, pH 10.2) was evaluated by measuring weight loss (%) over time and is summarized in Figure 8. Earlier degradation studies in phosphate buffer (100 mM, pH 7.4) showed no weight loss after incubating samples in this buffer at 37 °C for over a month (data not shown). Various factors such as temperature, pH, polymer end group and molecular weight affect the degradation rate of the polylactides and polyglycolides [68-78]. Studies by de Jong et al.[68] on the hydrolytic degradation of poly(lactic acid) suggest that lactic acid oligomers undergo faster degradation at higher pH (i.e., carbonate buffer). We observed similar accelerated degradation by incubating samples in carbonate buffer. After 4 weeks of incubation in this buffer, a measurable weight loss (PLA: 2.5%, PLA-NH_2: 4.9% and PLA-F: 10.0 %) was observed for all sample series.

As expected, the amino-activated PLA showed a higher degradation rate than untreated PLA, which can be explained by decreased hydrophobicity of these amino-activated samples in comparison to untreated PLA. The immobilization of TFICP could be expected to decrease the rate of hydrolysis of the ester bonds because of their hydrophobic protection against water and hydroxyl ions. But in fact, we observed that degradation rate was higher for the TFICP immobilized PLA samples even though they had the highest contact angle/ hydrophobicity of all samples in this series. One possible explanation could be a catalytic role of TFICP on the hydrolysis of ester bonds in polymer backbone. Another possibility is that the TFICP treatment

reduces the surface crystallinity of the PLA thus increasing water access for hydrolysis of PLA chains.

It also worth noting that at the end of the 12 weeks experiment time, weight loss was approximately same for all polymers studied here. The differences in degradation rate at shorter times are consistent with surface degradation – when the surface zone has hydrolyzed, then all that remains of each of the samples is the bulk PLA. We terminated the experiment at the end of third month since the PLA pellet disks started to disintegrate and this made it difficult for accurate weight measurements. Further investigation is required to understand and describe the degradation nature of TFICP immobilized PLA since hydrophobicity is not the only parameter that plays a role in its degradation rate.

2.4. *In vitro* assessment of cytotoxicity

To determine if harmful components leach from the PLA and surface modified PLA, conditioned medium was prepared by incubating samples in cell culture medium for 72h following the recommended procedure described in ISO 10993-5. NIH-3T3 fibroblast cells were then incubated with the conditioned media for 72 h. The cytotoxicity of the polymer pellet disks was evaluated by comparing the metabolic activity of NIH-3T3 cells treated with latex extract as a positive control and tissue culture polystyrene (TCPS) extract as a negative control using the MTT assay. MTT is a yellow tetrazolium salt that is reduced to form violet formazan crystals only in metabolically active cell mitochondria allowing us to quantify the number of living cells spectrophotometrically. The results were normalized with respect to the negative controls (untreated TCPS) (Figure 9). Neither PLA extracts nor modified PLA extracts had an adverse effect on the metabolic activity of fibroblast cells, whereas latex extracts killed most of the cells.

PLA devices were approved by the FDA for direct contact with biological fluids in the 1970's [79] and PLA is considered to be non-toxic [27, 80, 81]. Earlier studies also showed that amino-activated PLA improves cell attachment and proliferation [82-85].

In addition, cell viability was determined using the LIVE/DEAD cytotoxicity assay for membrane integrity. In this method, we used calcein AM (component A) which is a cell-permeant dye that converts to green fluorescent calcein in live cells by the presence of esterase activity. On the other hand, dead cells produce a red fluorescence due to the binding of EthD-1 (component B) to their nucleic acids. EthD-1 cannot enter live cells with the intact plasma membrane. Both calcein AM and EthD-1 components are virtually non-fluorescent before interacting with cells. NIH-3T3 fibroblast cells were incubated with sample extracts and prepared for LIVE/DEAD staining at various designated time points. Representative fluorescent microscopy images are shown in Figure 10. With respect to the total number of cells, very few dead (i.e. red) cells were observed in all samples except the latex extract which is known to be toxic to cells. Likewise, most cells stained green, revealing no indication of toxicity from the samples extracts. The MTT assay supported the LIVE/DEAD staining data (Figure 10).

2.5. Protein adsorption

2.5.1. Protein adsorption from pure protein solutions

The adsorption of human serum Alb and Fg onto the various polymer pellet disks and the 316SS from a pure Alb and Fg solution in cPBSzI (0.3 mg/ml and 0.03 mg/ml, respectively) are presented in Figures 11 and 12. These concentrations were chosen to correspond to the Alb and Fg concentration in 1% human plasma [86, 87]. After a 2 h adsorption time, TFICP immobilized PLA adsorbed a relatively greater amount of Alb than other samples. The Alb adsorption

decreased in the order of PLA-F > PLA > PLA-NH_2 > 316SS. After incubation with 2% SDS, higher amounts of Alb were retained on TFICP immobilized PLA as compared to all other samples tested. The lowest quantity of Alb was retained on PLA and amino-activated PLA pellet disks. Thus, a statistically significant amount of albumin was both adsorbed and retained on TFICP immobilized PLA compared to all other materials studied ($\alpha = 0.05$).

The trend observed for Fg adsorption and Fg retention was similar to that observed with Alb adsorption and retention, with greater amount of Fg adsorbed and retained on TFICP immobilized PLA than other samples tested.

2.5.2. Protein adsorption from binary protein solutions

The adsorption and retention of Alb and Fg onto modified polymer pellet disks from binary/competitive protein solutions are presented in Figure 13. To make these binary solutions, we prepared two identical Alb-Fg solutions in PBS based on the 1 % protein ratios observed in normal human blood plasma (Alb: 0.3 mg/ml and Fg: 0.03 mg/ml) [86] and then added radiolabeled Alb to one solution and radiolabeled Fg to the other.

Alb adsorption was in the range of 65-8 ng/cm^2 for the samples evaluated using binary protein solutions, following the same trend of pure protein solution. We observed higher Alb adsorption on the TFICP immobilized PLA and the amount of the adsorbed Alb decreased in the order similar to the pure protein solution described above. When both albumin and fibrinogen are present in the solution, samples overall adsorbed less albumin than from a single component Alb protein solution. The amount of the retained albumin after 24 h incubation in 2% SDS showed the same trend observed with retained Alb from pure protein solution. The highest amount of

retained Alb was once again greatest on TFICP immobilized PLA, while other samples retained negligible Alb after incubation with SDS.

In the case of Fg, both protein adsorption and retention from an Alb-Fg binary protein solution were also highest on TFICP immobilized PLA and decreased in the order similar to Alb adsorption and retention: PLA-F > PLA > PLA-NH_2 > 316SS. Overall, samples adsorbed less Fg in a binary protein solution compared to a pure protein solution. The Fg retention after SDS incubation was once again highest on TFICP immobilized PLA and decreased in the same order as Fg adsorption.

In both cases, the percent of retained protein after 24 h incubation in 2% SDS was numerically higher on TFICP immobilized PLA than on all other samples evaluated. After SDS elution, 21 ng/cm^2 (33%) of adsorbed albumin was retained on FTICP immobilized PLA, whereas less than 5 ng/cm^2 Alb is retained on other samples. Likewise, 25 ng/cm^2 (51 %) of adsorbed fibrinogen was retained on TFICP immobilized PLA, while less than 7 ng/cm^2 remained on other samples.

2.5.3. Protein adsorption from normal human plasma

To emulate the complex protein solutions that these surfaces might come into contact *in vivo*, we measured the Alb and Fg adsorption onto these surfaces in 1% citrated pooled human plasma. As expected, the amount of Alb and Fg protein adsorption from human plasma was lower than those measured in pure and binary protein solutions for all the samples tested (Figure 14). Both PLA and TFICP immobilized PLA had higher Alb adsorption than Fg, whereas, amino-activated PLA and 316SS adsorbed slightly more Fg than Alb (statistically significant for the 316SS).

After elution with 2% SDS and consistent with the pure and binary protein adsorption results, a greater amount of both Alb and Fg were retained on the TFICP immobilized PLA than the other

samples tested (Figure 15). In contrast to pure and binary protein solutions, Alb retention was greater than Fg on all polymer surfaces except 316SS. Alb (15 ng/cm^2) and Fg (10 ng/cm^2) were retained on TFICP immobilized PLA. Both Alb and Fg retention were slightly higher on PLA than amino-activated PLA. Of all the samples, 316SS retained the least adsorbed protein with marginally higher amount of Fg than Alb.

Table I presents the Alb/Fg ratio of the adsorbed and retained proteins. Earlier studies suggest that a high Alb/Fg ratio contributes to improved hemocompatibility of polymer surfaces [88]. The Alb/Fg protein adsorption ratios ranged from 0.6 to 1.3, with the highest value for TFICP immobilized PLA. Upon elution with 2 % SDS, the Alb/Fg ratio was increased for all the surfaces and ranged from 0.8 for 316SS to 1.5 for TFICP immobilized PLA.

Protein adsorption from binary solutions and from blood plasma measure the relative affinity of surfaces for a specific protein competing with other proteins. When protein adsorption was measured from pure protein solutions using concentrations close to that in 1% blood plasma, 0.3 mg/ml Alb (Figure 11), 316SS and amino-activated PLA had the lowest adsorbed Alb. On the other hand, TFICP immobilized PLA had the highest amount of protein adsorption and retention after incubating with 2% SDS. The higher retention of proteins has also been reported in earlier studies with fluorinated polymers [11, 18, 89]. Fluorinated surfaces have shown satisfactory clinical performance [56, 90, 91] and have been the material of choice for blood contact applications [92, 93]. Our observation of Alb protein adsorption and retention on fluorinated surfaces is consistent with the previous studies [18, 89].

There is little consensus over optimal methods for measuring blood compatibility [61, 94-101]. Generally, studies are focused on intrinsic pathway activation, platelet interaction and evaluation of adsorbed proteins. The focus of this study is on protein adsorption. The adsorption of blood

plasma proteins to synthetic material surfaces has been recognized as the precursor event to platelet adhesion/activation and thrombus formation [87, 102]. The dynamics of protein adsorption are related to the physical and chemical properties of the surfaces and proteins. The concentration of the proteins on the surface can be 1000 times higher than their initial concentration in plasma and adsorbed proteins can form a 2-10 nm monolayer [103]. In order to connect protein adsorption events to their effect on surface-induced clotting, we need to accurately measure the type and quantity of adsorbed proteins. Among more than 300 distinct blood plasma proteins [86], Fg has been shown to play a key role in platelet adhesion and coagulation [17, 104-107]. Albumin (Mw~ 66.5 kDa, pI = 4.9), a relatively inert protein, is the most abundant protein in blood with a concentration range from 35 to 50 mg/ml. Fibrinogen (Mw ~ 340 kDa, pI = 5.5) is a net negatively charged protein and has a concentration between 2-4.5 mg/ml in blood. Based upon a hypothesis by Horbett, adsorbed Fg even in low levels supports platelet adhesion and clotting [107-109]. On the other hand, increased albumin on the surface has long been thought to improve blood compatibility. Albumin has been used as a passivating surfaces against protein adsorption since a preadsorbed layer of Alb inhibits subsequent adhesion of fibrinogen and decreases *in vitro* platelet adhesion producing a potentially less thrombogenic surfaces [105, 110, 111]. We have modified that hypothesis to consider the amount of fibrinogen adsorbed to surfaces in competition with albumin and the retention of albumin. Thus, a higher Alb/Fg ratio could potentially improve hemocompatibility. Also, the surface retention of albumin ("albumin tight binding") has been proposed to play an important role in this hypothesis [18] to inhibit further displacement of albumin by fibrinogen (*i.e.*, Vroman effect).

2.6. Platelet adhesion and morphology

Scanning electron microscopy was used to visualize the morphology of adherent platelets. Samples were preadsorbed with 1% citrated normal human plasma and then exposed to the platelet rich plasma for 2 h at 37 °C. Samples were then washed to remove loosely attached platelets, fixed and critical point dried. SEM analysis showed noticeable differences in both amount and morphology of adherent platelets on the various samples (Figure 16). Amino-activated PLA displayed a larger number of adherent platelets compared to all other samples tested here. For a more holistic view, SEM images (Figure 17) were also taken at lower magnification (1000x). Platelets in their inactive form have a typical discoid or round shape and depending on the level of activation, their morphology changes. The relative morphological distributions (expressed as percentage of total platelets) are presented in table II and provides insight to the general degree of platelet activation. Platelets are categorized into four different groups: (I) discoid or round (II) dendritic (III) partially spread and (IV) fully spread (Figure 18). A larger percentage of adherent platelets on TFICP immobilized PLA were dendritic or partially spread whereas, adherent platelets on amino-activated PLA were mostly partially spread or fully spread. Conversely, PLA and 316SS had adherent platelets in all categories with larger percentage of them partially spread. Using this semi-quantitative method, the results suggested that platelets adhesion to TFICP immobilized surfaces was lower than other materials assessed here and they were less activating to platelets. It is worth noting that the platelet adhesion trend did not follow the trends observed for fibrinogen adsorption or retention. In fact, the more hydrophilic amino-activated PLA, which had the lowest amount of protein adsorption in all tested conditions, had the greatest number of activated platelets. Conversely, TFICP immobilized

PLA retained the highest amount of fibrinogen, but had the lowest number of visually countable adherent platelets.

For this study, samples were preadsorbed with 1% human plasma to mimic the relevant conditions of protein adsorption event. Based on the albumin passivation hypothesis, albumin enrichment at the surface of biomaterials is desirable for reducing platelet adhesion and activation. The highest amount of albumin was retained on TFICP immobilized PLA as shown in Figure 15. The Alb/Fg ratio (table I) was also the highest on these surfaces even though they retained relatively more amount of fibrinogen than other samples tested here.

3. Conclusions

In this work, we have explored a new approach for the functionalization of poly(lactic acid) surfaces with trifluoromethyl groups with a focus on improving its hemocompatibility. To achieve this goal, PLA surfaces were first activated with ammonia plasma to introduce amine functional groups. Later, these functional groups were used to conjugate TFICP (with terminal CF_3 groups) to the PLA surface using the reaction between primary amine and isocyanate on TFICP. It was shown that TFICP immobilized surfaces were more hydrophobicic than other samples and showed no sign of cytotoxicity toward NIH-3T3 fibroblast cells. Contrary to our expectations they hydrolytically degraded faster than PLA. Protein adsorption experiments with fluorinated PLA compared to untreated PLA and 316SS showed that TFICP immobilized surfaces adsorbed higher amount of the Alb and Fg in all protein solutions studies. In addition, we observed greater amount of retained Alb on TFICP immobilized surfaces after incubating with 2% SDS in all protein solutions studied here. The surface-induced thrombosis is a complex phenomenon and it is important to consider multiple assays to get a holistic picture of the blood

reaction to materials. Fluorinated surfaces, compared to other materials studied here, showed a relatively smaller number of adherent platelets and those platelets were less activated. Therefore, we hypothesize that these fluorinated surfaces will show improved blood compatibility *in vivo* as tight binding of Alb will contribute to improved blood compatibility by passivating these surfaces. Further studies on this passivation phenomenon with fluorinated surfaces is currently under investigation. It is important to pay a close attention to the events leading to thrombosis. In this regard, protein adsorption, which is the first event after implantation and occurs before platelets ever reach to the surface, is a viable research area.

Figures

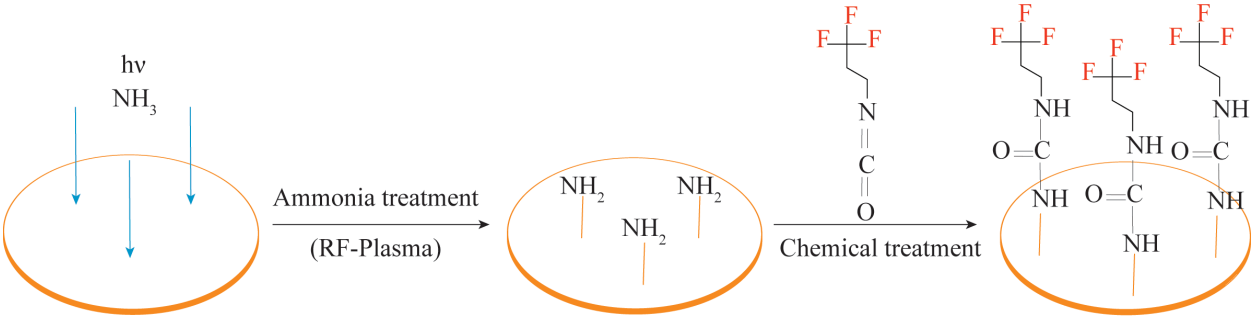

Figure 1. Schematic illustration showing surface fluorination of PLA with a two step strategy: first, surface activation with terminal amino groups using radio frequency plasma treatment with ammonia and subsequent immobilization of TFICP using the chemical reaction between the terminal amino groups on PLA and isocyanate functional groups on TFICP.

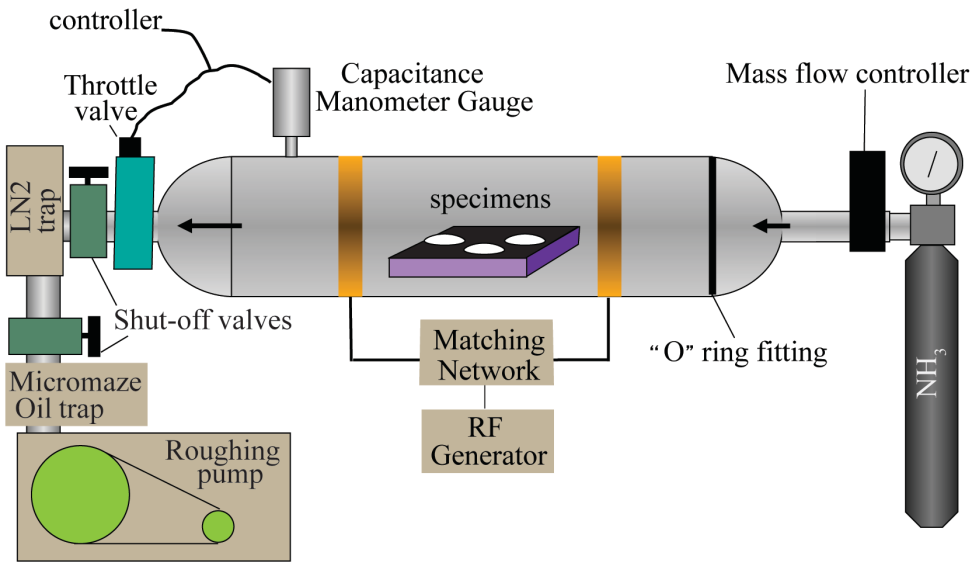

Figure 2. Schematic of radio frequency plasma deposition reactor and the location of samples in the reactor.

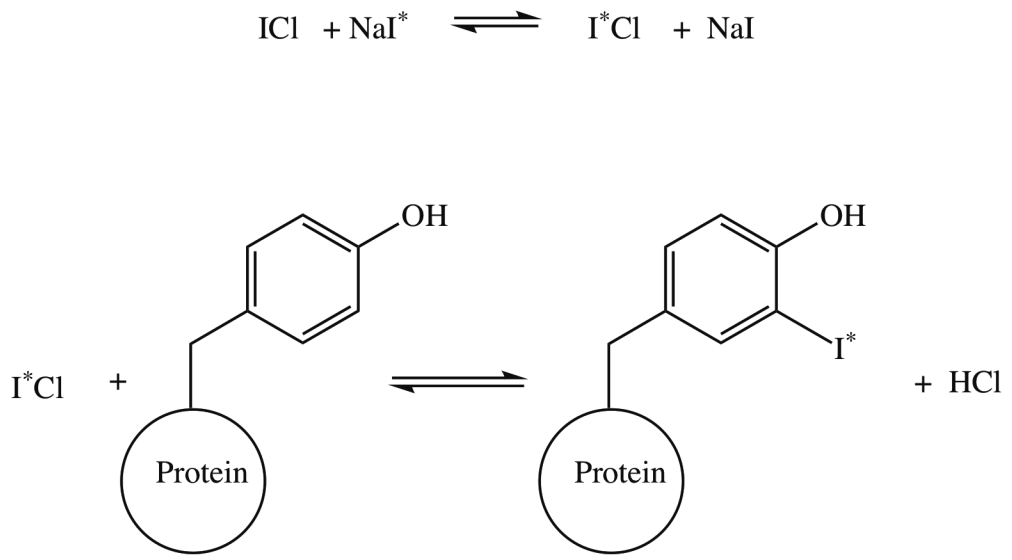

Figure 3. Protein iodination: First, nonradioactive iodine (I) in iodine monochloride (ICl) is replaced with radioactive iodine (I*). Then the tyrosine residue of the protein is tagged with a mixture of radioactive and nonradioactive ICl.

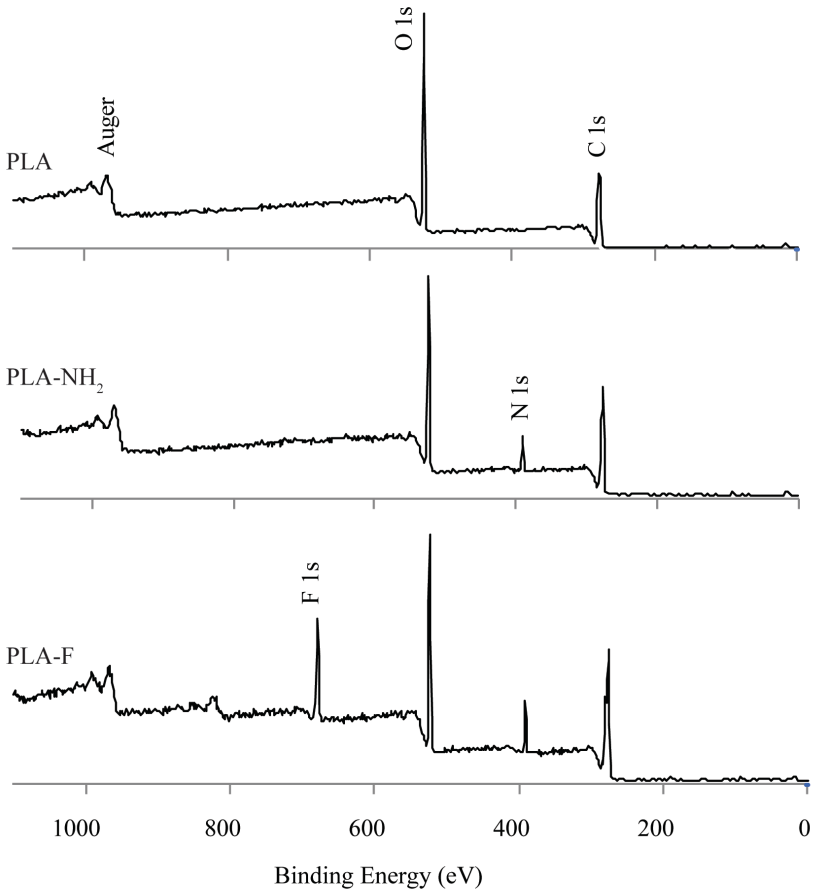

Figure 4. ESCA spectra of untreated PLA, amino-activated PLA (PLA-NH_2) and TFICP immobilized PLA (PLA-F). As excepted untreated PLA has only C 1s and O 1s peaks in the spectra whereas, PLA-NH_2 shows a distinct N 1s peak and PLA-F shows a sharp F 1s and N 1s peaks in addition to C 1s and O 1s peaks.

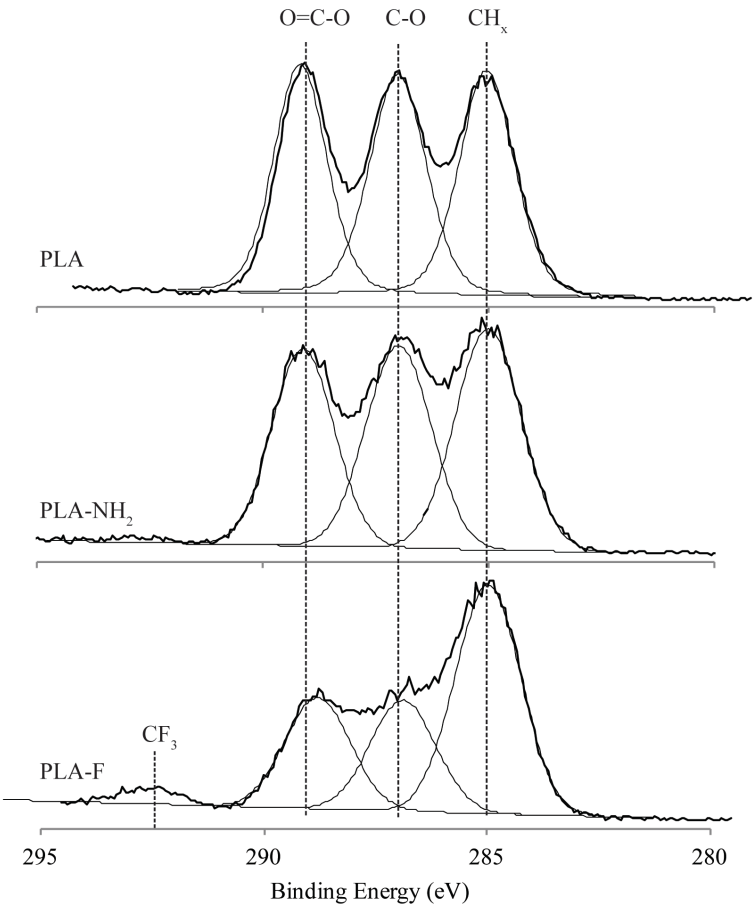

Figure 5. High resolution ESCA C 1s spectra and curve fitting of untreated PLA, amino-activated PLA (PLA-NH_2) and TFICP immobilized PLA (PLA-F). From left to right, peaks correspond to CF_3, O=C–O, C–O, and CH_3.

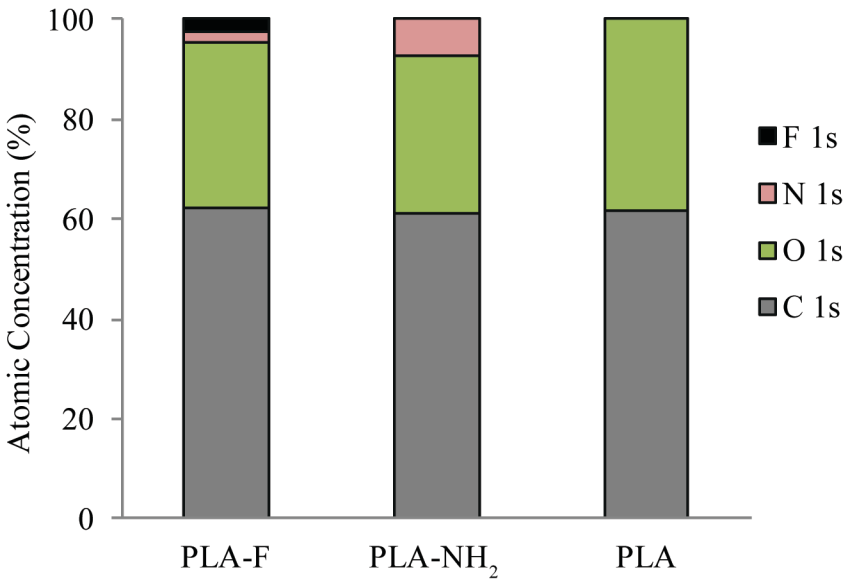

	Atomic Concentration (%)		
XPS Line	PLA-F	$PLA-NH_2$	PLA
C 1s	62.27	61.15	61.91
O 1s	38.10	31.69	38.10
N 1s	2.13	7.16	
F 1s	2.68		

Figure 6. ESCA atomic concentrations of the chemical components of untreated PLA, amino-activated PLA ($PLA-NH_2$) and TFICP immobilized PLA (PLA-F).

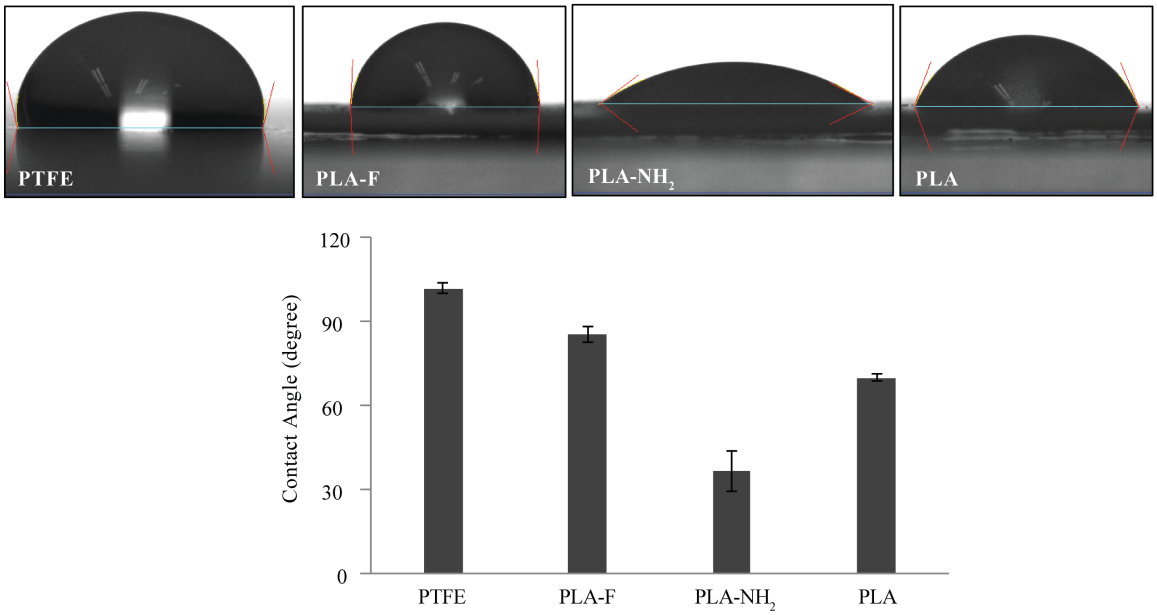

Figure 7. The profiles of water droplets on the surface of modified PLA measured by aqueous sessile drop goniometry and its comparison with PTFE.

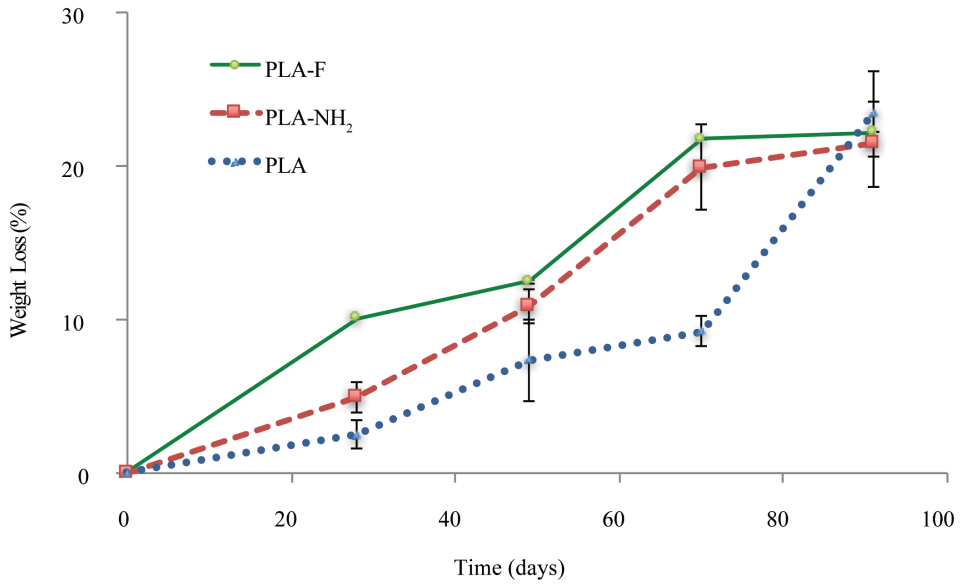

Figure 8. Degradation profile of untreated PLA, amino-activated PLA (PLA-NH_2) and TFICP immobilized PLA (PLA-F) at 37 °C in carbonate buffer, pH 10.2.

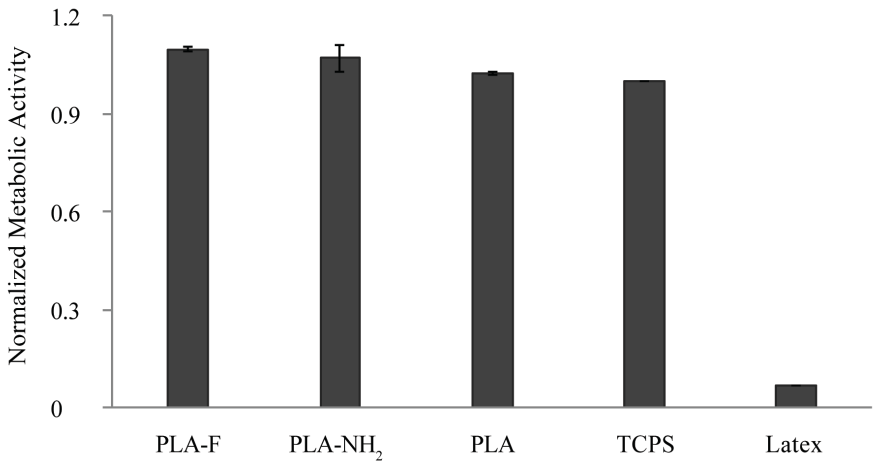

Figure 9. The relative metabolic activity of the NIH 3T3 cells treated with sample eluents, evaluated by the MTT assay, 24h after treatment and normalized with respect to the TCPS value. Latex and TCPS were used as positive and negative controls, respectively.

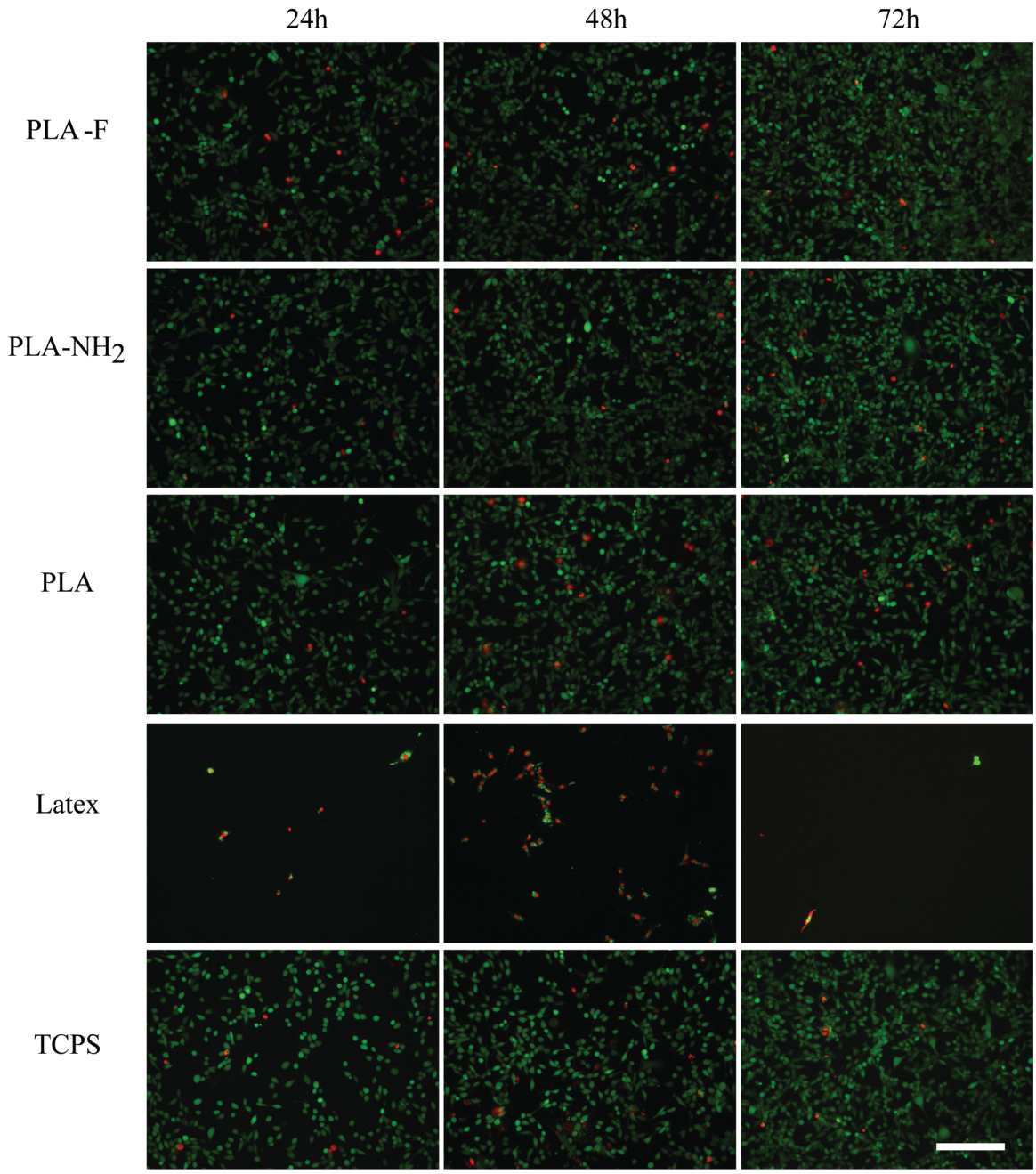

Figure 10. LIVE/DEAD cytotoxicity assay showed most cells were alive in all the samples series except positive control, latex, over the course of 72 h incubation with sample extracts. Green indicates live cells and red indicates dead cells. (Scale bar: 400 μm; n≥3)

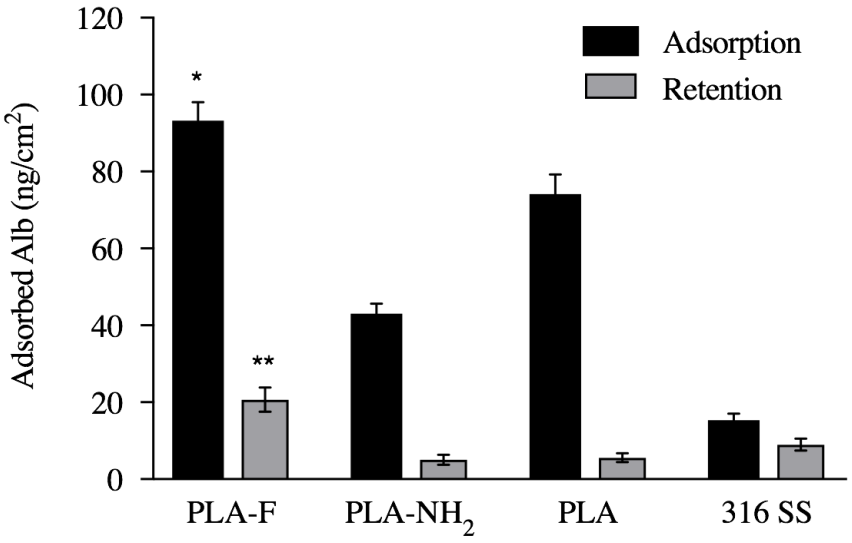

Figure 11. Protein adsorption from a pure Alb solution (0.3 mg/ml) in cPBSzI (black) and the retained Alb on the surfaces after 24 h elution with 2% SDS (pattern). Error bars indicate SEM, n=6. Single asterisk (*) or double asterisk (**) show statistically significant higher amount of adsorbed or retained Alb, respectively, on PLA-F as compared to all other materials tested (α= 0.05).

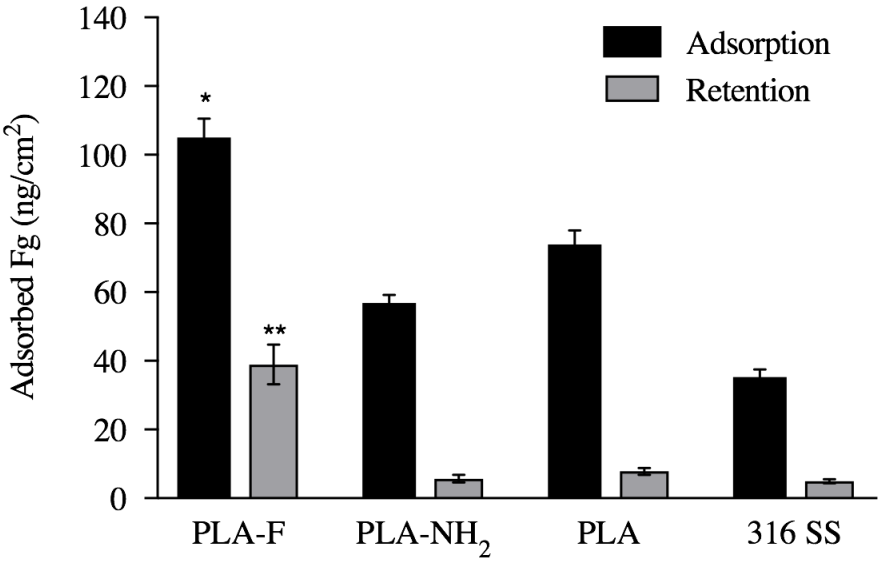

Figure 12. Protein adsorption from a pure Fg solution (0.03 mg/ml) in cPBSzI (black) and the retained Fg on the surfaces after 24 h elution with 2% SDS (pattern). Error bars indicate SEM, n=6. Single asterisk (*) or double asterisk (**) show statistically significant higher amount of adsorbed or retained Fg, respectively, on PLA-F as compared to all other materials tested (α= 0.05).

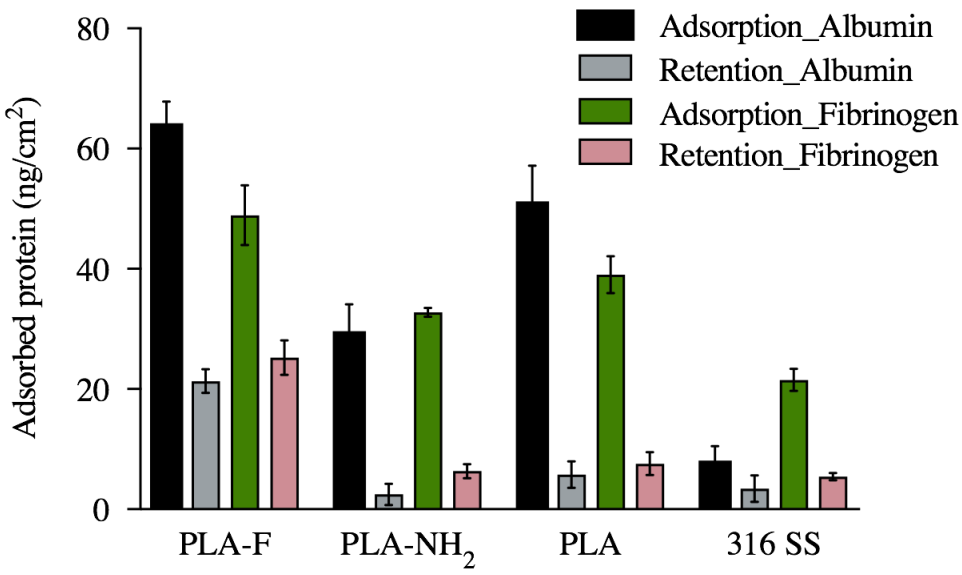

Figure 13. Competitive protein adsorption from binary solution (Alb: 0.3 mg/ml and Fg: 0.03mg/ml). Samples were incubated for 2 h in binary protein solutions in cPBSZI (black and green). The amount of retained protein on the surfaces was measured after 24 h incubation with 2% SDS (pattern and pink). Error bars indicate SEM, n=6. There is a statistically significant higher amount of both adsorbed Alb and Fg on PLA-F as compared to all other samples except PLA. There is a significantly greater amount of both retained Alb and Fg as compared to all other materials studied ($\alpha = 0.05$).

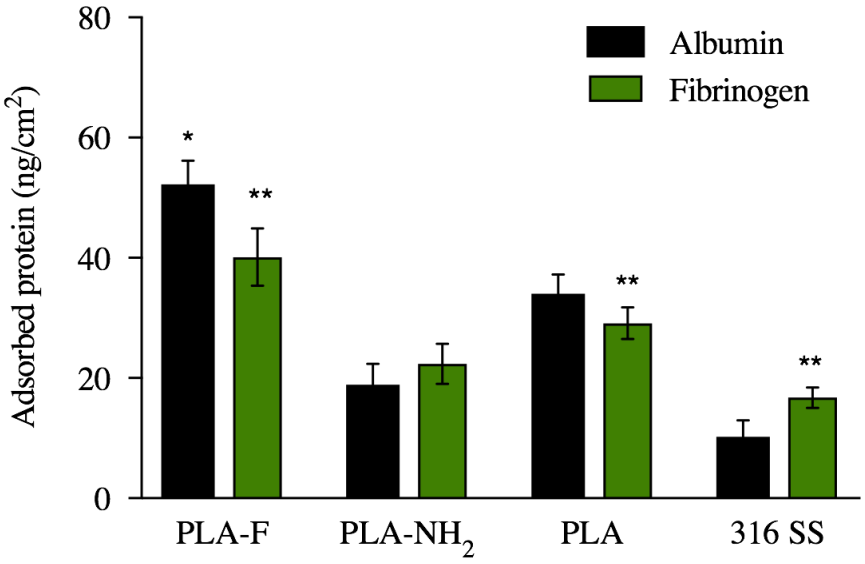

Figure 14. Protein adsorption from 1 % citrated normal human plasma. Black bars represent Alb adsorption and green bars show Fg adsorption. Error bars indicate SEM, n=6.There is a statistically significant (*) higher amount of adsorbed Alb on PLA-F as compared to all other samples. There is a statistically significantly difference (**) in the amount of adsorbed Alb as compared to the amount of adsorbed Fg in all materials studied except PLA-NH_2 (α= 0.05).

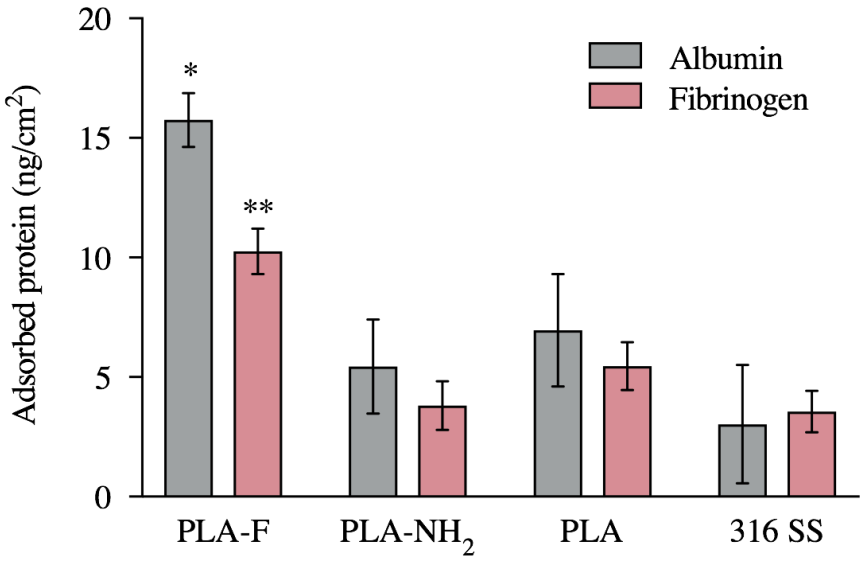

Figure 15. Protein retention from 1 % citrated normal human plasma after 24 h elution with 2% SDS. Retained Alb is shown in pattern and Fg is shown in pink. Error bars indicate SEM, n=6. Single asterisk (*) or double asterisk (**) show statistically significant differences in the amount of retained Alb or Fg, respectively, on PLA-F as compared to all other materials tested (α= 0.05).

Table I. Alb/Fg ratio from 1 % citrated normal human plasma after 2 h adsorption and subsequent elution with 2% SDS for 24 h

Sample	Alb/Fg Adsorption	Alb/Fg Retention
PLA-F	1.30	1.53
PLA-NH_2	0.84	1.43
PLA	1.17	1.27
316 SS	0.61	0.85

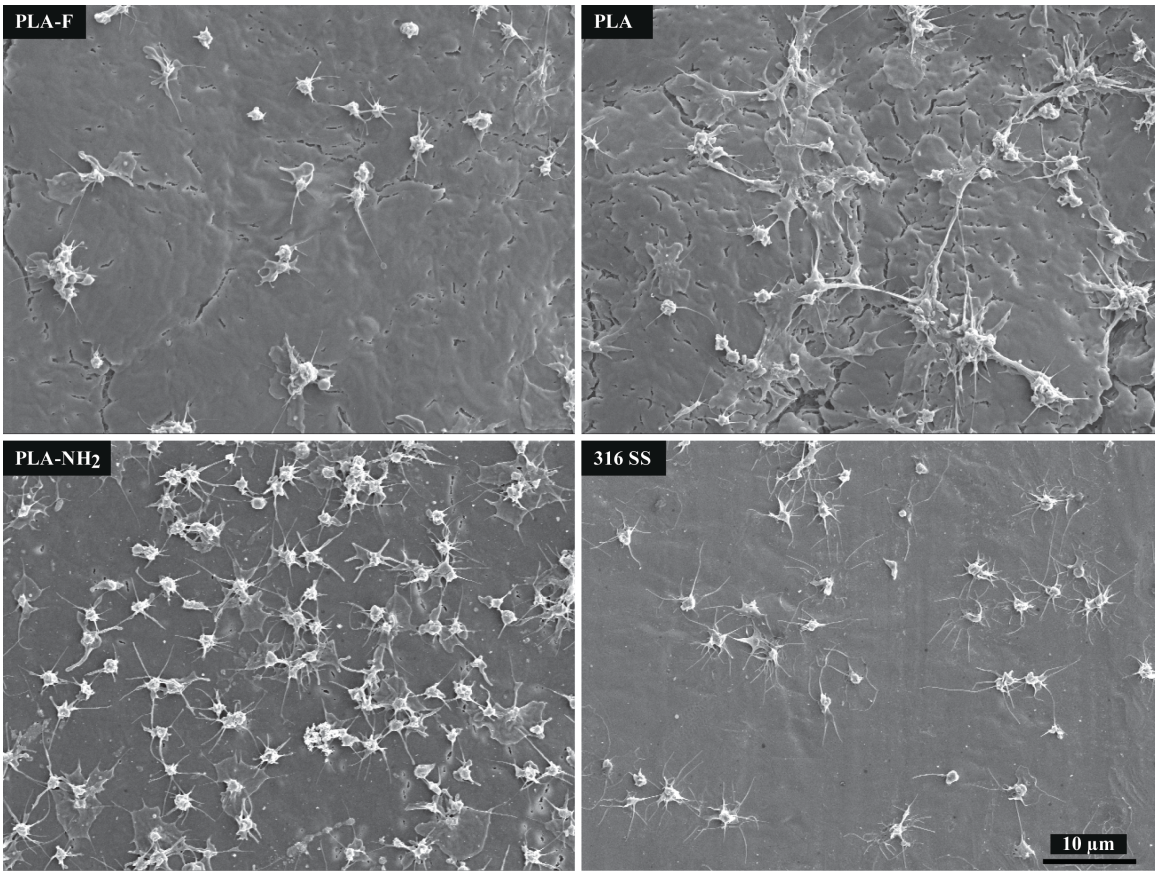

Figure 16. Scanning electron micrographs of adherent human platelets on the surfaces of untreated PLA, amino-activated PLA, TFICP immobilized PLA and 316SS. Samples were initially pre-incubated with 1% human plasma for 1.5 h. Samples were then incubated in the freshly prepared PRP for 2 h at 37 °C. Magnification x2000; scale bar 10 μm.

Table II. Percent (%) of platelets in each activation category determined from visual examination using SEM images (n=3). Platelet morphological categories were (I) discoid or round (II) dendritic (III) partially spread and (IV) fully spread. Samples were preadsorbed with 1% plasma before exposing to human PRP for 2 h at 37 ºC.

Sample	Discoid (%)	Dendritic (%)	Partially spread (%)	Fully spread (%)
PLA-F	13.3 ± 4.4	53.3 ± 18.2	26.7 ± 12.6	6.7 ± 3.8
PLA-NH_2	<1	9.2 ± 6.3	68.3 ± 11.2	22.5 ± 5.7
PLA	3.9 ± 1.8	23.5 ± 4.3	47.1 ± 14.2	25.5 ± 11.8
316 SS	2.3 ± 1.1	18.6 ± 7.7	67.4 ± 9.4	11.7 ± 3.1

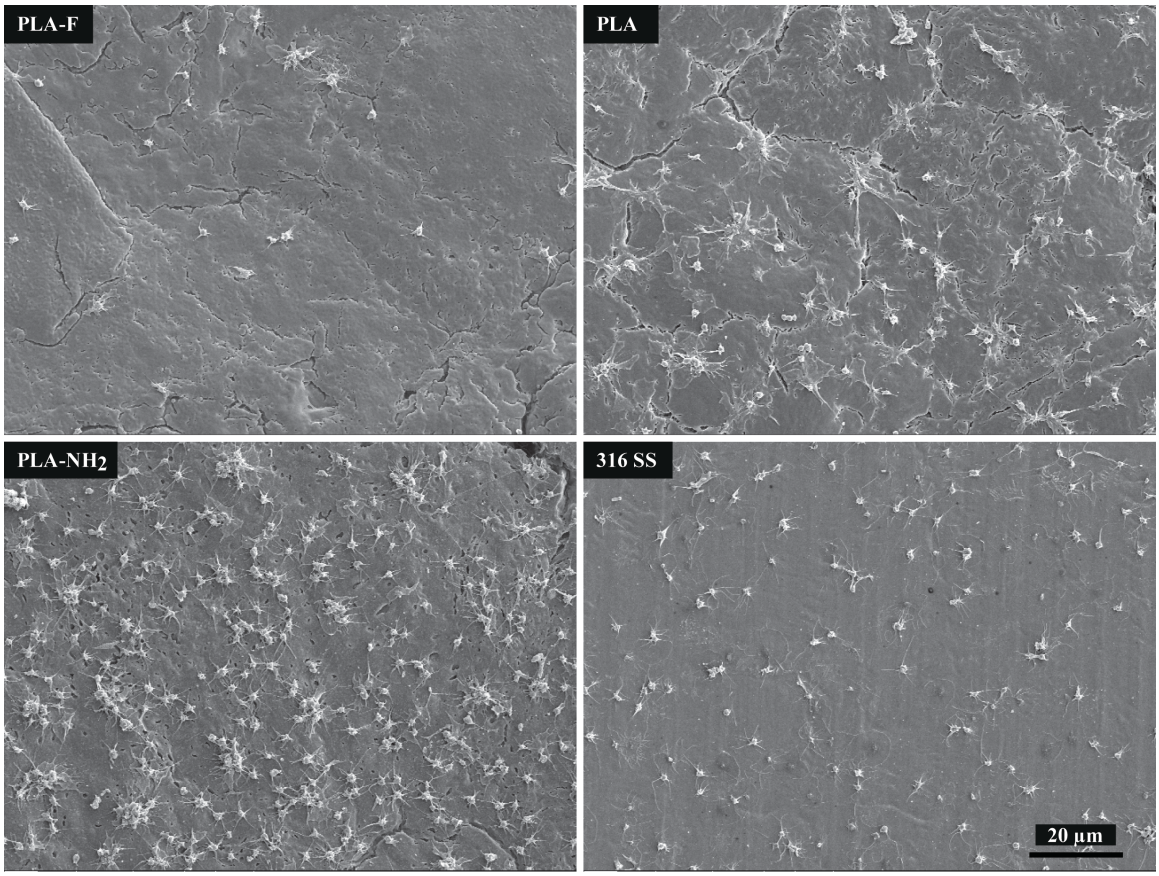

Figure 17. Scanning electron micrographs of adherent human platelets on the surfaces of TFICP immobilized PLA, untreated PLA, amino-activated PLA, and 316SS. Samples were initially pre-incubated with 1% plasma for 1.5 h and then exposed to the freshly prepared PRP for 2 h at 37 °C. Magnification 1000x; scale bar 20 μm.

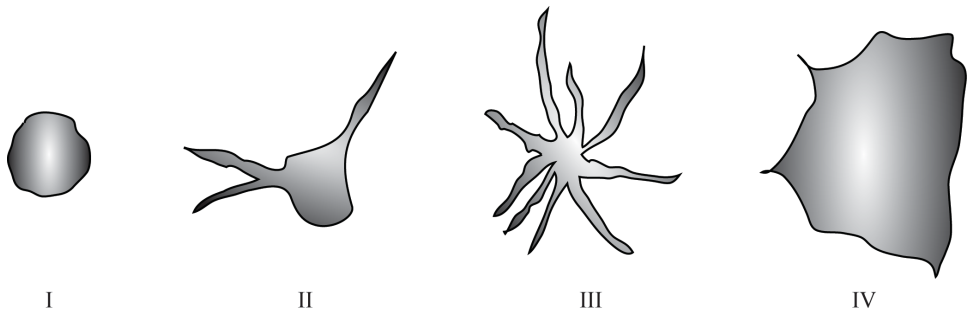

Figure 18. Schematic of representative images of platelets morphology divided into four shape categories to evaluate the extent of their activation. From left to right the morphological categories are: (I) discoid or round with no pseudopodia, (II) dendritic or early pseudopodia with no evidence of flattening, (III) partially spread or late pseudopodia and (IV) fully spread in which, hyaloplasm is extensively spread and there is do distinct pseudopodia.

Chapter 3

Bulk Fluorination of Poly(lactides)

1. Materials and Methods

1.1. Materials

3,3,3-Trifluorolactic acid (TFLA) and 2-bromopropionyl bromide (2-BPB) were purchased from Matrix Scientific (Columbia, USA) and Sigma-Aldrich, respectively and were used as received. Tin (II) 2-ethylhexanoate ($Sn(Oct)_2$) and benzyl alcohol were purchased from Sigma-Aldrich and purified by distillation prior to use. Acetonitrile (MeCN), dichloromethane (DCM) and triethylamine (NEt_3) was obtained from a Glass Contour solvent purification system. All other reagents and solvents were used as received from commercial sources. ^{1}H, ^{13}C and ^{19}F NMR analyses were carried out at room temperature in deuterated solvents on a Bruker AV700 or DRX499 MHz spectrometer. Chemical shifts are expressed in parts per million (ppm) downfield from tetramethylsilane with the residual protio-solvent used as chemical shift standard. ($CDCl_3$, ^{1}H: 7.26 ppm and ^{13}C: 77.16 ppm; CD_3CN, ^{1}H: 1.94 ppm and ^{13}C: 1.39 and 118.69 ppm).

1.2. Buffer solutions

The protein radiolabeling buffer used in this study is referred to CPBSz and contained 0.01M sodium phosphate, 0.01 M sodium citrate, 0.12 M sodium chloride, and 0.02 % sodium azide. Protein adsorption washing buffer is referred to CPBSzI and contained all the components of CPBSz and 10 mM NaI. All salts were reagent grade and purchase from Sigma-Aldrich (St.

Louis, MO) and used without further purification. Sodium dodecyl sulfate (SDS) (electrophoresis purity) was obtained from BioRad (Richmond, CA). A solution of 2% SDS was used to elute the adsorbed proteins.

1.3. Synthesis of CF_3-functionalized lactide monomer

Figure 1 shows the synthetic route for preparing trifluoromethyl-functionalized lactide (CF_3-LA) monomer. Under argon gas flow, 3,3,3-trifluorolactic acid (43 mmol) was dissolved in 100 ml dry acetonitrile in a flame-dried three-neck flask. The mixture was placed in an ice bath and dry triethylamine (56 mmol) was added to the reaction flask. Then equimolar of 2-bromopropionyl bromide (54 mmol) was mixed in 10 mL of dry acetonitrile and was added dropwise via syringe to the reaction flask. After the addition was complete, the ice bath was removed and the mixture was stirred at room temperature for 5 h. The resulting white precipitate was filtered off through Celite, and the filtrate was concentrated under reduced pressure. The resulting product was then dissolved in ethyl acetate and filtered again through Celite to remove any remaining salts. The removal of the ethyl acetate by rotary evaporation gave product (2b) as a brown oil.

To prepare the product (3), dry acetonitrile (700 ml) was added to a flame-dried three-neck flask under argon gas flow and placed in an ice bath. Next, sodium hydride (64.5 mmol) was added to the flask and stirred for 20 minutes. The product (2b) was dissolved in dry acetonitrile (100 ml) and was added dropwise to the flask using addition funnel over 45 minutes. The ice bath was removed and reaction mixture was stirred until it reached to room temperature. The reaction flask was then transferred to an oil bath and stirred overnight at 75 °C under Argon gas flow. At the end of reaction time, the oil bath was removed and the resulting mixture was cooled to room temperature. The reaction mixture was filtered off through Celite to remove white precipitate and

the acetonitrile was removed by rotary evaporation. The crude product was purified by silica gel flash column chromatography using dry premium grade silica gel and ethyl acetate: hexane mixture (1:2) as an eluent. The solvents were distilled off and the product was recrystallized from hexane/dichloromethane to give product (3) as a white powder. The product was a mixture of R, R/S, S and R,S diastereomers (31% yield).

1.4. Solution polymerization of CF_3-functionalized lactide monomer

Scheme 4 shows the solution polymerization of monomer (3) in dry toluene at 110 °C. A reaction flask containing a stir bar was fitted with septum, flame dried under vacuum, and charged with monomer (3) (1mmol) and filled with dry toluene (4 ml). Benzyl alcohol (0.01 mmol) and tin (II) 2-ethylhexanoate $Sn(Oct)_2$ (0.01 mmol) were added to the flask and used as an initiator and catalyst respectively. Prior to polymerization, the stock solution of benzyl alcohol and catalyst were prepared in dry benzene (0.1M). The flask was placed in an oil bath and heated for 20 h at 110 °C. The resulting mixture was cooled to room temperature and dried in a rotary evaporator and then dissolved in chloroform. The precipitate was filtered and chloroform was removed by the rotary evaporator. The polymer was further dissolved in methanol, filtered and concentrated in the rotary evaporator. The resulting product was dissolved again in chloroform and precipitated in excess hexane. Next, hexane was removed by the rotary evaporator to give a trifluoromethyl-functionalized poly(lactic acid) as a white powder (76% yield). Polymerization conversion, degree of polymerization (DP) and molecular weights of the polymer were determined by ^{1}H NMR analysis.

1.5. Sample preparation for surface analysis and protein adsorption studies

Glass cover slips (8mm and 15mm, ProSci Corp) were used to prepare samples for surface analysis, water contact angle measurements and protein adsorption studies. These cover slips were cleaned by putting them in an in-house fabricated holder and immersing in a 1/64 dilution of Isopanasol in Milli-Q water (C.R. Callen Corp, Seattle, WA) and ultrasonicating for 20 min. They were then washed three times with Milli-Q water by ultrasonicating them for 15 min and replacing the used water with fresh water each time. The cover slips were air dried and stored in a desiccator. Next, both sides of the coverslips were spin-coated with ethyl methacrylate-methacryoxysilane copolymer (EMA-silane) (2.5% w/v) and baked at 60 °C overnight. Coverslips were then immersed in ethyl acetate twice for 1 h and once for 5 min. The ethyl acetate was replaced with fresh ethyl acetate after each cycle and EMA-silane coated coverslips were air dried and stored in the desiccator. This pretreatment technique has been shown to prevent delamination of the polymer coatings on coverslips.

Polymer solutions (2.5% w/v) in chloroform were prepared and both sides of the EMA-silane coated coverslips were spin-coated at 4000 rpm for 20 seconds and air dried and stored in a desiccator until ready to use. For protein adsorption studies, 316 stainless steel (316 SS) were cut into 7x7 mm coupon and cleaned by ultrasonicatin in hexane, methylene chloride, acetone and methanol for 15 min for each solvent and then air dried and stored in a desiccator. For cytotoxicity studies, samples were soaked in 70 % ethanol for 2h and then washed with sterile PBS for 20 min.

1.6. Surface analysis of CF_3-functionalized poly(lactic acid)

The chemical composition of CF_3-poly(lactic acid) samples was determined by electron

spectroscopy for chemical analysis (ESCA) at the National ESCA and Surface Analysis Center for Biomedical Problems (NESAC/BIO, University of Washington, Seattle). A thin layer of the CF_3-poly(lactic acid) was coated on coverslips using the spin-coating technique as described above. Spectra were collected using a Surface Science SSX-100 spectrometer (Surface Science Instruments, Mountain View, CA) equipped with a monochromatic Al Kα x-ray source. The samples were analyzed at a 55° take-off angle probing the topmost 50-80 Å of the surface. Compositional survey scans (0-1000 eV) and high-resolution C1s scans were acquired at an analyzer pass energy of 150 eV with an x-ray spot size of approximately 1000 μm. High-resolution scan was then obtained at a pass energy of 50 eV and resolved into individual Gaussian peaks using a least-squares algorithm in the Service Physics SSI software. Peaks were identified and integrated to calculate the atomic percentage using the peak areas under the elemental curves and linear background function. Each peak was referenced to the C (1s) hydrocarbon peak at 285 eV to account for any binding energy shift. Samples were presoaked with water for 1 h before ESCA analysis.

1.7. Contact angle goniometry

Contact angle analysis evaluates the wettability of a surface by measuring the surface tension of a liquid droplet at its interface with a homogeneous surface. Advancing contact angles measurements on the sample surfaces were carried out by a Rame-Hart contact angle goniometer by the sessile drop technique using ultrapure water as the probing liquid [61, 62] using CAM 200 software provided with the instrument. Polymer coated coverslips (as described earlier) were placed on top of the sample platform and five droplets were added to obtain the advancing contact angle curve. At least three samples were measured for each group studied.

1.8. Cell culture

The mouse embryonic fibroblast cells (NIH-3T3) were purchased from American Type Culture Collection (ATCC, Manassas, VA, USA). Cells were cultured in Medium Dulbecco's Modified Eagle's Medium (DMEM), supplemented with 10% fetal bovine serum (FBS) and maintained according to ATCC recommended protocol.

1.9. *In vitro* cytotoxicity evaluation

To evaluate cytotoxicity, samples were incubated in the DMEM culture medium supplemented with 10% FBS at 37 °C for 24 hours to extract soluble substances. Latex and tissue culture polystyrene (TCPS) were used as the positive and negative controls, respectively. Cell viability assay was determined using 3-(4,5-dimethylthiazol-2-yl)-2,5-diphenyltetrazolium bromide (MTT) colorimetric method. This method is based on the reduction of the MTT (Sigma; St. Louis, MO) into formazan crystals by viable cells. NIH-3T3 cells were seeded into the 24-well tissue culture plate at an initial density of 50,000 cells per well and incubated for 24 h. The cell culture medium was then removed and replaced with the same amount of the extracting medium from samples and incubated for an additional 24 hours. The metabolic activity of the cells was measured by addition of 50 µl of MTT (5 mg/ml solution in PBS) to each well. The cells were incubated for an additional 2.5 h. After removing the MTT solution, 0.5 ml dimethyl sulfoxide was added to each well and incubated for 30 min to dissolve the formazen crystals. A 200μl aliquot from each well was transferred into a 96-well plate and the optical density of each well

was measured at 570nm using a microplate reader (tunable VERSAmax microplate reader, Molecular Devices; Sunnyvale, CA).

1.10. Live/Dead assay

To evaluate cell viability/cytotoxicity at various time points, we used a live/dead cell staining assay kit (Molecular Probes, Inc). NIH-3T3 cells (10000 cells/well) were seeded in 24-well plates and allowed to adhere overnight. Then culture media was removed and cells were treated with the sample eluents, which was prepared by incubating samples in the DMEM supplemented with 10% FBS at 37 °C for 24 hours. At the end of each time point culture media was removed and cells were prepared for microscopy following manufacturing protocol. Briefly, after aspirating cells and washing with PBS, we added 200 μl of a staining solution consisting of 2 μM ethidium homodimer (EthD-1) and 4 μM calcein AM for 20 min. The staining solution was then removed and replaced with phenol red-free DMEM for imaging. Cell attachment and morphology were examined on a Nikon TE200 inverted microscope using rhodamine and FITC filters to visualize EthD-1-stained (dead) and calcein AM-stained (live) cells, respectively. Images were acquired in pseudocolored, greyscale, and combined using ImageJ software.

1.11. Protein radiolabeling

We used the iodine monochloride (ICl) method developed by Helmkamp et al. [63] and modified by Horbett [64] to radiolabel human fibrinogen (Fg, FIB 3 2642P, Enzyme research, South Bend, IN) and human albumin (Alb, A8763, Sigma, St. Louis, MO). An ICl stock solution consisted of 0.02 M ICI, 2.0 M NaCl, 0.02 M KC1, and 1.0 M HC1.

In this method, radioactive ("hot") $Na^{125}I$ iodide (Perkin Elmer, Waltham, MA) is mixed with

nonradioactive ("cold") iodine monochloride. Hot ICl is formed by rapid iodide-iodine exchange. The iodine is substituted in the tyrosine residues (Figure S2) of the protein [65]. The degree of substitution can be tuned by adjusting the stoichiometry, i.e. the ICl to protein ratio. We used a 3:1 ICl to protein molar ratio for labeling Fg and a 2:1 ICl/protein molar ratio for labeling Alb.

At the end of the reaction, the unbound ^{125}I is separated from the radiolabeled protein by transferring the reaction mixture to a disposable size-exclusion chromatography column (#732-2010 EconoPac 10DG, BioRad, Hercules, CA). Typically, two passes through the desalting columns are required to sufficiently remove the free iodine. Radiolabeled Alb and Fg were aliquoted and stored at -80˚C and used within two weeks.

1.12. Protein adsorption and retention

Protein adsorption was performed by incubating samples with radiolabeled protein for 2 h at physiological temperature (37 °C). A standard protein concentration equivalent to 1% plasma concentration was used for each individual protein adsorption experiment. This corresponded to a concentration of 0.3 mg/ml for Alb and 0.03 mg/ml for Fg.

Prior to protein adsorption, samples were placed into 1.5 ml polystyrene cups and equilibrated by submersion in 0.75 ml of degassed cPBSzI (pH 7.4) for one hour at room temperature. cPBSzI is the cPBSz to which 10 mM NaI was added. The buffers used for adsorption studies are prepared the day before and adjusted to pH 7.4 with sodium hydroxide. Approximately, 1 L cPBSzI was vacuum degassed for 2 hours prior to use as a protein diluent or equilibrant. The citrate is added both as a buffer compound and a calcium chelator to inhibit the calcium-dependent proteases,

which are common to blood and blood products. Shortly before use, a 2x concentration stock protein solutions (0.6 mg/ml Alb or 0.06 mg/ml Fg) and 2 % citrated pooled plasma solutions were made and enough ^{125}I-labeled protein was added to the unlabeled protein solution to get a minimum of a 2:1 signal-to-noise ratio (~50 cpm/ng). Since the specific activity of the ^{125}I protein was high, only a small quantity of that was required to add to unlabeled protein solutions. Thus, the initial protein concentrations did not change significantly.

Protein adsorption experiments were initiated by mixing 0.75 ml of the 2x concentration stock solution to the samples soaking in cPBSzI to yield a final protein concentration consistent with 1% plasma solution. At the end of the 2 h adsorption time, samples were rinsed three times with 1 ml fresh cPBSzI buffer and then transferred to counting tubes. The radioactivity is measured after a one minute count with the Cobra II gamma counter (Packard Instruments). The amount of adsorbed protein was calculated from the retained radioactivity after correcting for the background, the specific activity of the stock protein solution, radioactivity decay and the exposed surface area of both sides the sample.

Protein retention was measured by storing samples for 24 h with 1 ml of 2% sodium dodecyl sulfate (SDS). Samples were then removed from the counting tubes and carefully rinsed with fresh cPBSzI three times and transferred into new gamma counter tubes for measuring the specific activity of the retained proteins.

1.13. Statistical analysis

All statistical analyses were performed using GraphPad Prism 7 for MacOSX (GraphPad Software, La Jolla California USA). Significant differences amongst sample groups were

evaluated by one-way analysis of variance (ANOVA) applying Dunnett's multiple comparisons test. Statistical significance assumed for $p < 0.05$, unless otherwise noted.

2. Results and Discussions:

2.1. CF_3-functionalized lactide monomer synthesis

Substituted lactide have been known for over four decades with the synthesis of alkyl-substituted lactide originally reported by Schöllkopf et al. in 1978 [112] using the route outlined in Scheme 1. The method involves step-by-step condensation, starting from an α-hydroxyl acid (1) and an α-haloacyl halide (2). This synthesis method has proven to be quite versatile and was reported previously for preparing various alkyl and benzyl substituted lactides [32, 36, 37, 43, 44, 113-115]. Inspired by Schollkopf's original method, we further extended the substitution span to include halogens or halocarbons (Scheme 2). With appropriate selection of α-hydroxyl acid and α-haloacyl halide, we have been able to introduce a library of potential halogenated polyesters (Scheme S1). The suggested α-hydroxyl acid precursors, each with a unique Chemical Abstracts Service (CAS) number, contain at least one halogen at their structure. These precursors are either commercially available or their synthesis procedures are reported in the literature. The library is divided into five categories: (1-4) containing only one of F, Cl, Br or I and (5) is a combination of two different halogens.

To explore the possibility of this method, as an example we chose commercially available 3,3,3-trifluorolactic acid as a starting precursor due to the relevance of CF_3 functional group to biological applications. Previous studies on substituted lactides all consisted of hydrocarbon chains in various lengths and the fluorocarbon substituent has never been described. CF_3-functionalized lactide was prepared by analogue reaction described by Schöllkopf et al.

However, applying exact reaction conditions described earlier did not yield stable CF_3-functionalized lactide. Fluorine is the most electronegative element in the periodic table and it can potentially add further challenges to the reaction progress by attracting electrons and limiting them from participating in the desired reaction. To overcome this issue, we modified the synthesis method as shown in Figure 1 and Scheme 3. First, 3,3,3-trifluorolactic acid (1) was reacted with 2-bromopropionyl bromide to form an intermediate anhydride (2a), followed by intramolecular acyl-transfer giving carboxylic acid intermediate (2b). Then under basic condition carboxylate intermediate (2c), derived from (2b), undergoes nucleophilic substitution to yield the desired cyclic lactide monomer (3). Each separate addition of the bases, NEt_3 in first step and NaH in second step, was considered to act as an HBr scavenger and also contribute to the formation of carboxylates. The original method using a one-portion addition of NEt_3 did not produce a desired yield probably due to presence of CF_3 group on the asymmetric center. Formation of (2b) directly from (1) might also be considered. However, in the presence of NEt_3 we speculate that this reaction does not dominate because the reactivity of secondary hydroxy group of (1) is lower than carboxylate anion [116].

The course of the reaction, formation of intermediate ester (2b) along with consumption of TFLA, was monitored by thin layer chromatography (ethyl acetate: hexane 1:2 eluent mixture, R_f: 0.65). The formation of cyclic monomer (3), ring closure, imposed more challenges probably due to the hydrolysis of final product. Various modifications were tried [40, 116-118] but the best yield was obtained using dry acetonitrile and sodium hydride (NaH). The use of NaH as a strong non-nucleophilic base instead of NEt_3 resulted in higher yield. Subtle variations in the reaction conditions including type and separate addition of the base in each step of the reaction

sequence, solvent and temperature significantly affected the synthesis outcome compared to Schöllkopf's original method. The photos of the reaction setup are shown in Figure 2-7.

^{1}H-NMR and ^{13}C-NMR (700 MHz, acetonitrile-d_3) spectra of the CF_3-functionalized lactide monomer are shown in Figures 8 and 9 respectively. The ^{1}H-NMR spectrum shows characteristic peaks related to the cyclized monomer. The methyl and methine protons can be identified as a doublet near δ: 1.6 and a quartet near δ: 5.2. A quartet near δ: 5.7 is associated with CF_3 group in functionalized lactide and clearly shows the formation of the CF_3-functionalized lactide monomer. The product is a mixture of R, S (87%) and R, R/S,S (13%) diastereomers as determined by ^{1}H-NMR. The structure of the functionalized monomer was further confirmed by ^{13}C-NMR. Carbon-fluorine couplings resulting from carbons of the CF_3 groups can be identified as a quartet (d) at δ: 120 ppm. Two singlets at δ: 14.4 ppm and 72.58 ppm were assigned to carbons of CH_3 (a) and CH (c) groups. Another quartet (b) at δ: 72 ppm was ascribed to the carbon next to the CF_3 group in the monomer structure. In addition, 2D-NMR (Figure 10) and ^{19}F-NMR (Figure 11) confirm the formation of the monomer.

2.2. Ring-opening polymerization

Generally two methods have been used to prepare poly(lactide): (i) ring-opening polymerization of cyclic diesters or (ii) direct polycondensation of α-hydroxycarboxylic acids [119-122]. The reaction mechanism of these polymerization methods has been extensively investigated. Typically direct polycondensation of lactide generates low molecular weight polymer whereas, ROP yield polymers with different terminal groups, and higher molecular weight [123, 124]. The monomer to initiator ratio also effects the molecular weight of the resulting polymer. Both water and alcohols can be used as initiators. Therefore, to achieve high molecular weight, water should

be removed from all synthesis precursors and the reactant system [124]. This is considered to be challenging since water is the byproduct of polycondensation which favors depolymerization and eventually leads to low molecular weight polymer [125]. Therefore, controlled ROP in the presence of metal catalysts is the preferred method to obtain high molecular weight polymer. Tin(II) 2-ethylhexanoate $Sn(Oct)_2$ is the most commonly used catalyst for the preparation of polylactides for medical applications [25, 126-129]. This catalyst not only has good polymerization properties but it is also accepted by Food and Drug Administration (FDA) as a food additive and it is the catalyst of choice for biomedical applications.

The bulk polymerization of lactide using $Sn(Oct)_2$ in the presence of water or alcohol as an initiator at relatively high temperature (110-220 ºC) is the classic method for preparing poly(lactic acid). Scheme 4 and Figure 12 show the ROP of CF_3-functionalized lactide monomer at 110 °C using $Sn(Oct)_2$ and benzyl alcohol as the initiator alcohol due to (i) its low volatility at around the chosen temperature range, (ii) benzyl ^{1}H-NMR signal at δ 7.4 ppm can be used to estimate the conversion and degree of polymerization and (iii) by removing the benzyl protecting group with H_2/Pd, the resulting polymer would be suitable for further functionalization using its reactive carboxylic acid end group [35].

Figures 13 and 14 show the ^{1}H-NMR and ^{13}C-NMR spectra of the CF_3-functionalized poly(lactic acid). Replacing the methyl group of lactide with a trifluoromethyl group did not significantly affect the polymerization rate of the functionalized monomer. The molecular weights of the substituted polymers were determined by end group analysis using ^{1}H-NMR. The signals from both MALS and DRI detectors in the gel permeation chromatography (GPC) method using THF as an eluent were too weak to obtain the molecular weight of the polymer. In addition, ^{19}F NMR spectra of both the CF_3-substituted monomer and the polymer are shown in Figure 15. We

observed Peak broadening in the polymer spectrum, which indicates a distribution of polymer chains with various molecular weights.

2.3. ESCA analysis

The XPS wide scan spectrum of the CF_3-functionalized poly(lactic acid) is shown in Figure 16 (top). In addition to C and O peaks, the F 1s peak is also present in the spectrum and no additional elements were detected. A C1s high resolution XPS spectrum (HRXPS) of CF_3-functionalized poly(lactic acid) is also presented in Figure 16 (bottom). After spectral resolution into component Gaussian peaks, we can see that the spectral envelop is comprised of four primary C peaks: (1) a 285.0 eV peak corresponding to carbon with three bonds to hydrogen (CH_3, hydrocarbons), (2) a 288.2 eV peak corresponding to carbon with one bond to oxygen (C-O, this peak is usually at 286.5 eV and due to the proximity of the CF_3 it shifted to higher binding energy: inductive effect), (3) a 289.9 eV peak corresponding to carbons with three bonds to oxygen (O=C–O) and a 293.5 eV peak corresponding to C-F_3. The surface chemical composition of PLA and PLA-F have been also calculated. The PLA films have about 62% of carbon and 38% of oxygen, a C/O ratio of 1.6 (O/C ratio of 0.6) with no other detectable elements. Whereas, PLA-F has 51.3 % of carbon, 28.9 % of oxygen and about 19.8% of fluorine with C/O ratio of 1.8.

2.4. Contact angles

Contact angle is an important parameter related to surface energetics, which has been commonly used to evaluate the hydrophobicity of a solid surface. Higher contact angle reflects higher hydrophobicity and lower surface energy [130-134]. We used the sessile drop technique to

measure the contact angle of CF_3-functionalized poly(lactic acid). The resulting static contact angles are shown in Figure 17 and were compared to the contact angle of the smooth polytetrafluoroethylene (PTFE) sheet. We observed significant differences in contact angles between CF_3-functionalized poly(lactic acid) as compared with other samples studied here. As expected, smooth PTFE sheet has the highest hydrophobicity with contact angle: 102±1.8°. The contact angle of the CF_3-functionalized poly(lactic acid) increased to 88.2±1.5º as compared to PLA (contact angle: 70±1.3º). This noticeable increase in the contact angle of the CF_3-functionalized poly(lactic acid) was expected with the introduction of the fluorine in PLA-F structure. Previous studies with perfluoro compounds also reported reduced surface energies, which allows only weak interaction between the surface and liquid [53, 67, 135-137]. The presence of the inert trifluoromethyl groups is responsible for these observations [138-141].

2.5. *In vitro* assessments of cytotoxicity

To evaluate the cytotoxicity of the CF_3-functionalized poly(lactic acid) and to determine if harmful products were leaching out from the polymer, conditioned medium was prepared by incubating samples in cell culture media according to ISO 10993-5. Then NIH-3T3 fibroblast cells were incubated with these material extracts. At designated times, the media was removed and cytotoxicity of the samples was evaluated by comparing with the metabolic activity of cells treated with latex extracts as a positive control using the MTT assay. MTT is a yellow tetrazolium salt that is reduced to form violet formazan crystals only in metabolically active cell mitochondria allowing us to quantify the number of living cells by a spectrophotometrically method. The results were normalized with respect to the negative controls (TCPS) that were not treated with any agents (Figure 18). There was no adverse effect on the metabolic activity of

fibroblast cells treated with sample extracts and their MTT level was always above the 70% toxicity limit defined by ISO 10993-5.

LIVE/DEAD cytotoxicity assay was also performed to test the membrane integrity of the cells treated with sample eluents. In this method we used two fluorescent components: Calcein AM (component A) and ethidium homodimer-1 (EthD-1) (component B). Calcein AM is a virtually nonfluorescent cell-permeant dye that converts to the intensely green fluorescent calcein in live cells by the presence of adequate esterase activity. Whereas, EthD-1 binds to the nucleic acid of dead cells, producing a bright red fluorescence. EthD-1 cannot enter live cells with the intact plasma membrane. Both components are virtually non-fluorescent before interacting with cells. Representative LIVE/DEAD fluorescent microscopy images of the NIH 3T3 fibroblast cells that were incubated with samples extracts over the course of 72 h are shown in Figure 19. Cell morphology was normal at all time points and with respect to the total number of cells, very few dead (i.e., red) cells could be observed in all samples except the positive control latex that is known to be cytotoxic. Likewise, most cells stained green, indicating low level of toxicity from the samples extracts. The MTT assay supported the LIVE/DEAD data. PLA devices were approved by the FDA for direct contact with biological fluids as early as 1970's [79] and are considered to be non-toxic [27, 80, 81]. Comparing and contrasting the results obtained from both MTT and LIVE/DEAD staining assays shows the similar nontoxic nature of the CF_3-functionalized poly(lactic acid).

2.7. Protein adsorption

2.6.1. Protein adsorption from pure protein solutions

The adsorption of human serum Alb and Fg onto the polymer coated coverslips and the 316 SS from a pure Alb (0.3 mg/ml) and Fg (0.03 mg/ml) solution in cPBSzI are shown in Figures 20 and 21. The Alb and Fg concentrations were chosen to correspond to the concentration of these proteins in 1% human plasma [86, 87]. At the end of a 2 h adsorption time, both F-PLA and PVDF-HFP adsorbed relatively higher amount of Alb than other samples. The Alb adsorption decreased in the order of F-PLA and PVDF-HFP > PLA > 316 SS. After incubation with 2% SDS, higher amounts of Alb were retained on both F-PLA and PVDF-HFP as compared to PLA and 316 SS. Statistically significant higher amounts of albumin was adsorbed and retained on both F-PLA and PVDF-HFP as compared to all other materials studied ($\alpha = 0.05$). There was no statistically significant difference between the Alb adsorption and retention between F-PLA and PVDF-HFP.

Similar adsorption and retention trends were observed for pure Fg solution in cPBSzI with relatively greater amount of adsorbed and retained Fg on PVDF-HFP. The Fg adsorption decreased in the order of PVDF-HFP > F-PLA > PLA > 316 SS. Once again, both F-PLA and PVDF-HFP retained relatively higher amounts of Fg after elution with 2 % SDS.

2.6.2. Protein adsorption from binary/competitive protein solutions

The adsorption and retention of Alb and Fg onto the polymer coated coverslips and the 316 SS from binary/competitive protein solutions is shown in Figure 22. To make these binary solutions, we prepared two identical solutions containing both Alb and Fg in PBS based on the 1 % protein ratios observed in normal human blood plasma (Alb: 0.3 mg/ml and Fg: 0.03 mg/ml). Nest radiolabeled Alb was added to one solution and radiolabeled Fg to the other.

The Alb adsorption and retention trend in binary solutions was similar to the trend observed in pure protein solutions. Alb adsorption was in the range of 22-86 ng/cm^2 and once again F-PLA and PVDF-HFP both adsorbed and retained the higher amount of Alb as compared to PLA and 316 SS. Only a negligible amount of Alb (less than 3 ng/cm^2) was retained on these samples after elution with 2% SDS.

In the case of Fg, protein adsorption from an Alb-Fg binary protein solution was highest on PVDF-HFP (85 ng/cm^2) and F-PLA (83 ng/cm^2) and decreased in the order of: PVDF-HFP > PLA-F > PLA > 316 SS. When both albumin and fibrinogen are present in the solution, samples overall adsorbed less Fg than from a pure Fg protein solution. The amount of the retained Fg after elution with 2% SDS was similar to the trend observed with retained Fg from pure protein solution. The highest amount of retained Fg was once again greater on PVDF-HFP (22 ng/cm^2) and F-PLA (20 ng/cm^2) and decreased in the same order as Fg adsorption.

In both cases, the amount of retained protein after elution with 2% SDS was statistically higher on F-PLA and PVDF-HFP than on all other samples tested here.

2.6.3. Protein adsorption from normal human plasma

Blood is a complex fluid and contains more than 300 different proteins. To mimic the complex protein solutions that these surfaces might come into contact *in vivo*, we measured the protein adsorption onto these surfaces in 1% citrated pooled human plasma (Figure 23). Human blood was drawn following the procedure described earlier and plasma was collected after removing blood cells by two step centrifugations and diluted to 1 % plasma by adding cPBSz buffer.

Overall, the amount of adsorbed Alb and Fg from human plasma was noticeably lower than those measured in pure and binary protein solutions. All samples had higher Alb adsorption than Fg

except 316 SS. In addition, F-PLA and PVDF-HFP both adsorbed statistically higher amount of Alb as compared to PLA and 316 SS.

Figure 24 Shows the protein retention after elution with 2% SDS. Once again, a statistically higher amount of both Alb and Fg were retained on the PVDF-HFP (Alb: 13 ng/cm^2, Fg: 14 ng/cm^2) and F-PLA (Alb: 11 ng/cm^2, Fg: 10 ng/cm^2) as compared to PLA and 316 SS. Of all the samples, 316SS retained the least adsorbed protein with marginally higher amount of Alb than Fg.

The Alb/Fg ratio of the adsorbed and retained proteins from 1% human plasma is shown in table I. The Alb/Fg protein adsorption ratios ranged from 0.8 to 1.7, with the highest value for F-PLA. Upon elution with 2 % SDS, the Alb/Fg ratio changed for all the surfaces and ranged from 0.92 to 1.44. Protein adsorption from blood plasma provides a more holistic view of the relative affinity of surfaces for a specific protein competing with other proteins in a complex mixture of human plasma. When protein adsorption was measured from pure, binary and 1% plasma protein solutions, PLA and 316 SS had the lowest adsorbed and retained Alb and Fg. On the other hand, F-PLA and PVDF-HFP had the highest amount of protein adsorption and retention after incubating with 2% SDS.

Our observation of protein adsorption and retention on fluorinated surfaces is consistent with the previous studies which reported the higher retention of proteins on these surfaces [11, 18, 89]. Fluorinated materials have been approved for use in various blood-contacting applications due to their satisfactory clinical performance [56, 90-93].

Although there is a no universal guidelines for blood compatibility evaluation of synthetic materials, studies are generally focused on blood plasma protein adsorption, platelet interaction and intrinsic pathway activation [8, 61, 94-101, 142]. Protein adsorption at biomaterials surfaces

is considered as the initial event after implantation and considered central to the ultimate outcome. Protein adsorption depends on the physiochemical properties of both proteins and surfaces. Upon contact, proteins from plasma can be adsorbed to the biomaterials surface in the order of seconds and form a 2-10 nm monolayer, resulting in a high concentration of the proteins at interface as compared to their concentrations in plasma [87, 102, 103]. The current research focuses on the interaction of two distinct blood plasma proteins, albumin and fibrinogen, with the newly developed fluoropolymer surfaces. Albumin is the most abundant blood protein (concentration: 35-50 mg/ml) and has high affinity for circulating free fatty acids. It been shown that highly hydrophobic surfaces can develop a strong interactions with albumin and retain it on their surfaces. This is considered a potentially thromboresistive effect since a preadsorbed layer of albumin inhibits the subsequent adsorption of fibrinogen.

Fg (concentration: 2-4.5 mg/ml) has been shown to play a key role in initiating coagulation and adsorbed Fg, even at low levels, can trigger platelet adhesion and activation [17, 104-109].

According to the albumin passivation theory, a confluent, preadsorbed layer of albumin on biomaterials surfaces can decrease the subsequent adhesion of fibrinogen and reduce the *in vitro* platelet adhesion resulting in potentially less thrombogenic surfaces [110, 111]. Two mechanisms were proposed to explain the passivation effect of adsorbed albumin layer: (1) blockage of surface active sites that prevents surface contact-initiating step, and (2) complexing of the surface-bound albumin with surface contact-activated materials such as plasma proteins [143]. We have modified this hypothesis and introduced the Alb/Fg ratio to include the fibrinogen adsorption in competition with albumin. Earlier studies suggest that a high Alb/Fg ratio contributes to improved hemocompatibility of polymer surfaces [88]. Also, the high albumin retention known as “albumin tight binding” should be taken into consideration in order

to consider a more comprehensive view of the events at blood biomaterial interfaces. This is particularly important since protein adsorption from blood plasma involves a complex series of adsorption and displacement steps known as the “Vroman effect”. This competitive protein exchange is a general phenomenon and occurs when a protein mixture adsorbs to a surface and then these early adsorbers are subsequently displaced by high affinity binding proteins that are present in the solution. The high retention of albumin on fluorinated surfaces indicates the tendency of these to resist the displacement of albumin by fibrinogen [144-146].

3. Conclusions

In this chapter, we have developed a novel method for preparing CF3-functionalized poly(lactic acid). First, we synthesized the CF3-functionalized monomer and then adopted the ROP to prepare the subsequent polymer. As expected the resulting polymer showed higher hydrophobicity relative to unmodified PLA. There was no sign of cytotoxicity from material extracts as confirmed by both MTT and LIVE/DEAD staining methods on NIH-3T3 mouse fibroblast cells.

This approach can potentially extend the range of physiochemical properties and biomedical applications of polylactides. Further optimization of the reaction and the development of effective purification techniques will enable us to obtain polymer in higher molecular weights. In addition, our ongoing studies are aimed at investigating the physiochemical properties such as degradability and thermal characteristics. Both PVDF-HFP and CF3-functionalized poly(lactic acid) have been demonstrated to adsorb and retain (after incubation with 2% SDS) higher amount of the albumin and fibrinogen in single and binary protein solutions and plasma. Along with a higher Alb/Fg ratio, we hypothesize that these fluoropolymers will demonstrate enhanced

thromboresistivity in vivo. Additional investigations will be carried out to address the blood compatibility of this new class of degradable polyesters by analyzing platelet interactions under flow conditions.

Figures:

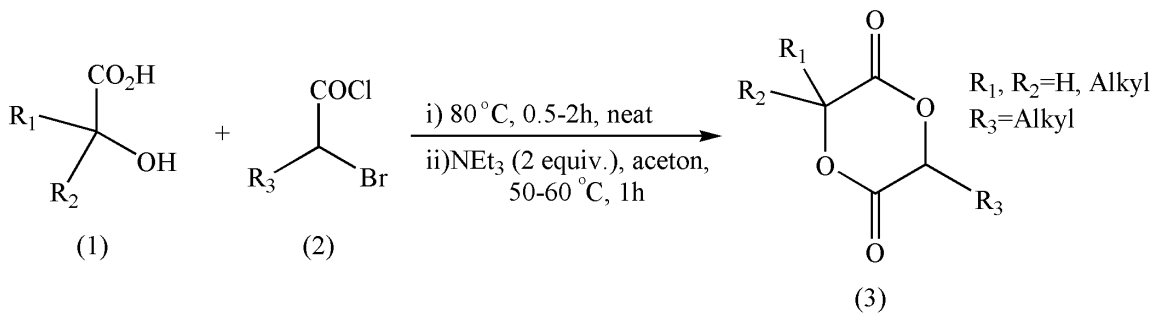

Scheme 1. Synthesis of alkyl-substituted lactide by Schollkopf's method.

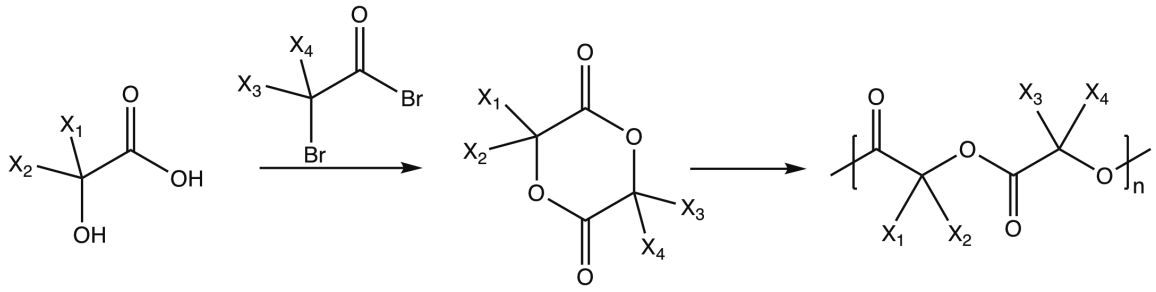

Scheme 2. General synthesis approach of halogen-substituted lactide monomer and subsequent halogenated polymer. At least one of x_1 or x_2 is halogen or halocarbon.

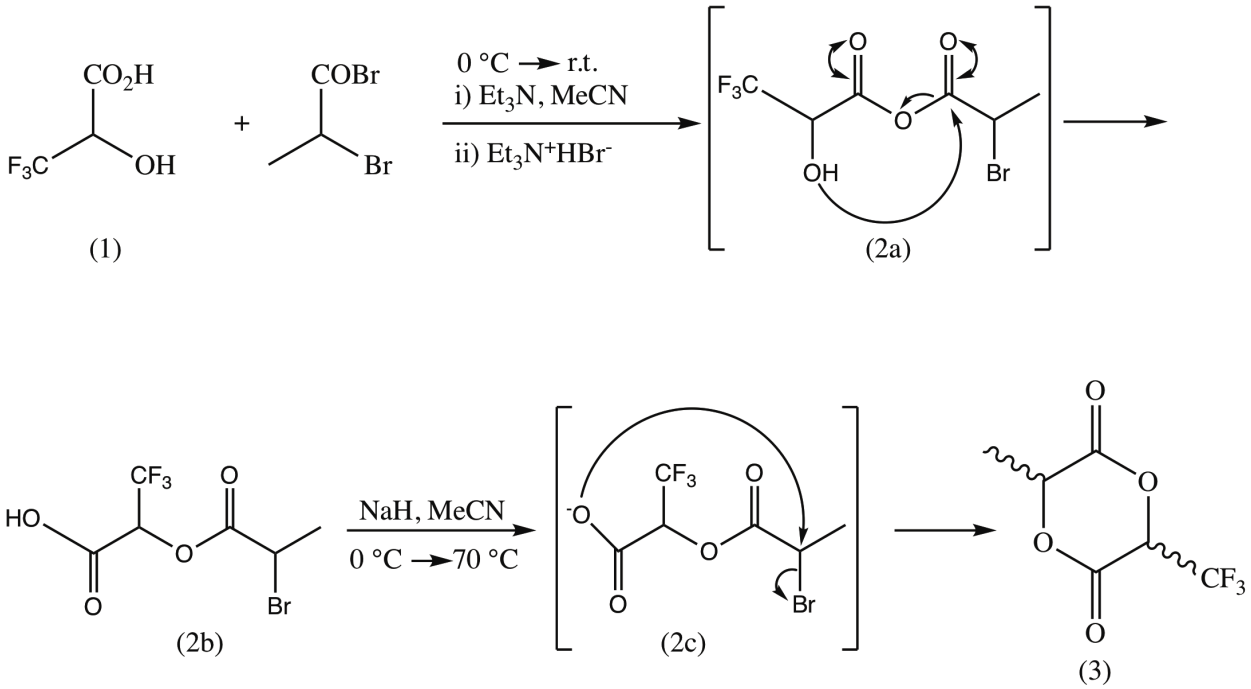

Scheme 3. Preparation of trifluoromethyl-functionalized lactide monomer and proposed cyclocondensation mechanism.

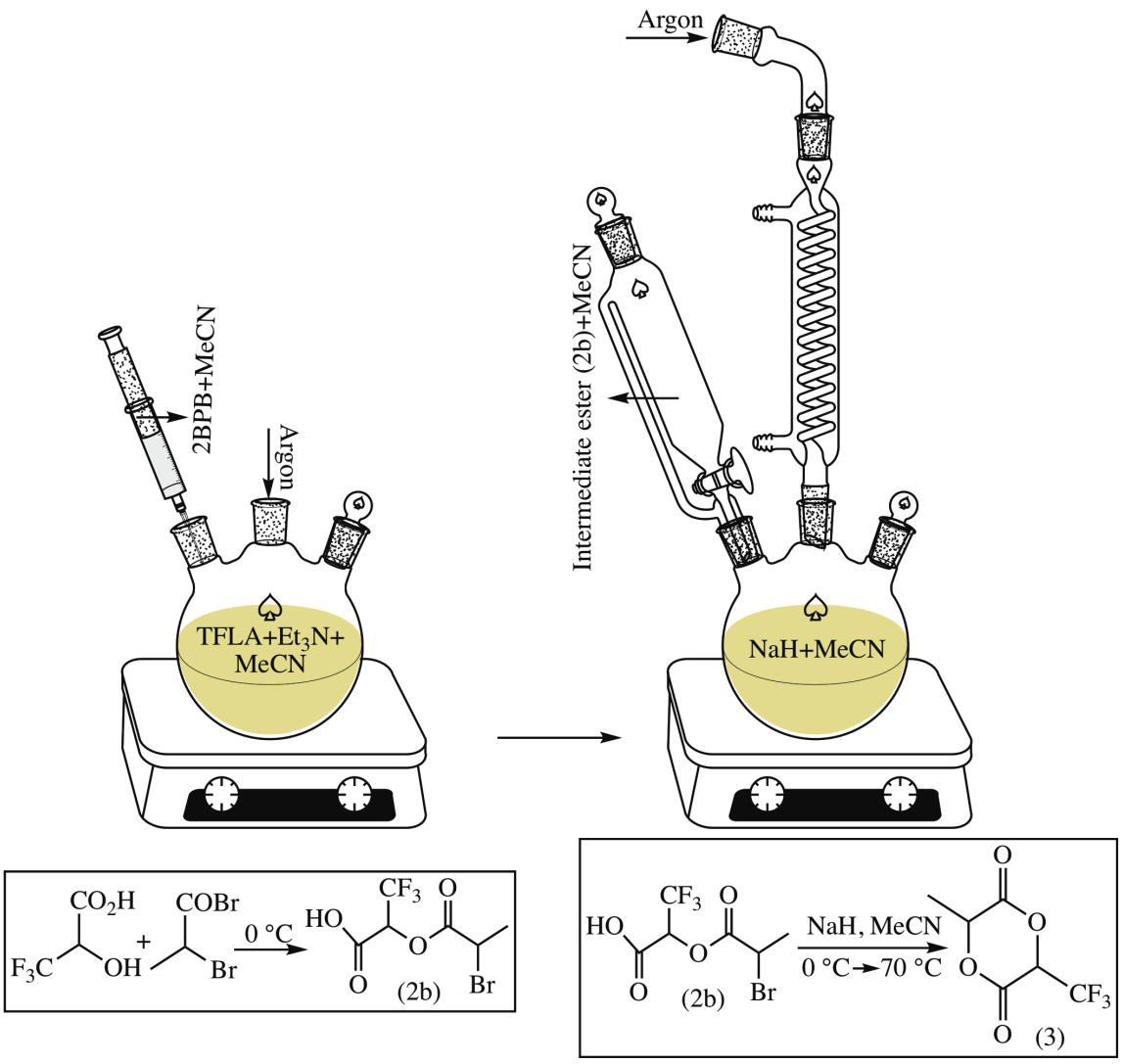

Figure 1. Illustration of the reaction setup and synthesis conditions used for preparing trifluoromethyl-functionalized lactide monomer.

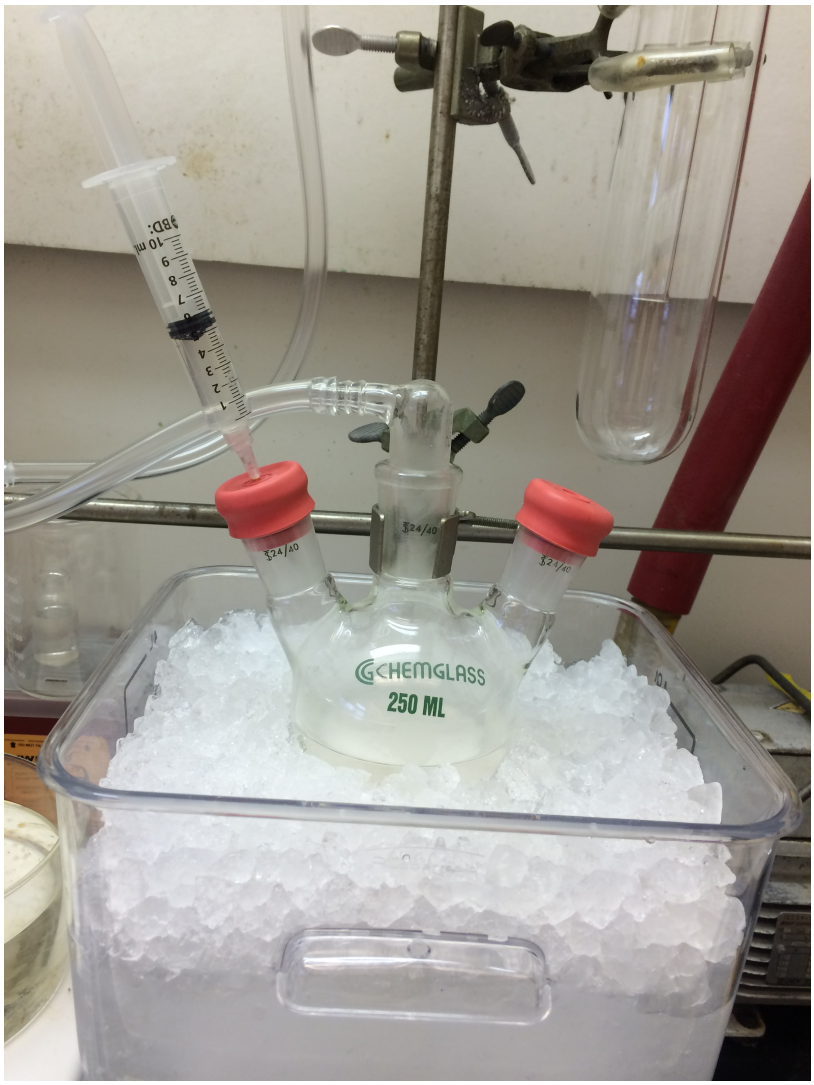

Figure 2. Apparatus for synthesis of trifluoromethyl-functionalized lactide monomer (dropwise addition of 2BPB).

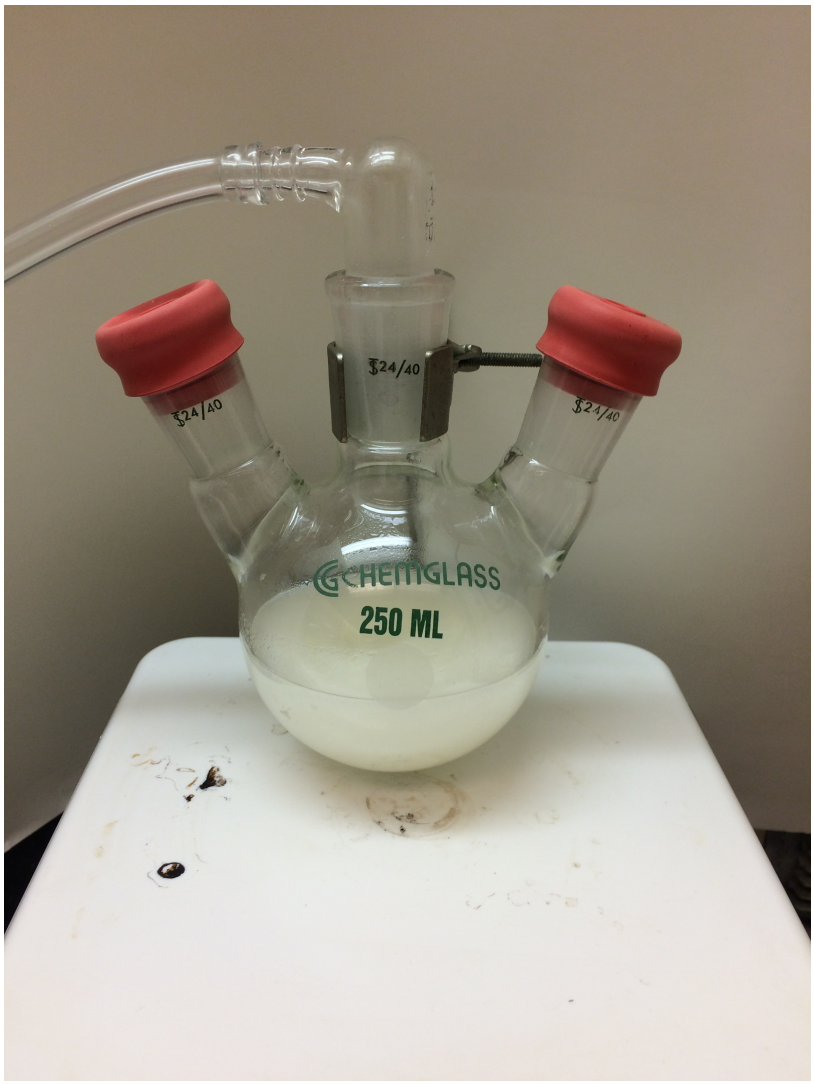

Figure 3. Apparatus for synthesis of trifluoromethyl-functionalized lactide monomer (stirring at room temperature).

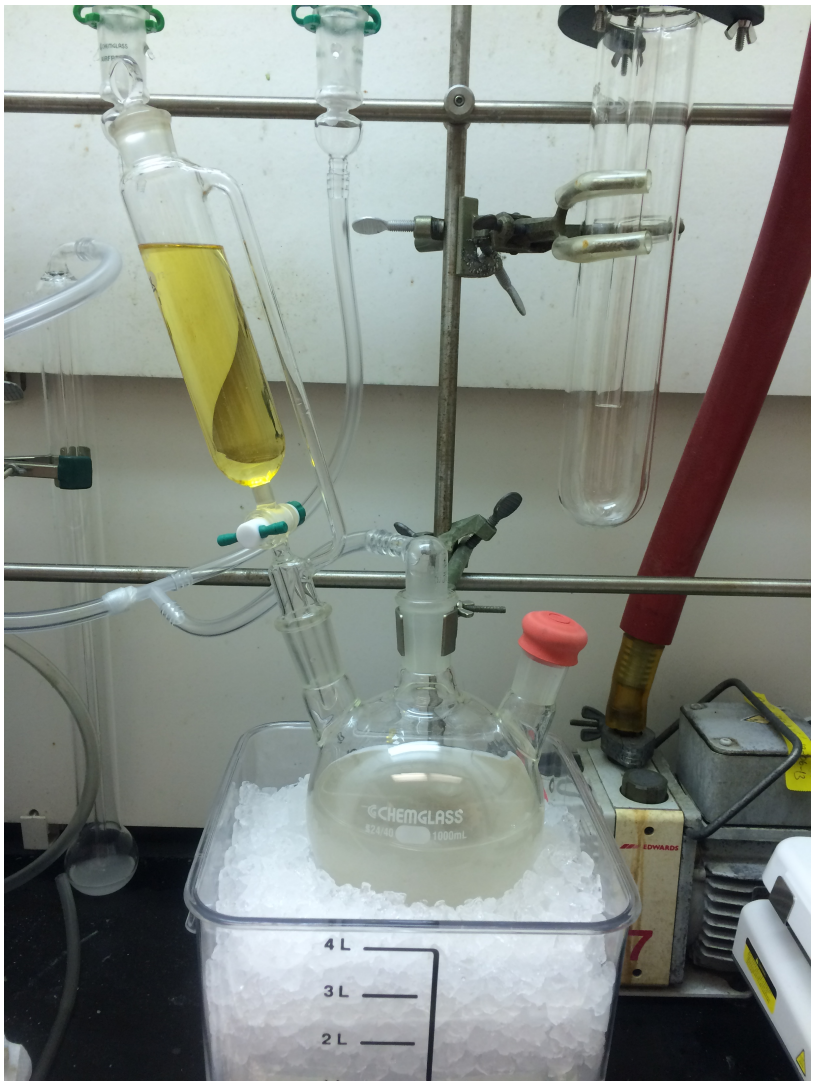

Figure 4. Apparatus for synthesis of trifluoromethyl-functionalized lactide monomer (dropwise addition of intermediate ester 2 to the acetonitrile and sodium hydride mixture in round bottom flask).

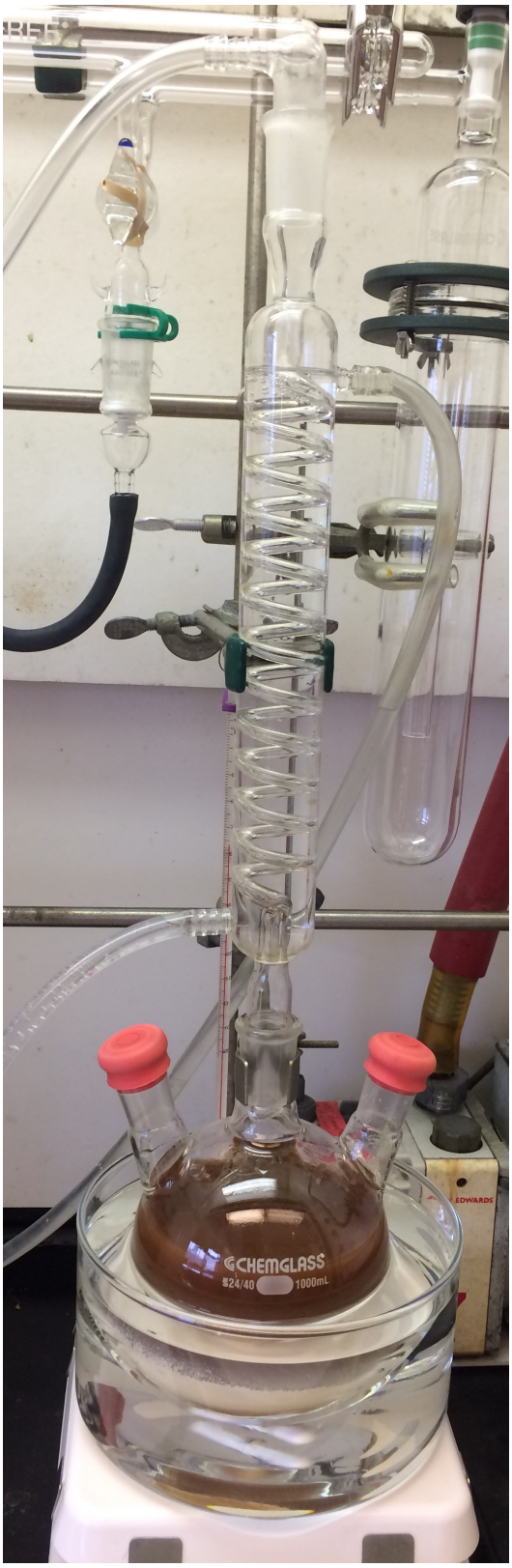

Figure 5. Apparatus for synthesis of trifluoromethyl-functionalized lactide monomer (ring closure).

Figure 6. Apparatus for synthesis of trifluoromethyl-functionalized lactide monomer: (concentration of monomer).

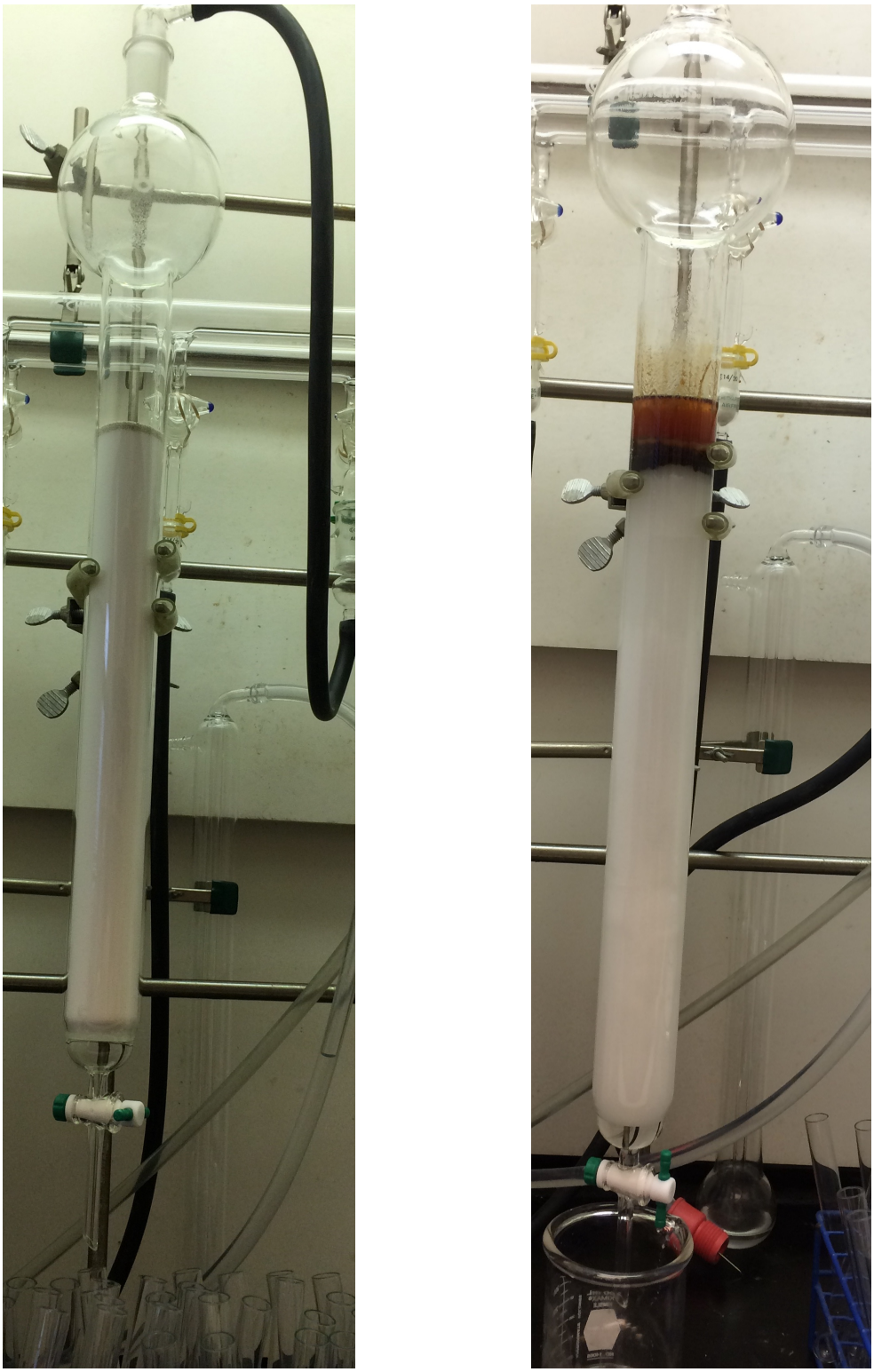

Figure 7. Apparatus for purification of trifluoromethyl-functionalized lactide monomer (column chromatography).

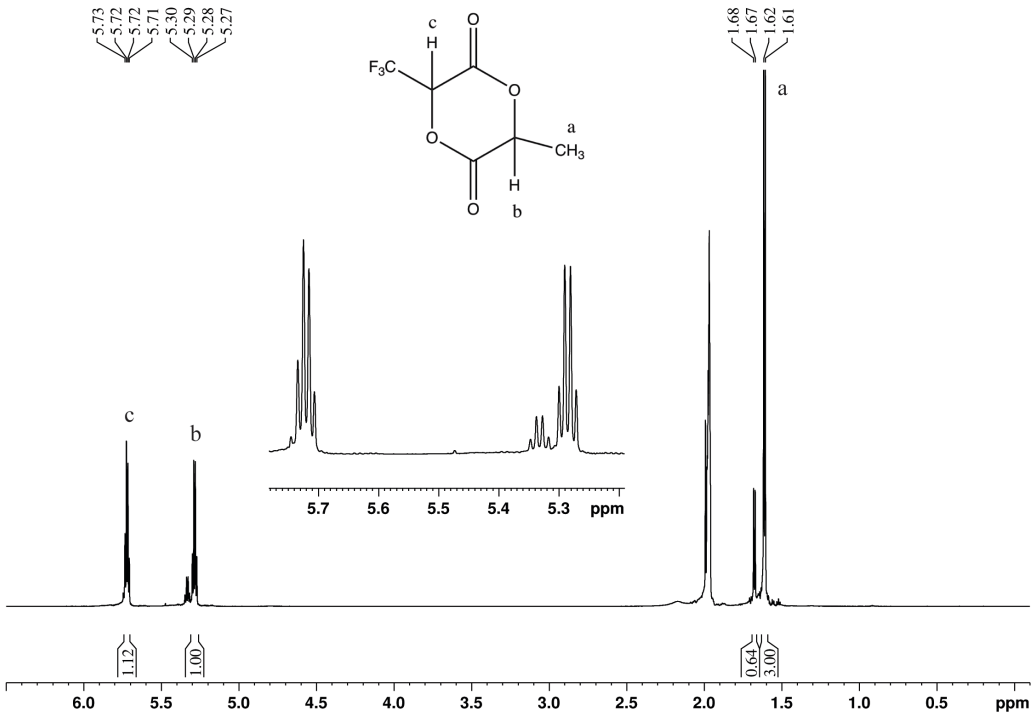

Figure 8. ^{1}H-NMR spectra (700 MHz, CD_3CN) of trifluoromethyl-functionalized lactide monomer.

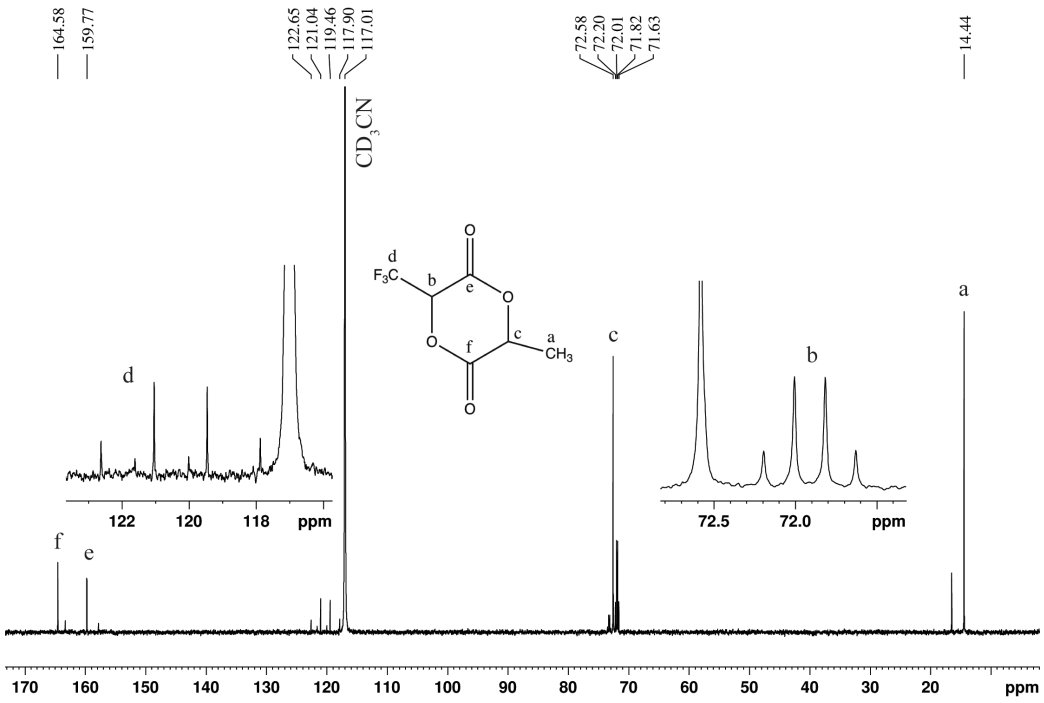

Figure 9. ^{13}C-NMR spectra (700 MHz, CD_3CN) of trifluoromethyl-functionalized lactide monomer.

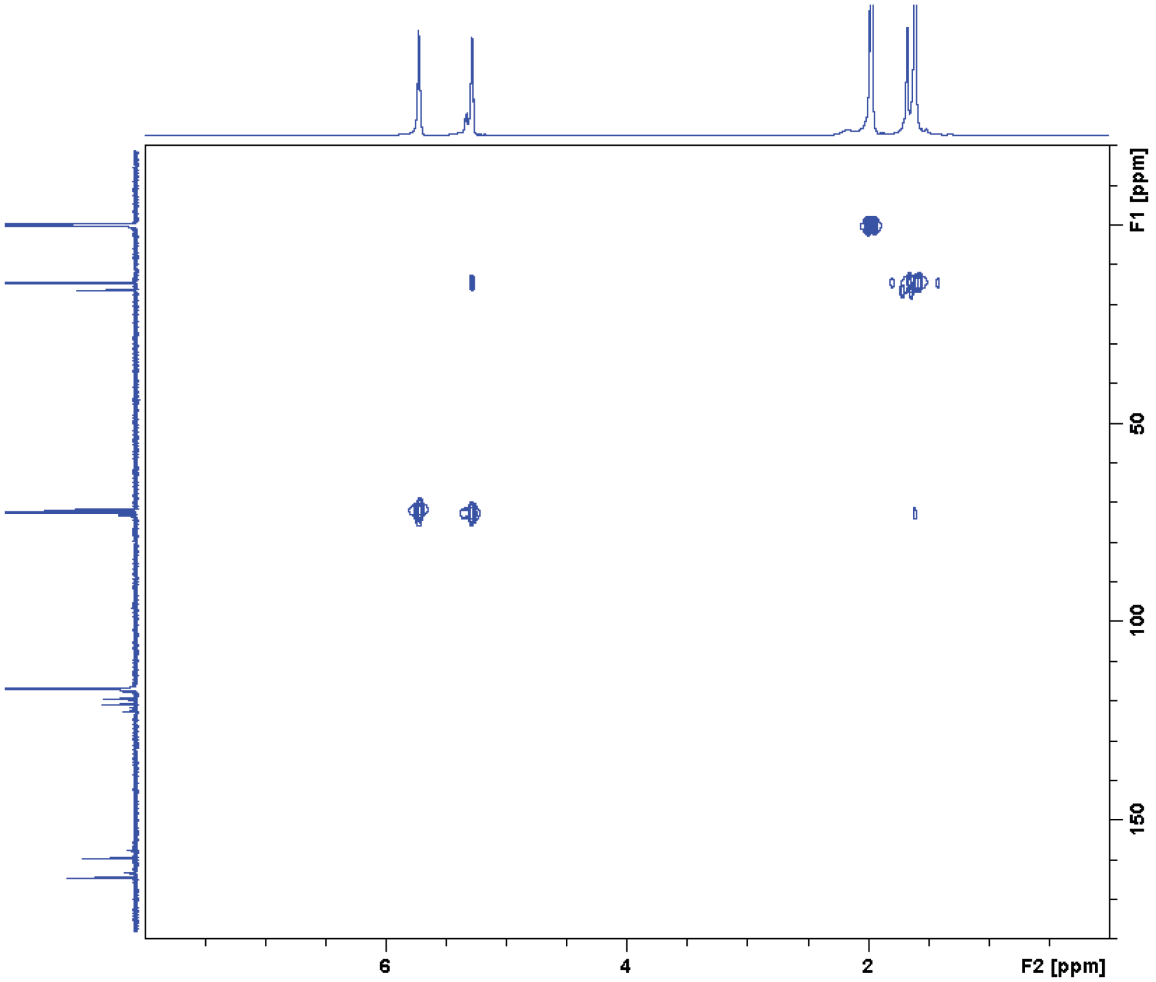

Figure 10. 2D-NMR spectra (700 MHz, CD_3CN) of trifluoromethyl-functionalized lactide monomer.

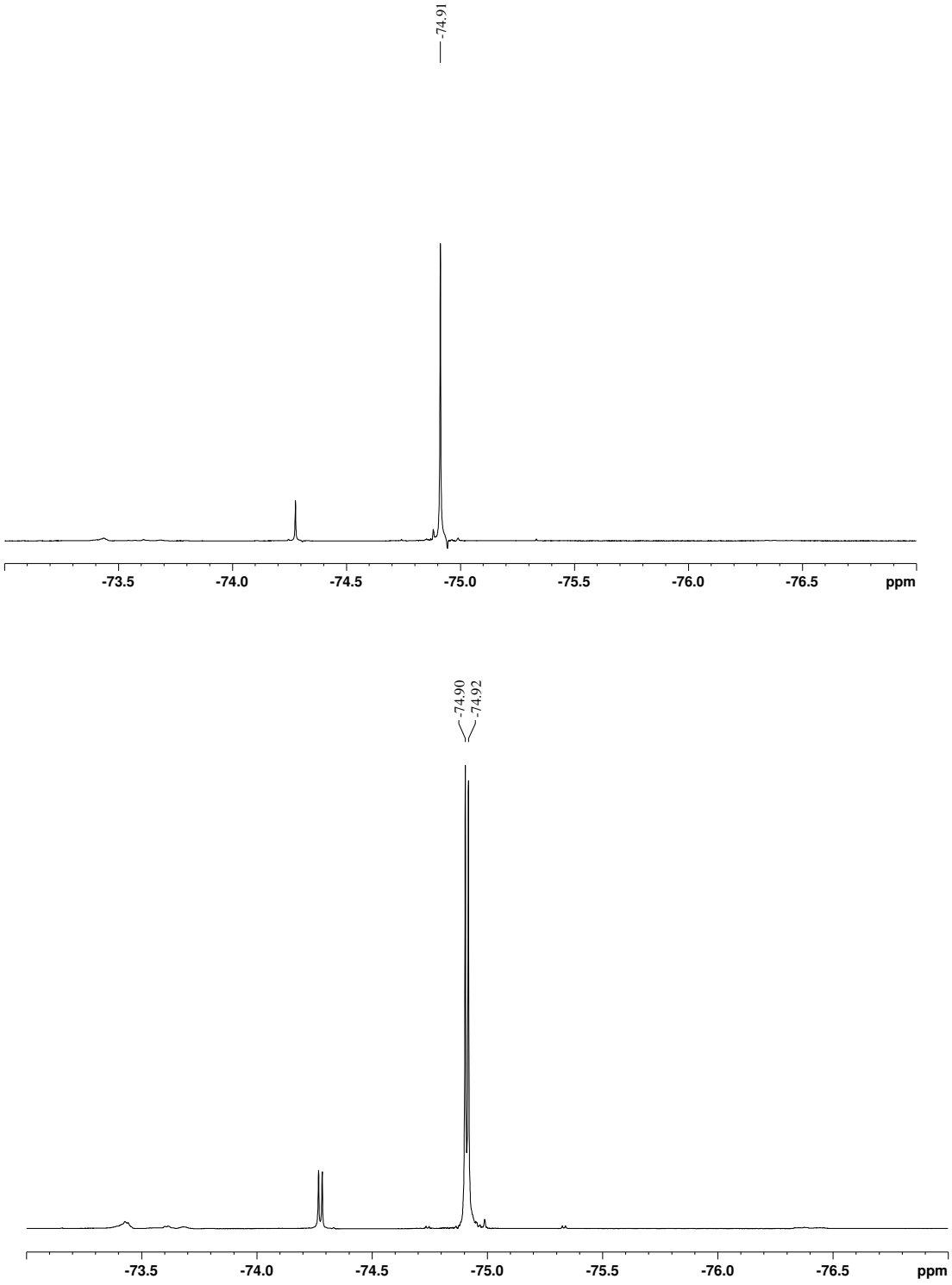

Figure 11. ^{19}F-NMR spectra (500 MHz, CD_3CN) of trifluoromethyl-functionalized lactic acid monomer. Top spectra show the ^{19}F, with ^{1}H decoupling and bottom spectra the ^{19}F, without ^{1}H decoupling.

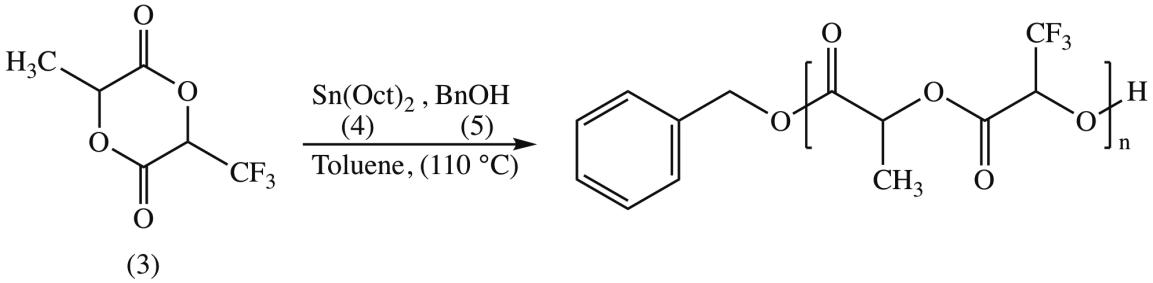

Scheme 4. Ring-opening polymerization of trifluoromethyl-functionalized poly(lactic acid) and polymerization conditions.

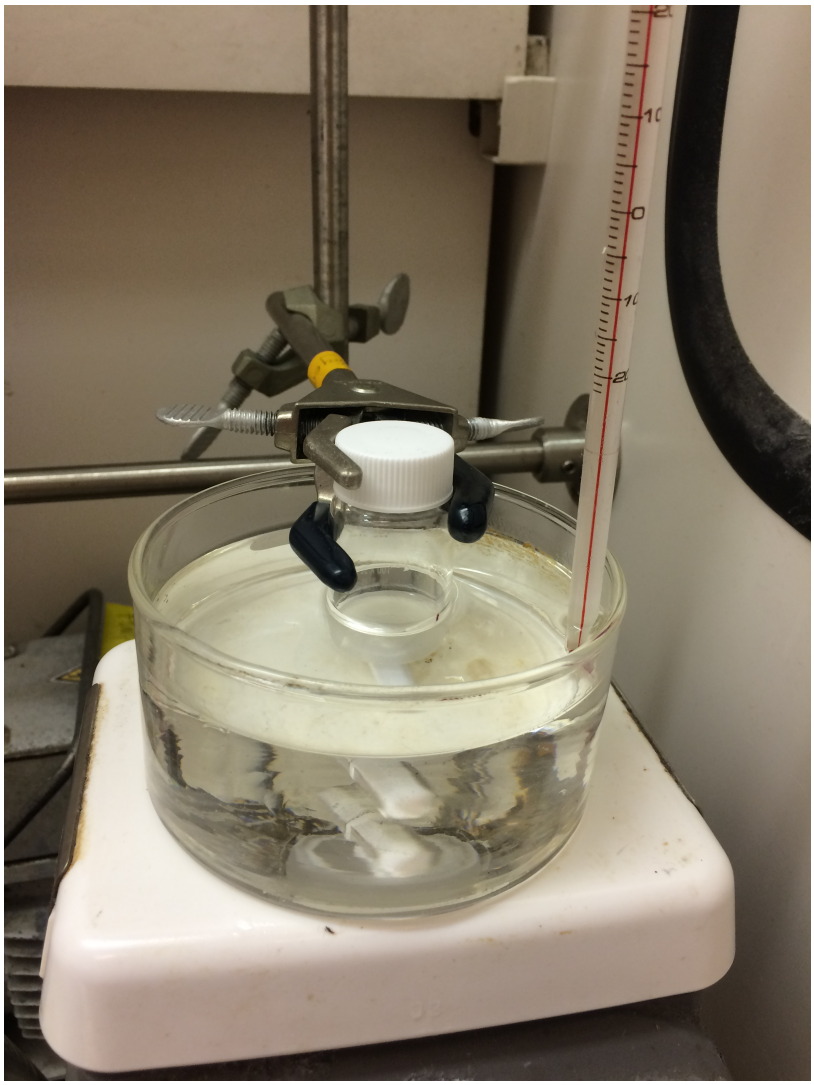

Figure 12. Apparatus for ring-opening polymerization.

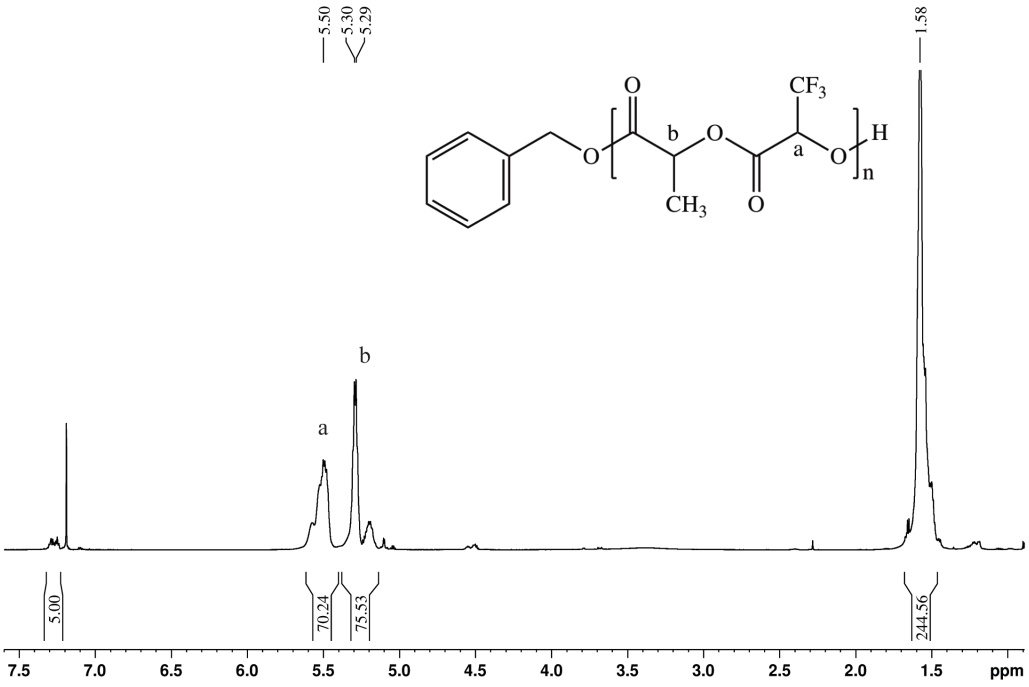

Figure 13. ^{1}H-NMR spectra (700 MHz, $CDCl_3$) of trifluoromethyl-functionalized poly(lactic acid).

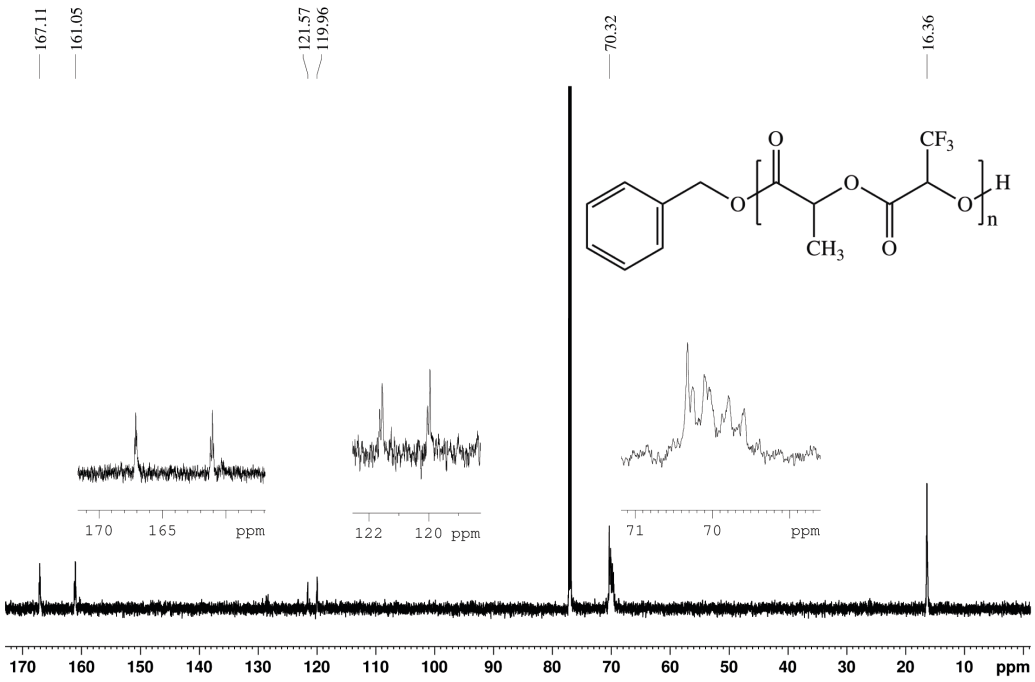

Figure 14. ^{13}C-NMR spectra (700 MHz, $CDCl_3$) of trifluoromethyl-functionalized poly(lactic acid).

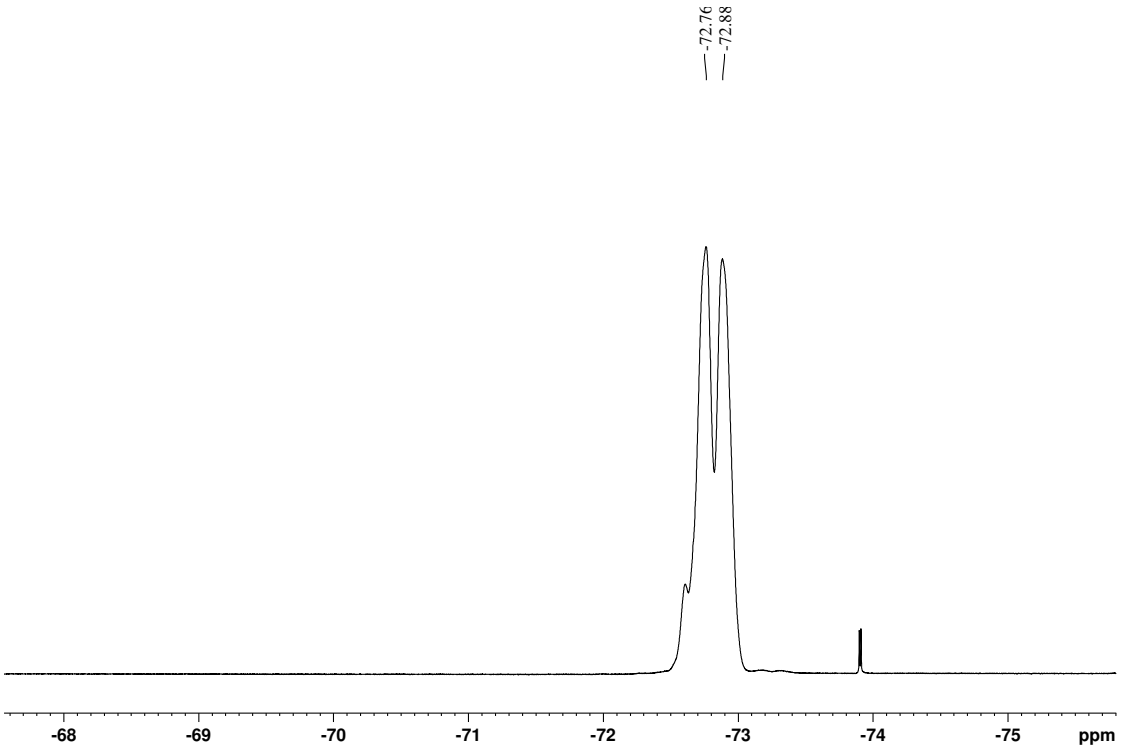

Figure 15. ^{19}F-NMR spectra (500 MHz, $CDCl_3$) of trifluoromethyl-functionalized poly(lactic acid).

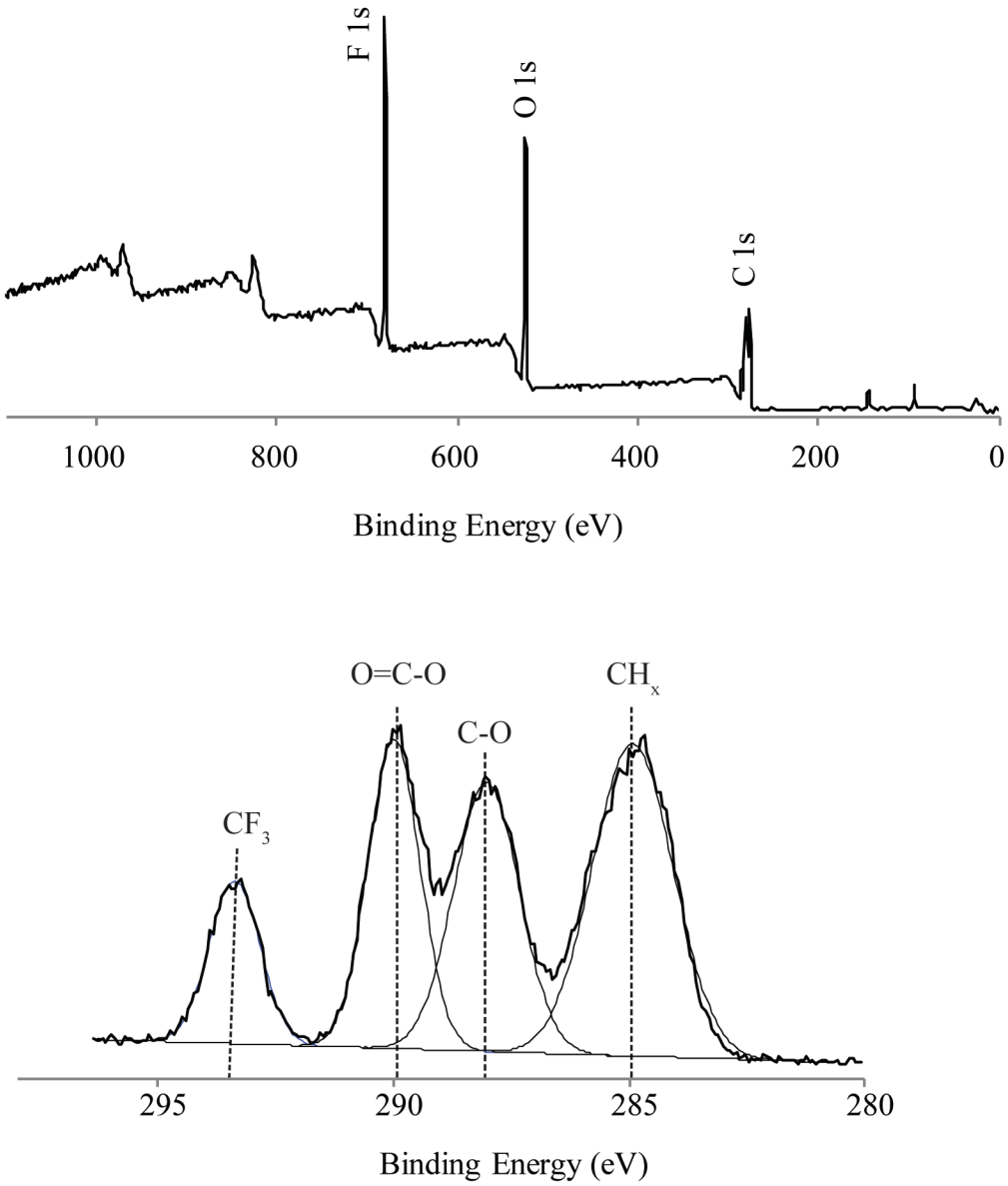

Figure 16. ESCA spectra of trifluoromethyl-functionalized poly(lactic acid) (top) and its high-resolution C1s spectrum and curve fitting (bottom). From left to right, the peaks correspond to CF_3, O=C–O, C–O, and CH_3. In the top wide-scan spectrum. in addition to C1s and O1s peaks, we observed an F1s peak.

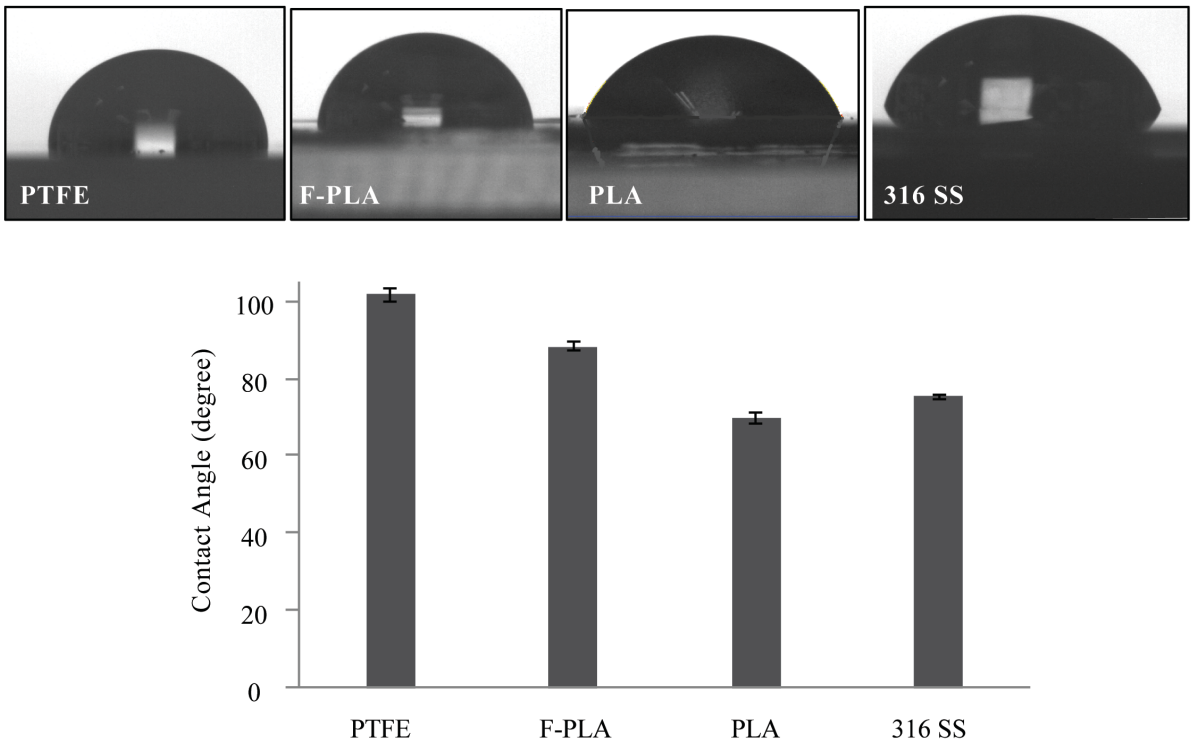

Figure 17. The profiles of water droplets on the surface of trifluoromethyl-functionalized poly(lactic acid) (F-PLA) measured by aqueous sessile drop goniometry and its comparison with PTFE.

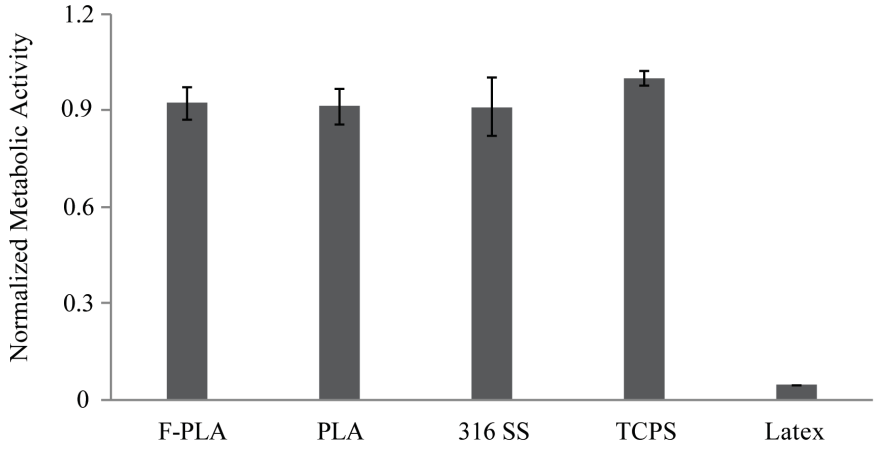

Figure 18. The relative metabolic activity of the NIH-3T3 cells incubated with sample extracts for 24h. The results are normalized with respect to the TCPS's value. Latex and TCPS were used as positive and negative controls, respectively.

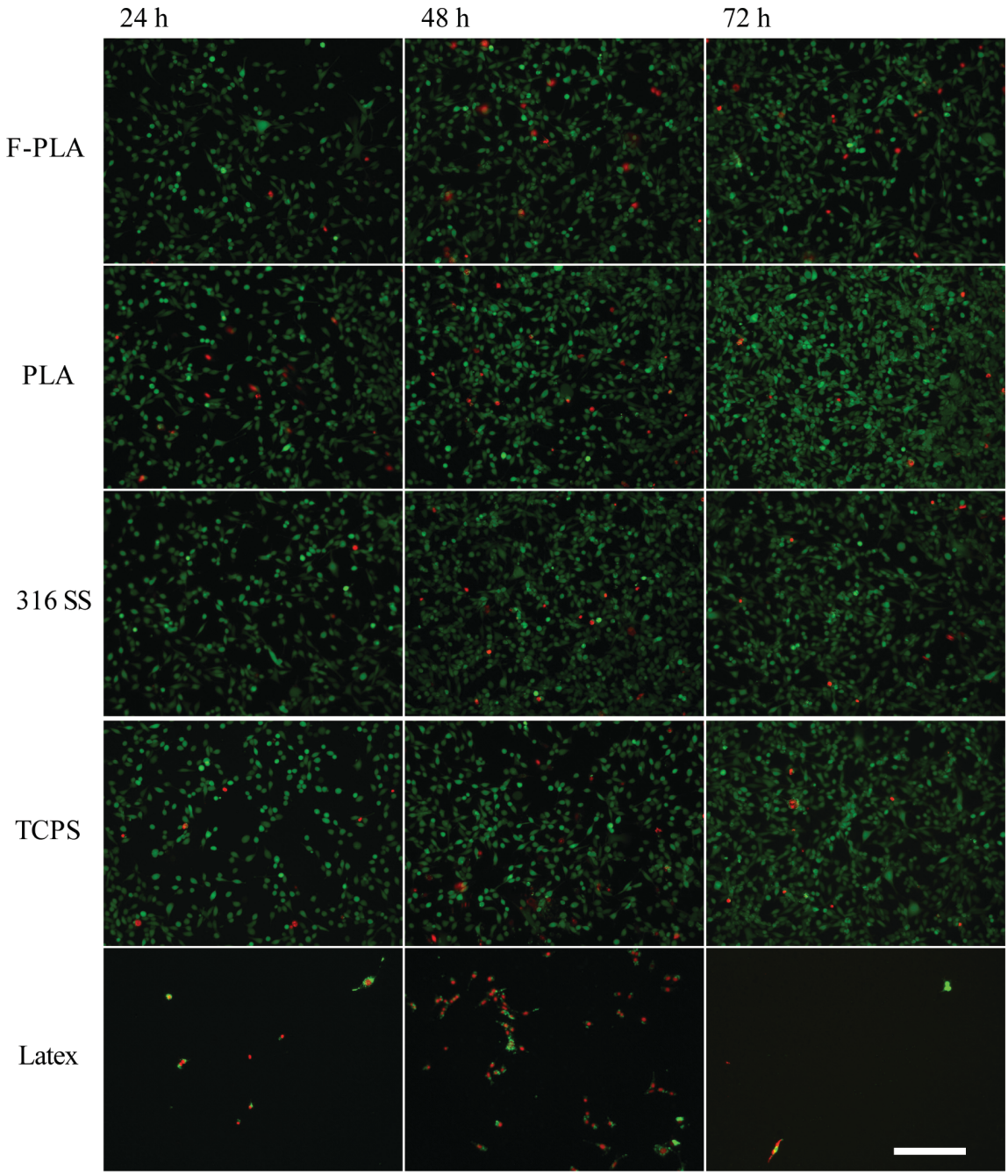

Figure 19. LIVE/DEAD staining of NIH-3T3 cells treated with trifluoromethyl-functionalized poly(lactic acid) extracts and its comparison with positive (latex) and negative (TCPS) controls. Calcein is staining live (green), and propidium iodide is staining dead cells (red). Over the course of 72 h incubation with sample extracts, majority of cells stained green in all the samples tested here except positive control. (Scale bar: 400 μm.)

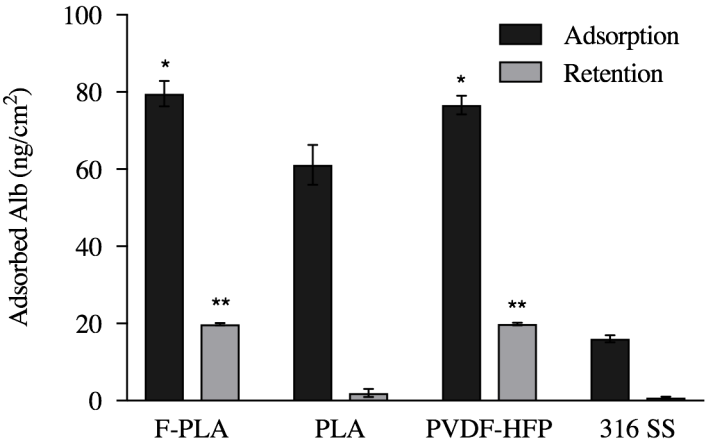

Figure 20. Protein adsorption from a pure Alb solution (0.3 mg/ml) in cPBSzI and the retained Alb on the surfaces after 24 h elution with 2% SDS. Single asterisk (*) shows statistically significant higher amount of adsorbed Alb on both F-PLA and PVDF-HFP as compared to PLA and 316 SS. Double asterisk (**) shows statistically significant higher amount of retained Alb on both F-PLA and PVDF-HFP as compared to all other materials tested ($\alpha \leq 0.05$). There was no statistically significant difference in Alb adsorption and retention between F-PLA and PVDF-HFP. Error bars indicate SEM, n=6.

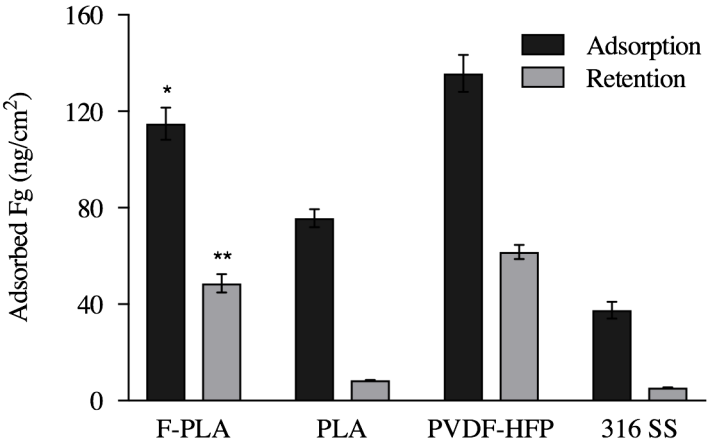

Figure 21. Protein adsorption from a pure Fg solution (0.03 mg/ml) in cPBSzI and the retained Fg on the surfaces after 24 h elution with 2% SDS. Single asterisk (*) and double asterisk (**) show statistically significant difference between the amount of adsorbed and retained Fg on F-PLA as compared to all other materials tested here ($\alpha \leq 0.05$). Error bars indicate SEM, n=6.

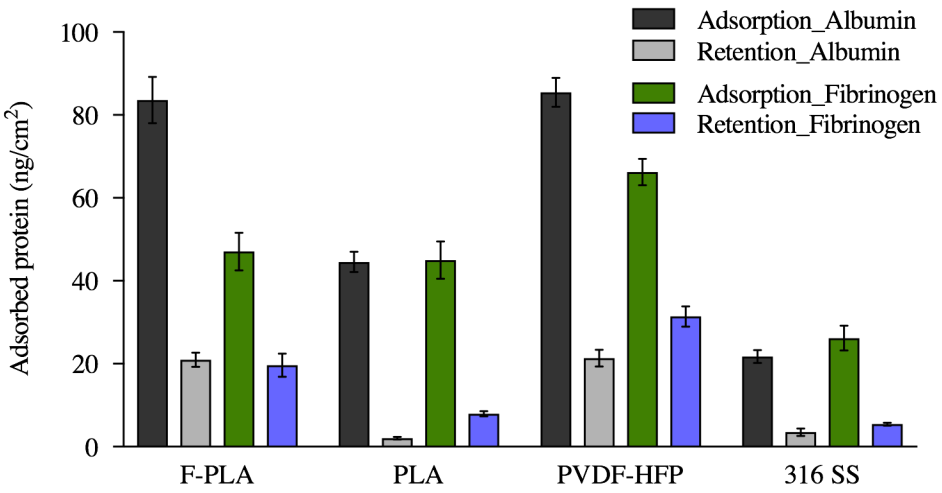

Figure 22. Competitive protein adsorption from binary solution (Alb: 0.3 mg/ml and Fg: 0.03mg/ml). Samples were incubated for 2 h in binary protein solutions in cPBSZI (black and gray). The amount of retained protein on the surfaces was measured after 24 h incubation with 2% SDS (green and blue). There is a statistically significant greater amount of both adsorbed and retained Alb on F-PLA as compared to all other samples except PVDF-HFP. There is a significantly higher amount of retained Fg on both F-PLA and PVDF-HFP as compared to PLA and 316 SS ($\alpha \leq 0.05$). Error bars indicate SEM, n=6.

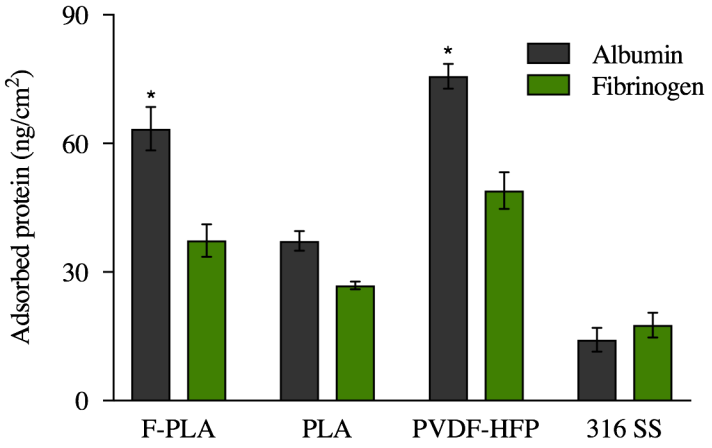

Figure 23. Protein adsorption from 1 % citrated normal human plasma. Black bars represent Alb adsorption and green bars show Fg adsorption. Single asterisk (*) shows statistically significant higher amount of adsorbed Alb on both F-PLA and PVDF-HFP as compared to all other samples ($\alpha \leq 0.05$). Error bars indicate SEM, n=6.

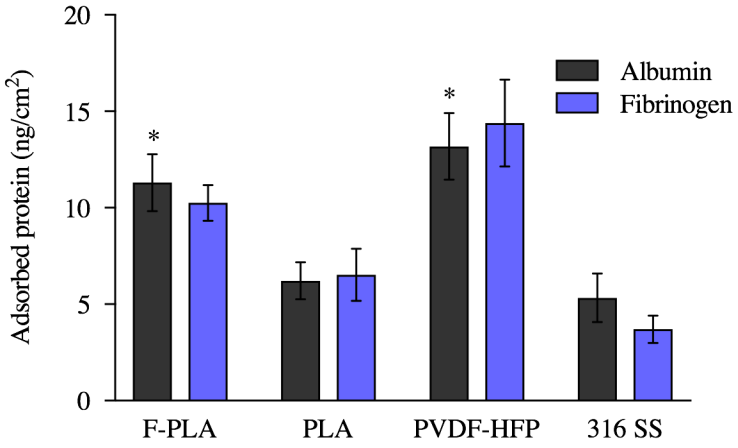

Figure 24. Protein retention from 1 % citrated normal human plasma after 24 h elution with 2% SDS. Retained Alb is shown in black and retained Fg is shown in blue. Single asterisk (*) shows statistically significant higher amount of retained Alb on both F-PLA and PVDF-HFP as compared to PLA and 316 SS ($\alpha \leq 0.05$). Error bars indicate SEM, n=6.

Table I. Alb/Fg ratio of different samples after 2 h adsorption in 1 % citrated normal human plasma and subsequent elution with 2% SDS for 24 h

Sample	Alb/Fg Adsorption	Alb/Fg Retention
F-PLA	1.70	1.10
PLA	1.39	0.95
PVDF-HFP	1.55	0.92
316 SS	0.80	1.44

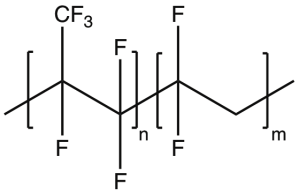

Scheme 5. Polymer structures of PVDF-HFP.

Supporting Information: S1

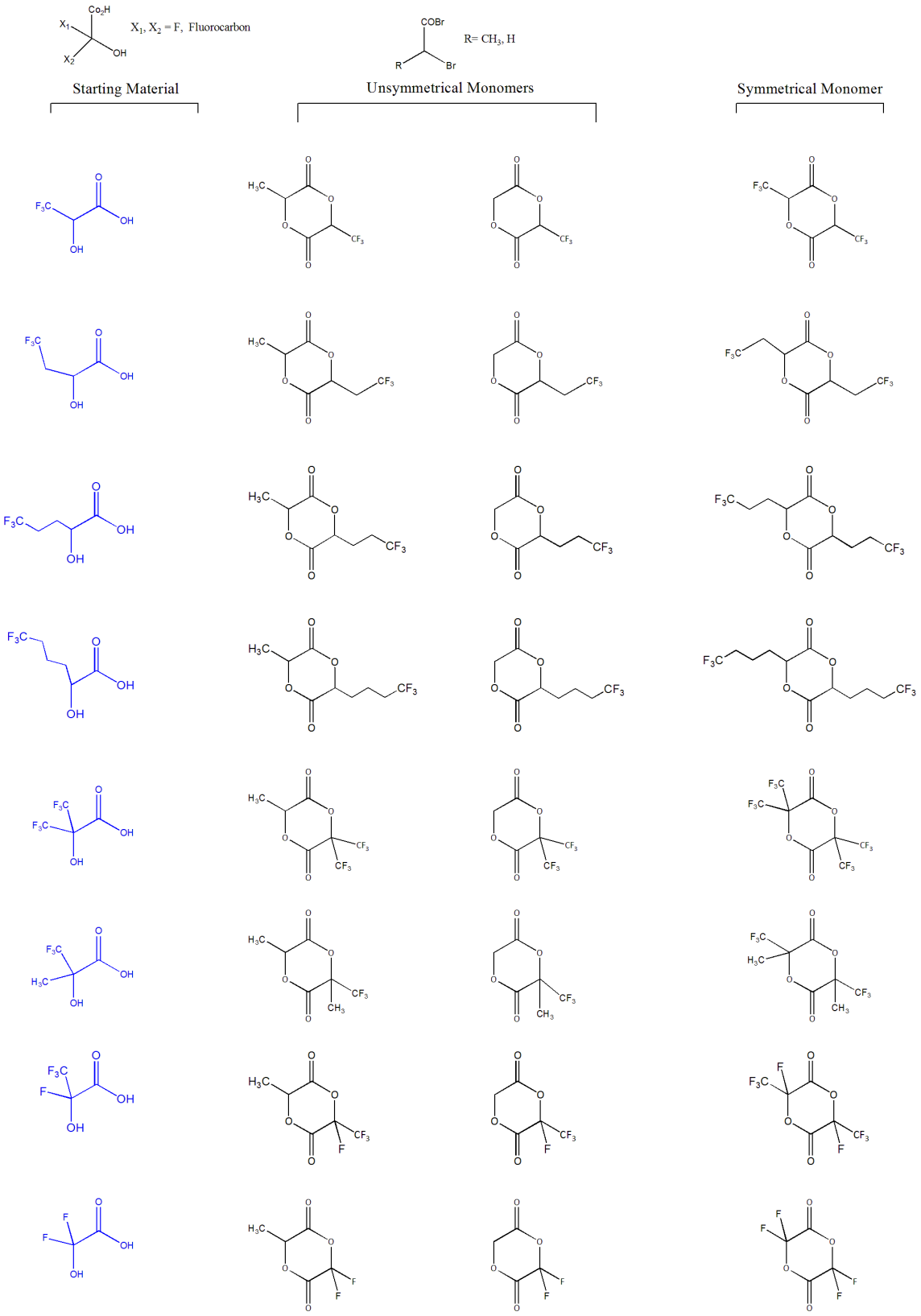

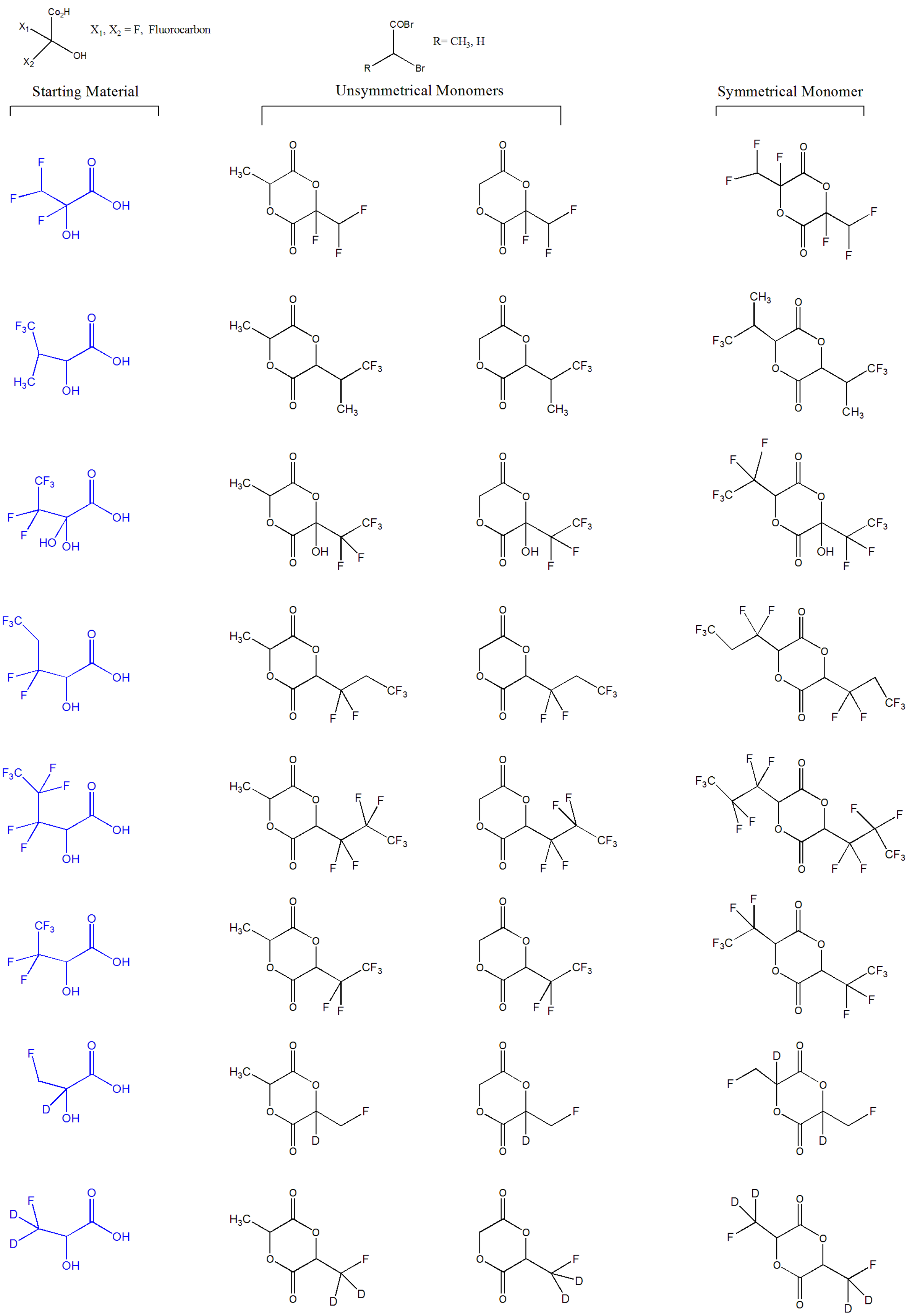
X1, X2 = F, Fluorocarbon
R= CH3, H
Starting Material
Unsymmetrical Monomers
Symmetrical Monomer

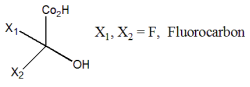

X_1, X_2 = F, Fluorocarbon

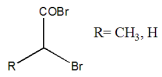

R= CH_3, H

Starting Material | Unsymmetrical Monomers | Symmetrical Monomer

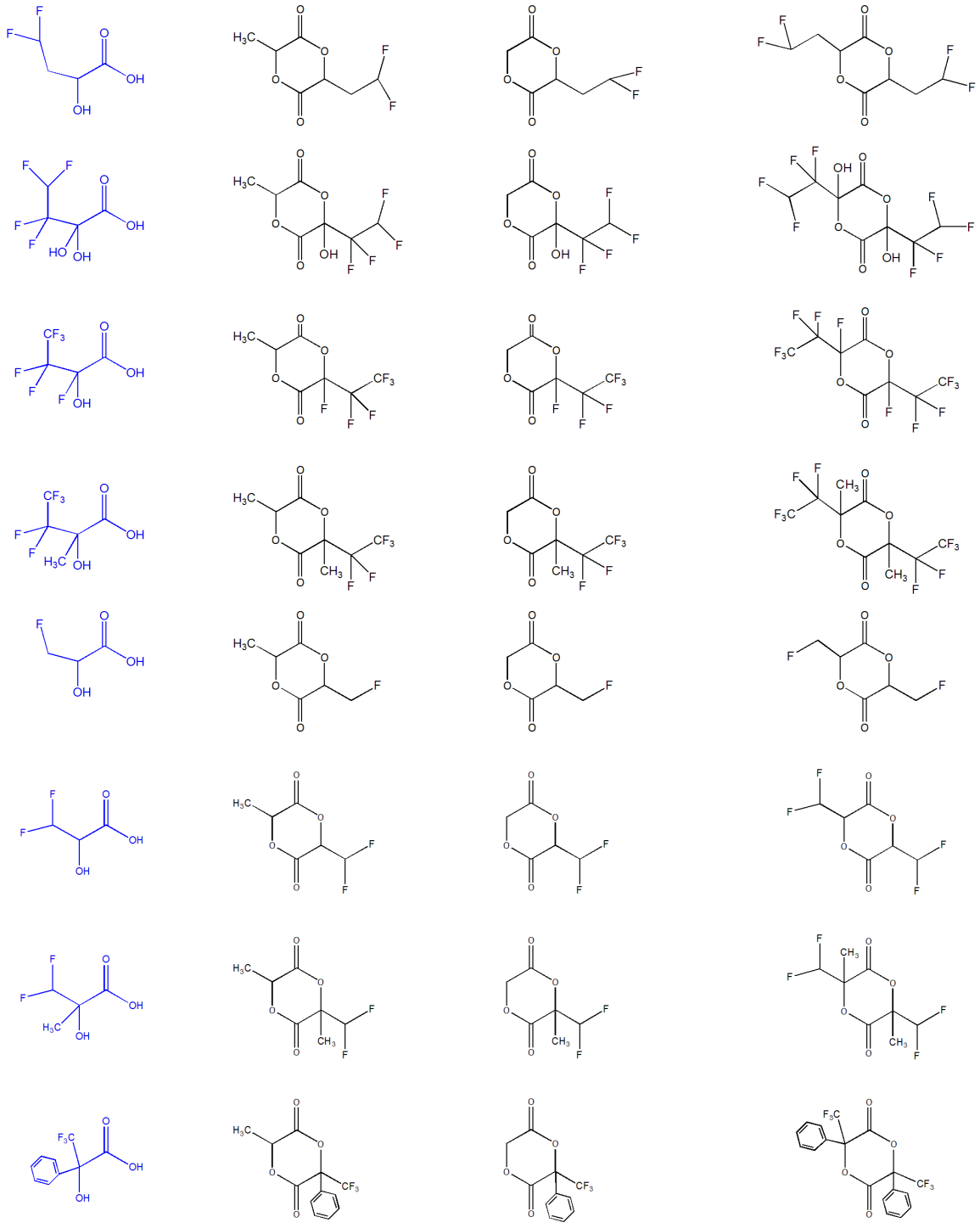

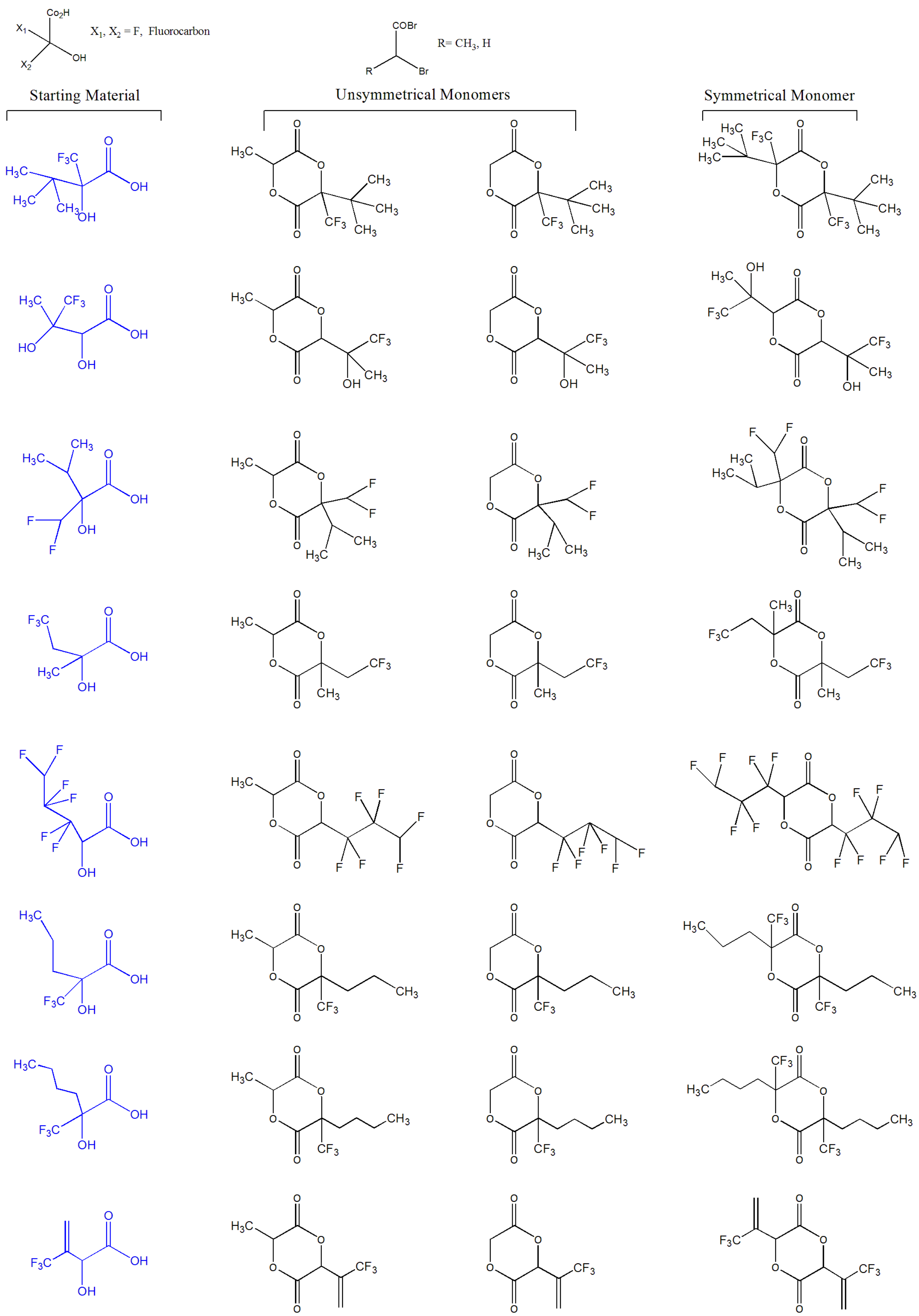
X1, X2 = F, Fluorocarbon
R= CH3, H
Starting Material
Unsymmetrical Monomers
Symmetrical Monomer

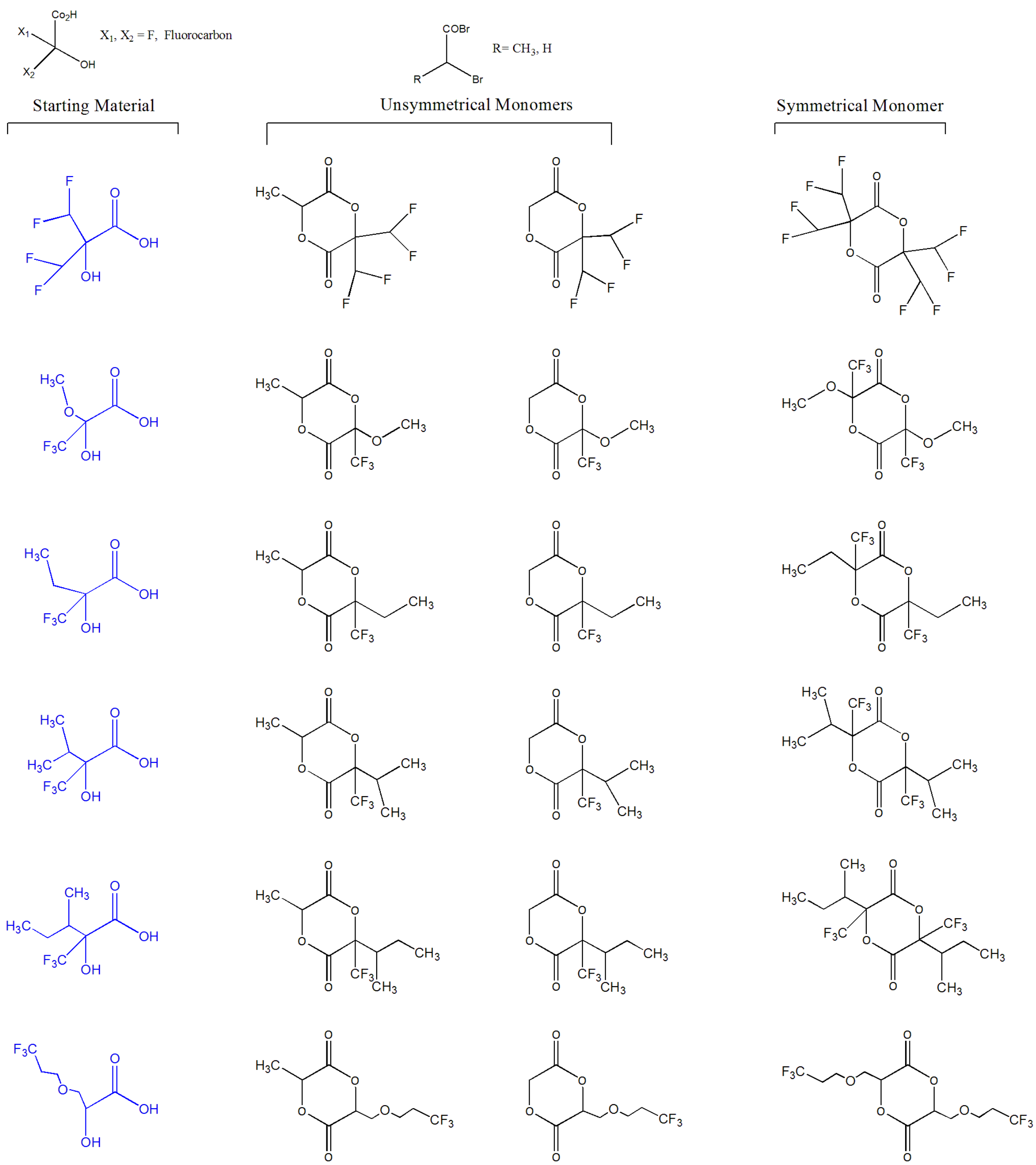
X1, X2 = F, Fluorocarbon
R= CH3, H
Starting Material
Unsymmetrical Monomers
Symmetrical Monomer

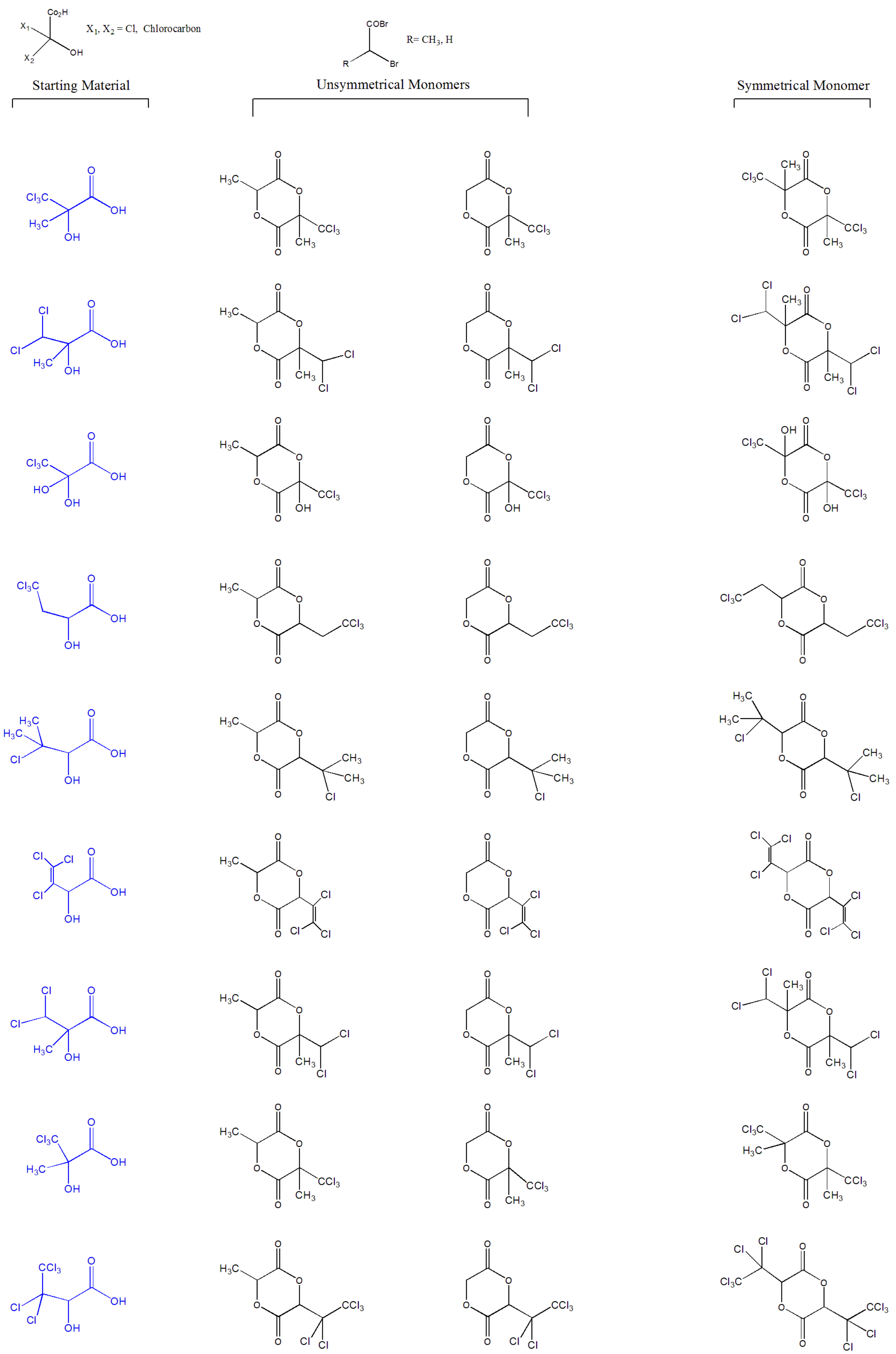
X_1, X_2 = Cl, Chlorocarbon
R= CH_3, H
Starting Material
Unsymmetrical Monomers
Symmetrical Monomer

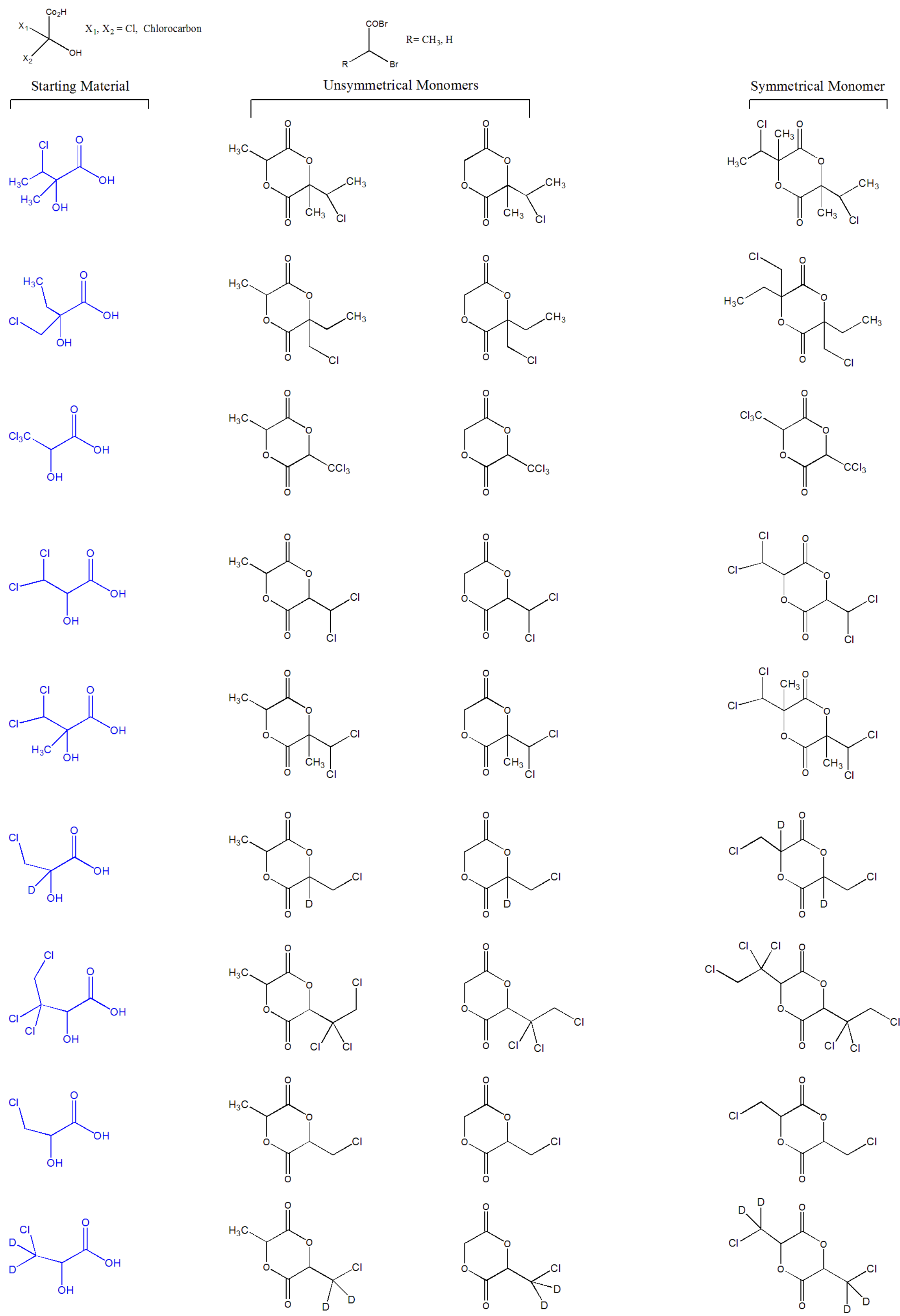
X1, X2 = Cl, Chlorocarbon
R= CH3, H
Starting Material
Unsymmetrical Monomers
Symmetrical Monomer

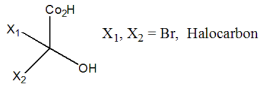

X_1, X_2 = Br, Halocarbon

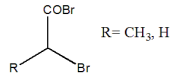

R= CH_3, H

Starting Material

Unsymmetrical Monomers

Symmetrical Monomer

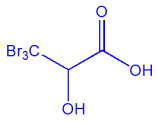

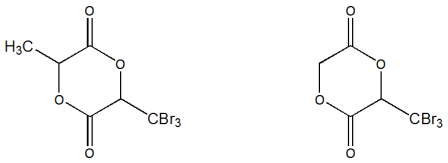

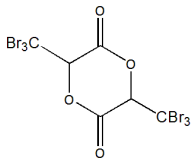

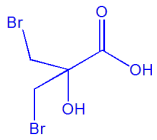

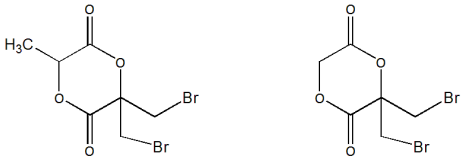

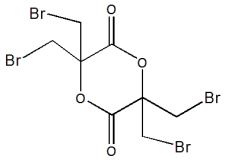

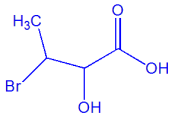

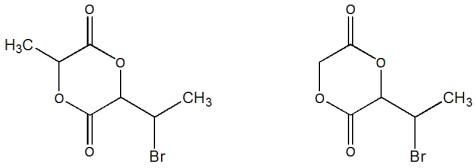

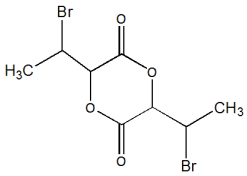

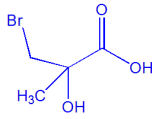

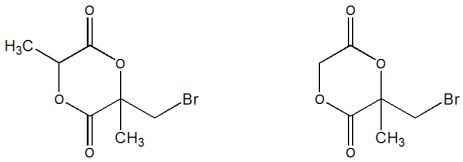

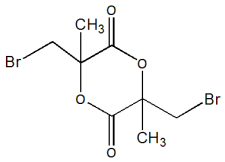

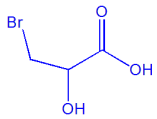

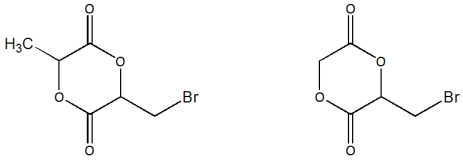

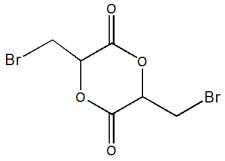

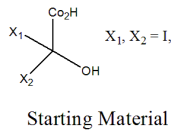

X_1, X_2 = I, Halocarbon

R= CH_3, H

Starting Material

Unsymmetrical Monomers

Symmetrical Monomer

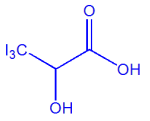

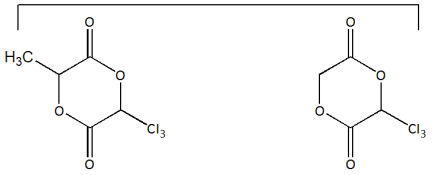

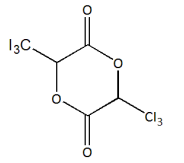

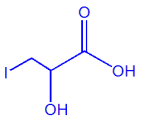

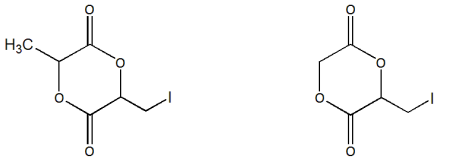

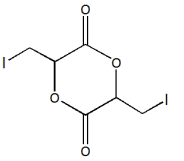

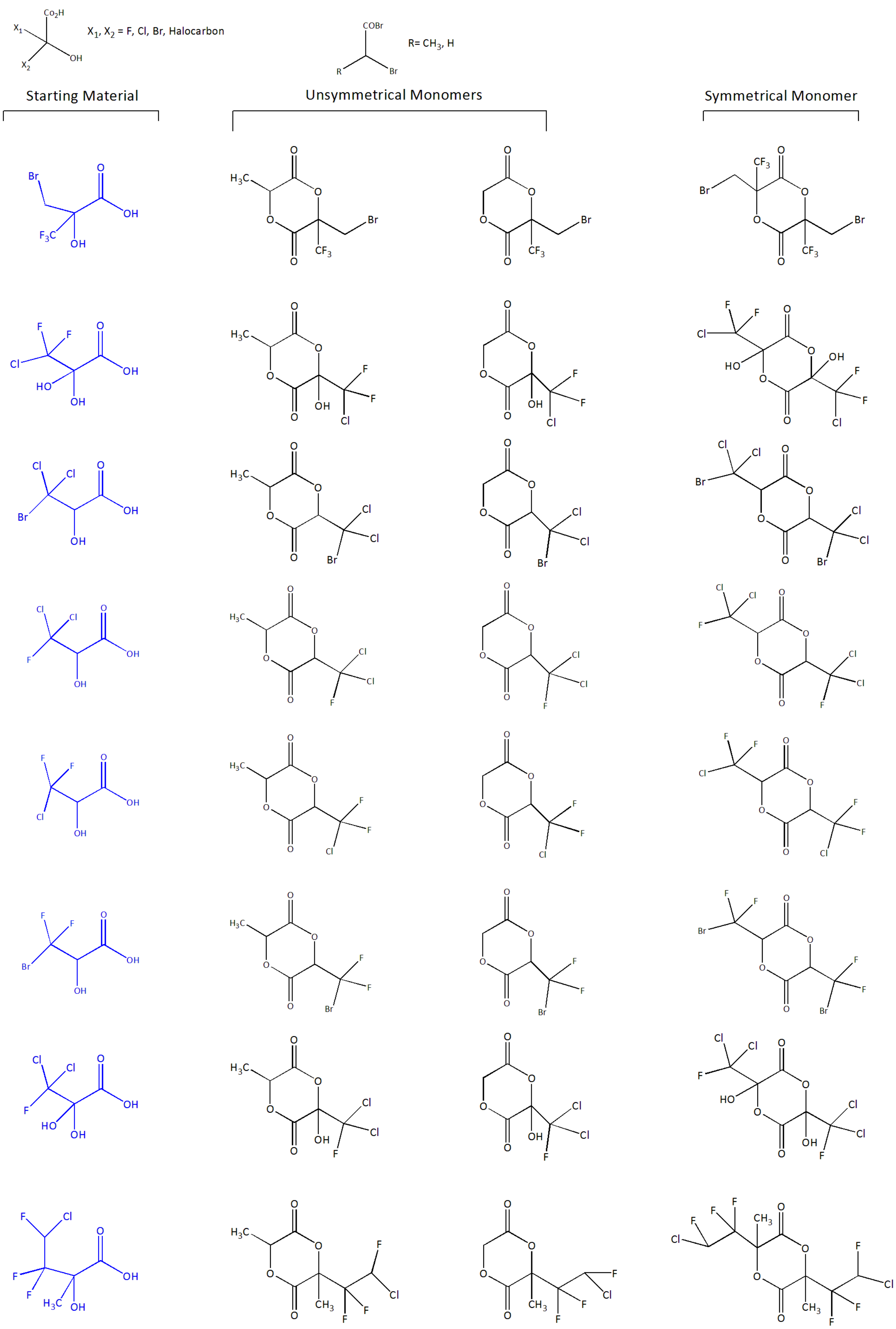
X1, X2 = F, Cl, Br, Halocarbon
R= CH3, H
Starting Material
Unsymmetrical Monomers
Symmetrical Monomer

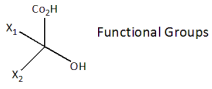

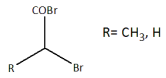

Starting Material

Unsymmetrical Monomers

Symmetrical Monomer

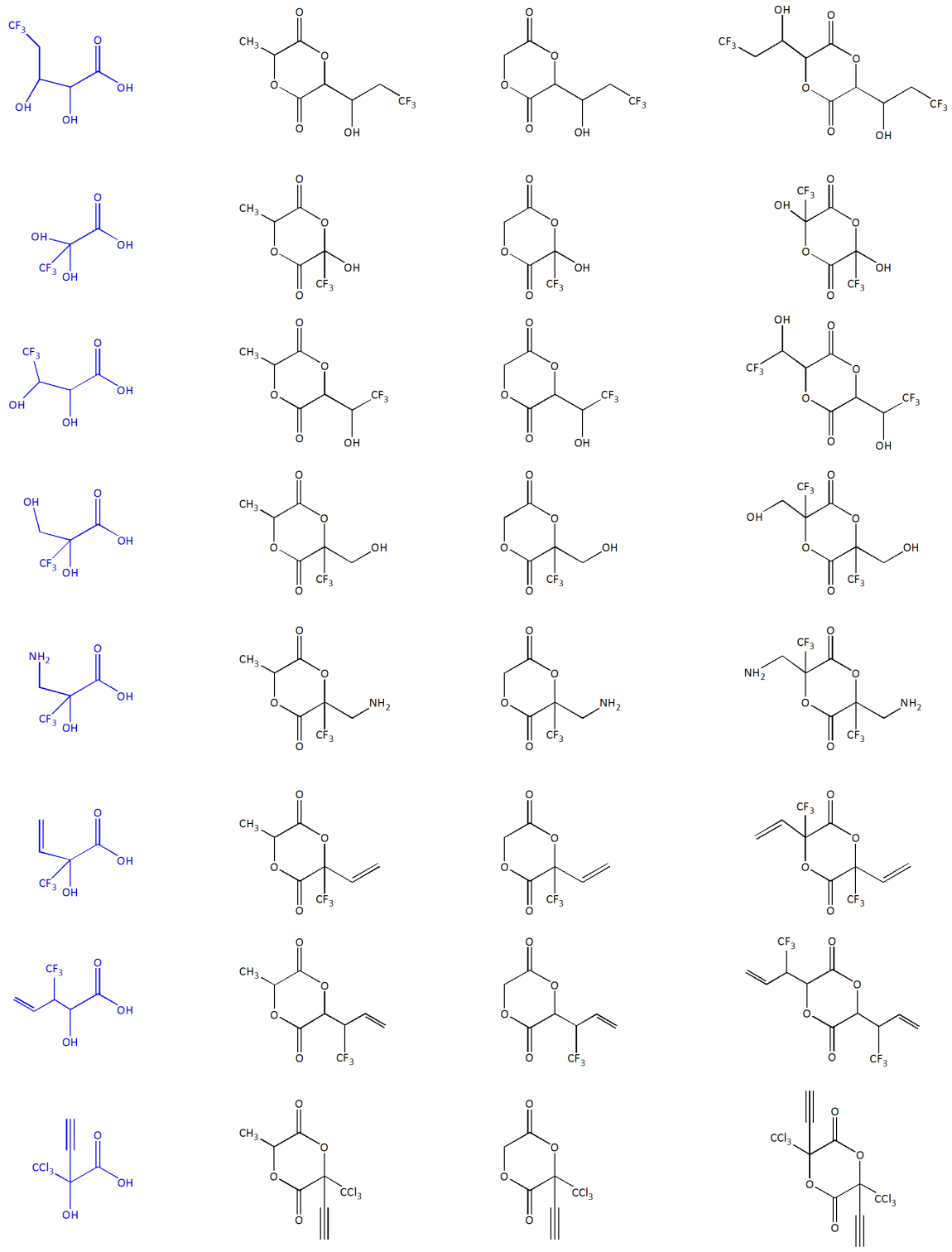

Reference:

[1] D. Mozaffarian, E.J. Benjamin, A.S. Go, D.K. Arnett, M.J. Blaha, M. Cushman, S.R. Das, S. de Ferranti, J.-P. Després, H.J. Fullerton, V.J. Howard, M.D. Huffman, C.R. Isasi, M.C. Jiménez, S.E. Judd, B.M. Kissela, J.H. Lichtman, L.D. Lisabeth, S. Liu, R.H. Mackey, D.J. Magid, D.K. McGuire, I. Mohler, Emile R, C.S. Moy, P. Muntner, M.E. Mussolino, K. Nasir, R.W. Neumar, G. Nichol, L. Palaniappan, D.K. Pandey, M.J. Reeves, C.J. Rodriguez, W. Rosamond, P.D. Sorlie, J. Stein, A. Towfighi, T.N. Turan, S.S. Virani, D. Woo, R.W. Yeh, M.B. Turner, Heart Disease and Stroke Statistics—2016 Update, Circulation, 2016, pp. e38-e360.

[2] S.J. Brener, D.J. Kereiakes, C.A. Simonton, A. Rizvi, W. Newman, K. Mastali, J.C. Wang, R. Caputo, R.S. Smith Jr, S.-W. Ying, D.E. Cutlip, G.W. Stone, Everolimus-eluting stents in patients undergoing percutaneous coronary intervention: Final 3-year results of the Clinical Evaluation of the XIENCE V Everolimus Eluting Coronary Stent System in the Treatment of Subjects With de Novo Native Coronary Artery Lesions trial, American heart journal 166(6) (2013) 1035-1042.

[3] F. Otsuka, R.A. Byrne, K. Yahagi, H. Mori, E. Ladich, D.R. Fowler, R. Kutys, E. Xhepa, A. Kastrati, R. Virmani, M. Joner, Neoatherosclerosis: overview of histopathologic findings and implications for intravascular imaging assessment, European heart journal 36(32) (2015) 2147-59.

[4] J.A. Ormiston, P.W. Serruys, E. Regar, D. Dudek, L. Thuesen, M.W.I. Webster, Y. Onuma, H.M. Garcia-Garcia, R. McGreevy, S. Veldhof, A bioabsorbable everolimus-eluting coronary stent system for patients with single de-novo coronary artery lesions (ABSORB): a prospective open-label trial, The Lancet 371(9616) (2008) 899-907.

[5] D.J. Kereiakes, S.G. Ellis, J.J. Popma, P.J. Fitzgerald, H. Samady, J. Jones-McMeans, Z. Zhang, W.F. Cheong, X. Su, O. Ben-Yehuda, G.W. Stone, Evaluation of a fully bioresorbable vascular scaffold in patients with coronary artery disease: design of and rationale for the ABSORB III randomized trial, American heart journal 170(4) (2015) 641-651 e3.

[6] S.G. Ellis, D.J. Kereiakes, D.C. Metzger, R.P. Caputo, D.G. Rizik, P.S. Teirstein, M.R. Litt, A. Kini, A. Kabour, S.O. Marx, J.J. Popma, R. McGreevy, Z. Zhang, C. Simonton, G.W. Stone, Everolimus-Eluting Bioresorbable Scaffolds for Coronary Artery Disease, The New England journal of medicine 373(20) (2015) 1905-15.

[7] R.A. Byrne, Bioresorbable Vascular Scaffolds—Will Promise Become Reality?, N Engl J Med, 2015.

[8] I. Reviakine, F. Jung, S. Braune, J.L. Brash, R. Latour, M. Gorbet, W. van Oeveren, Stirred, shaken, or stagnant: What goes on at the blood-biomaterial interface., Blood Rev., 2017, pp. 11-21.

[9] K.S. Lavery, C. Rhodes, A. Mcgraw, M.J. Eppihimer, Anti-thrombotic technologies for medical devices, Adv. Drug Deliv. Rev., Elsevier B.V., 2017, pp. 2-11.

[10] A.M. Garfinkle, A.S. Hoffman, B.D. Ratner, L.O. Reynolds, S.R. Hanson, Effects of a tetrafluoroethylene glow discharge on patency of small diameter Dacron vascular grafts, Transactions American Society for Artificial Internal Organs 30 (1984) 432-439.

[11] D. Kiaei, A.S. Hoffman, B.D. Ratner, T.A. Horbett, L.O. Reynolds, Interaction of blood with gas discharge treated vascular grafts, J. Appl. Polmer. Sci: Appl. Polymer Sym 42 (1988) 269.

[12] T.M. Massa, W.G. McClung, M.L. Yang, J.Y.C. Ho, J.L. Brash, J.P. Santerre, Fibrinogen adsorption and platelet lysis characterization of fluorinated surface-modified polyetherurethanes, J. Biomed. Mater. Res., 2007, pp. 178-185.

[13] J.C. Lin, S.L. Tiong, C.Y. Chen, Surface characterization and platelet adhesion studies on fluorocarbons prepared by plasma-induced graft polymerization, J Biomater Sci Polym Ed, 2000, pp. 701-714.

[14] T.-Y. Liu, W.-C. Lin, L.-Y. Huang, S.-Y. Chen, M.-C. Yang, Surface characteristics and hemocompatibility of PAN/PVDF blend membranes, Polym. Adv. Technol., 2005, pp. 413-419.

[15] R. Lilenfeld, N.M. Popadiuk, P. Steinheuser, E. Menezes, Surgical filaments from vinylidene fluoride copolymers, Google Patents, 1986.

[16] D.M. Paton, Ashton, Timothy R., Maini, Roshan Fluorinating polymer surfaces, United States Patent number 5356668 (Oct 18,1994).

[17] W.B. Tsai, Q. Shi, J.M. Grunkemeier, C. McFarland, T.A. Horbett, Platelet adhesion to radiofrequency glow-discharge-deposited fluorocarbon polymers preadsorbed with selectively depleted plasmas show the primary role of fibrinogen., J Biomater Sci Polym Ed, 2004, pp. 817-840.

[18] L.M. Szott, C.A. Irvin, M. Trollsas, S. Hossainy, B.D. Ratner, Blood compatibility assessment of polymers used in drug eluting stent coatings, Biointerphases, 2016, p. 029806.

[19] S. Tajbakhsh, F. Hajiali, A comprehensive study on the fabrication and properties of biocomposites of poly(lactic acid)/ceramics for bone tissue engineering, Mater. Sci. Eng. C-Mater. Biol. Appl. 70 (2017) 897-912.

[20] P. Saini, M. Arora, M. Kumar, Poly(lactic acid) blends in biomedical applications, Adv. Drug Deliv. Rev. 107 (2016) 47-59.

[21] G. Narayanan, V.N. Vernekar, E.L. Kuyinu, C.T. Laurencin, Poly (lactic acid)-based biomaterials for orthopaedic regenerative engineering, Adv. Drug Deliv. Rev. 107 (2016) 247-276.

[22] Y. Ramot, M. Haim-Zada, A.J. Domb, A. Nyska, Biocompatibility and safety of PLA and its copolymers, Adv. Drug Deliv. Rev. 107 (2016) 153-162.

[23] S. Farah, D.G. Anderson, R. Langer, Physical and mechanical properties of PLA, and their functions in widespread applications - A comprehensive review, Advanced Drug Delivery Reviews 107 (2016) 367-392.

[24] H. Tian, Z. Tang, X. Zhuang, X. Chen, X. Jing, Biodegradable synthetic polymers: Preparation, functionalization and biomedical application, Progress in Polymer Science 37(2) (2012) 237-280.

[25] S. Slomkowski, S. Penczek, A. Duda, Polylactides—an overview, Polymers for Advanced Technologies 25(5) (2014) 436-447.

[26] J.M. Becker, R.J. Pounder, A.P. Dove, Synthesis of Poly(lactide)s with Modified Thermal and Mechanical Properties, Macromolecular rapid communications 31(22) (2010) 1923-37.

[27] R.M. Rasal, A.V. Janorkar, D.E. Hirt, Poly(lactic acid) modifications, Progress in Polymer Science 35(3) (2010) 338-356.

[28] D. Bourissou, S. Moebs-Sanchez, B. Martín-Vaca, Recent advances in the controlled preparation of poly(α-hydroxy acids): Metal-free catalysts and new monomers, Comptes Rendus Chimie 10(9) (2007) 775-794.

[29] D.E. Borchmann, N.T. Brummelhuis, M. Weck, GRGDS-Functionalized Poly(lactide)-graft-poly(ethylene glycol) Copolymers: Combining Thiol-Ene Chemistry with Staudinger Ligation, Macromolecules 46(11) (2013) 4426-4431.

[30] C. Regnier-Delplace, O.T. du Boullay, F. Siepmann, B. Martin-Vaca, P. Demonchaux, O. Jentzer, F. Danède, M. Descamps, J. Siepmann, D. Bourissou, PLGAs bearing carboxylated side

chains: Novel matrix formers with improved properties for controlled drug delivery, Journal of Controlled Release, Elsevier B.V., 2013, pp. 256-267.

[31] Y. Yu, J. Zou, C. Cheng, Synthesis and biomedical applications of functional poly(α-hydroxyl acid)s, Polym. Chem. 5(20) (2014) 5854-5872.

[32] M. Yin, G.L. Baker, Preparation and Characterization of Substituted Polylactides, Macromolecules, American Chemical Society 1999, pp. 7711-7718.

[33] G.L. Baker, M.R. Smith, Process for the preparation of polymers of dimeric cyclic esters, Google Patents, 2002.

[34] T. Trimaille, R. Gurny, M. Moller, Poly(hexyl-substituted lactides): novel injectable hydrophobic drug delivery systems, Journal of biomedical materials research. Part A 80(1) (2007) 55-65.

[35] T. Trimaille, M. Möller, R. Gurny, Synthesis and ring-opening polymerization of new monoalkyl-substituted lactides, Journal of Polymer Science Part A: Polymer Chemistry 42(17) (2004) 4379-4391.

[36] F. Jing, M.R. Smith, G.L. Baker, Cyclohexyl-Substituted Polyglycolides with High Glass Transition Temperatures, Macromolecules, 2007, pp. 9304-9312.

[37] T. Liu, T.L. Simmons, D.A. Bohnsack, M.E. Mackay, M.R. Smith, G.L. Baker, Synthesis of Polymandelide: A Degradable Polylactide Derivative with Polystyrene-like Properties, Macromolecules, 2007, pp. 6040-6047.

[38] M. Leemhuis, N. Akeroyd, J.A.W. Kruijtzer, C.F. van Nostrum, W.E. Hennink, Synthesis and characterization of allyl functionalized poly(α-hydroxy)acids and their further dihydroxylation and epoxidation, European Polymer Journal 44(2) (2008) 308-317.

[39] M. Leemhuis, C.F. van Nostrum, J.A.W. Kruijtzer, Z.Y. Zhong, M.R. ten Breteler, P.J. Dijkstra, J. Feijen, W.E. Hennink, Functionalized Poly(α-hydroxy acid)s via Ring-Opening Polymerization: Toward Hydrophilic Polyesters with Pendant Hydroxyl Groups, Macromolecules, American Chemical Society 2006, pp. 3500-3508.

[40] W.W. Gerhardt, D.E. Noga, K.I. Hardcastle, A.s.J. García, D.M. Collard, M. Weck, Functional Lactide Monomers: Methodology and Polymerization, Biomacromolecules, 2006, pp. 1735-1742.

[41] D.E. Noga, T.A. Petrie, A. Kumar, M. Weck, A.s.J. García, D.M. Collard, Synthesis and Modification of Functional Poly(lactide) Copolymers: Toward Biofunctional Materials, Biomacromolecules, 2008, pp. 2056-2062.

[42] X. Jiang, E.B. Vogel, M.R. Smith, G.L. Baker, Amphiphilic PEG/alkyl-grafted comb polylactides, Journal of Polymer Science Part A: Polymer Chemistry 45(22) (2007) 5227-5236.

[43] Q. Zhang, H. Ren, G.L. Baker, Synthesis and click chemistry of a new class of biodegradable polylactide towards tunable thermo-responsive biomaterials, Polym. Chem., 2015, pp. 1275-1285.

[44] X. Jiang, E.B. Vogel, M.R. Smith, G.L. Baker, "Clickable" Polyglycolides: Tunable Synthons for Thermoresponsive, Degradable Polymers, Macromolecules, 2008, pp. 1937-1944.

[45] K. Muller, C. Faeh, F. Diederich, Fluorine in pharmaceuticals: looking beyond intuition, Science 317(5846) (2007) 1881-6.

[46] Y. Yamamoto, T. Kurohara, M. Shibuya, CF3-Substituted semisquarate: a pluripotent building block for the divergent synthesis of trifluoromethylated functional molecules, Chem. Commun., Royal Society of Chemistry, 2015, pp. 1-4.

[47] P.A. Champagne, J. Desroches, J.D. Hamel, M. Vandamme, J.F. Paquin, Monofluorination of Organic Compounds: 10 Years of Innovation, Chemical reviews 115(17) (2015) 9073-174.

[48] J. Wang, M. Sanchez-Rosello, J.L. Acena, C. del Pozo, A.E. Sorochinsky, S. Fustero, V.A. Soloshonok, H. Liu, Fluorine in pharmaceutical industry: fluorine-containing drugs introduced to the market in the last decade (2001-2011), Chemical reviews 114(4) (2014) 2432-506.

[49] P.R. Savoie, J.T. Welch, Preparation and utility of organic pentafluorosulfanyl-containing compounds, Chemical reviews 115(2) (2015) 1130-90.

[50] O.A. Tomashenko, V.V. Grushin, Aromatic trifluoromethylation with metal complexes, Chemical reviews 111(8) (2011) 4475-521.

[51] K.L. Kirk, Fluorination in Medicinal Chemistry: Methods, Strategies, and Recent Developments, Org. Process Res. Dev., 2008, pp. 305-321.

[52] H.L. Yale, The Trifluoromethyl Group in Medical Chemistry, Journal of Medicinal and Pharmaceutical Chemistry 1(2) (1959) 121-133.

[53] D. Han, L. Zhu, Y. Chen, W. Li, X. Wang, L. Ning, Synthesis of fluorinated monomer and formation of hydrophobic surface therefrom, RSC Adv., Royal Society of Chemistry, 2015, pp. 22847-22855.

[54] R.Y. Kannan, H.J. Salacinski, P.E. Butler, G. Hamilton, A.M. Seifalian, Current status of prosthetic bypass grafts: a review., J. Biomed. Mater. Res. Part B Appl. Biomater., 2005, pp. 570-581.

[55] A.I. Cassady, N.M. Hidzir, L. Grøndahl, Enhancing expanded poly(tetrafluoroethylene) (ePTFE) for biomaterials applications, Journal of Applied Polymer Science 131(15) (2014) n/a-n/a.

[56] J.P. Eiberg, O. Røder, M. Stahl-Madsen, N. Eldrup, P. Qvarfordt, A. Laursen, M. Greve, T. Flörenes, O.M. Nielsen, C. Seidelin, T. Vestergaard-Andersen, T.V. Schroeder, Fluoropolymer-coated Dacron Versus PTFE Grafts for Femorofemoral Crossover Bypass: Randomised Trial, European Journal of Vascular and Endovascular Surgery, 2006, pp. 431-438.

[57] J.G. Riess, M.P. Krafft, Fluorinated materials for in vivo oxygen transport (blood substitutes), diagnosis and drug delivery., Biomaterials, 1998, pp. 1529-1539.

[58] S. Petersen, D.G. Gliesche, G. Kurtbay, R. Begunk, M. Boeck, V. Hopf, H.K. Kroemer, K.-P. Schmitz, H.E. Meyer zu Schwabedissen, K. Sternberg, Tailored surface design of biodegradable endovascular implants by functionalization of poly (L-lactide) with elastin-like proteins, Journal of Biomedical Engineering and Informatics 2(1) (2015).

[59] S. Petersen, A. Strohbach, R. Busch, S.B. Felix, K.P. Schmitz, K. Sternberg, Site-selective immobilization of anti-CD34 antibodies to poly(l-lactide) for endovascular implant surfaces, Journal of biomedical materials research. Part B, Applied biomaterials 102(2) (2014) 345-55.

[60] S. Sato, D. Gondo, T. Wada, S. Kanehashi, K. Nagai, Effects of various liquid organic solvents on solvent-induced crystallization of amorphous poly(lactic acid) film, J. Appl. Polym. Sci., 2012, pp. 1607-1617.

[61] B.D. Ratner, Biomaterials science an introduction to materials in medicine, 3rd ed. ed., Elsevier/Academic Press, Amsterdam ;, 2013.

[62] A. Ulman, An introduction to ultrathin organic films : from Langmuir-Blodgett to self-assembly, Academic Press, Boston :, 1991.

[63] R.W. Helemkamp, R.L. Goodland, W.F. Bale, I.L. Spar, L.E. Mutschler, High Specific Activity Iodination of Gamma-Globulin with Iodine-131 Monochloride, Cancer Res., 1960, pp. 1495-1500.

[64] T.A. Horbett, Adsorption of proteins from plasma to a series of hydrophilic-hydrophobic copolymers. II. Compositional analysis with the prelabeled protein technique., J. Biomed. Mater. Res., 1981, pp. 673-695.

[65] S.G. Dawids, Test procedures for the blood compatibility of biomaterials, Kluwer Academic Publishers, Dordrecht ;, 1993.

[66] C. Skoglund, J. Wetterö, T. Skogh, C. Sjöwall, P. Tengvall, T. Bengtsson, C-reactive protein and C1q regulate platelet adhesion and activation on adsorbed immunoglobulin G and albumin, Immunol Cell Biol, 2008, pp. 466-474.

[67] W. Ming, J. Laven, R. van der Linde, Synthesis and Surface Properties of Films Based on Solventless Liquid Fluorinated Oligoester, Macromolecules, 2000, pp. 6886-6891.

[68] S.J. De Jong, E.R. Arias, D. Rijkers, C.F. van Nostrum, J.J. Kettenes-Van den Bosch, W.E. Hennink, New insights into the hydrolytic degradation of poly (lactic acid): participation of the alcohol terminus, Polymer, Elsevier, 2001, pp. 2795-2802.

[69] F. von Burkersroda, L. Schedl, A. Gopferich, Why degradable polymers undergo surface erosion or bulk erosion, Biomaterials, 2002, pp. 4221-4231.

[70] J. Shen, D.J. Burgess, Accelerated in-vitro release testing methods for extended-release parenteral dosage forms, Journal of Pharmacy and Pharmacology, 2012, pp. 986-996.

[71] G. Schliecker, C. Schmidt, S. Fuchs, T. Kissel, Characterization of a homologous series of d,l-lactic acid oligomers; a mechanistic study on the degradation kinetics in vitro, Biomaterials, 2003, pp. 3835-3844.

[72] L. Xu, K. Crawford, C.B. Gorman, Effects of Temperature and pH on the Degradation of Poly(lactic acid) Brushes, Macromolecules, 2011, pp. 4777-4782.

[73] H.-M. Chen, C.-X. Feng, W.-B. Zhang, J.-H. Yang, T. Huang, N. Zhang, Y. Wang, Hydrolytic degradation behavior of poly(l-lactide)/carbon nanotubes nanocomposites, Polymer Degradation and Stability, Elsevier Ltd, 2013, pp. 198-208.

[74] C.F. van Nostrum, T.F.J. Veldhuis, G.W. Bos, W.E. Hennink, Hydrolytic degradation of oligo(lactic acid): a kinetic and mechanistic study, Polymer, 2004, pp. 6779-6787.

[75] S. Bose, S.S. Keller, A. Boisen, K. Almdal, Microcantilever sensors for fast analysis of enzymatic degradation of poly (d, l-lactide), Polymer Degradation and Stability, Elsevier Ltd, 2015, pp. 1-8.

[76] F. Codari, S. Lazzari, M. Soos, G. Storti, M. Morbidelli, D. Moscatelli, Kinetics of the hydrolytic degradation of poly(lactic acid), Polymer Degradation and Stability, Elsevier Ltd, 2012, pp. 2460-2466.

[77] R.M. Felfel, K.M.Z. Hossain, A.J. Parsons, C.D. Rudd, I. Ahmed, Accelerated in vitro degradation properties of polylactic acid/phosphate glass fibre composites, J Mater Sci, 2015, pp. 3942-3955.

[78] X. Hu, C.B. Gorman, Resisting protein adsorption on biodegradable polyester brushes, Acta biomaterialia, Acta Materialia Inc., 2014, pp. 3497-3504.

[79] L. Xiao, B. Wang, G. Yang, M. Gauthier, Poly (lactic acid)-based biomaterials: synthesis, modification and applications, INTECH Open Access Publisher2012.

[80] G. Schmidmaier, K. Baehr, S. Mohr, M. Kretschmar, S. Beck, B. Wildemann, Biodegradable polylactide membranes for bone defect coverage: biocompatibility testing, radiological and histological evaluation in a sheep model., Clin Oral Implants Res, 2006, pp. 439-444.

[81] K.A. Athanasiou, G.G. Niederauer, C.M. Agrawal, Sterilization, toxicity, biocompatibility and clinical applications of polylactic acid/polyglycolic acid copolymers., Biomaterials, 1996, pp. 93-102.

[82] Y. Jiao, J. Xu, C. Zhou, Effect of Ammonia Plasma Treatment on the Properties and Cytocompatibility of a Poly(L-Lactic Acid) Film Surface, J Biomater Sci Polym Ed, 2012, pp. 763-777.

[83] Y. Wan, C. TU, J. Yang, J. Bei, S. Wang, Influences of ammonia plasma treatment on modifying depth and degradation of poly(l-lactide) scaffolds, Biomaterials, 2006, pp. 2699-2704.

[84] Z.-X. Xu, T. Li, Z.-M. Zhong, D.-S. Zha, S.-H. Wu, F.-Q. Liu, W.-D. Xiao, X.-R. Jiang, X.-X. Zhang, J.-T. Chen, Amide-linkage formed between ammonia plasma treated poly(D,L-lactide acid) scaffolds and bio-peptides: Enhancement of cell adhesion and osteogenic differentiation in vitro, Biopolymers, 2011, pp. 682-694.

[85] J. Yang, J. Bei, S. Wang, Improving cell affinity of poly(D,L-lactide) film modified by anhydrous ammonia plasma treatment, Polym. Adv. Technol., 2002, pp. 220-226.

[86] N.L. Anderson, N.G. Anderson, The human plasma proteome: history, character, and diagnostic prospects., Mol. Cell Proteomics, 2002, pp. 845-867.

[87] I.H. Jaffer, J.C. Fredenburgh, J. Hirsh, J.I. Weitz, Medical device-induced thrombosis: what causes it and how can we prevent it?, J Thromb Haemost, 2015, pp. S72-S81.

[88] D.J. Lyman, L.C. Metcalf, D.J. Albo, K.F. Richards, J. Lamb, The Effect of Chemical Structure and Surface Properties of Synthetic Polymers on the Coagulation of Blood III. ASAIO Journal 20(1) (1974) 474-478.

[89] J.L. Bohnert, B.C. Fowler, T.A. Horbett, A.S. Hoffman, Plasma gas discharge deposited fluorocarbon polymers exhibit reduced elutability of adsorbed albumin and fibrinogen., J Biomater Sci Polym Ed, 1990, pp. 279-297.

[90] E. Grube, B. Chevalier, P. Smits, V. Džavík, T.M. Patel, A.S. Mullasari, J. Wöhrle, M. Stuteville, C. Dorange, U. Kaul, S.V. Investigators, The SPIRIT V Study, JCIN, Elsevier Inc., 2011, pp. 168-175.

[91] H.J. Erli, R. Marx, O. Paar, F.U. Niethard, M. Weber, D.C. Wirtz, Surface pretreatments for medical application of adhesion., Biomed Eng Online, 2003, p. 15.

[92] L. Pedrini, M. Dondi, A. Magagnoli, F. Magnoni, E. Pisano, E. Del Giudice, M. Santoro, Evaluation of thrombogenicity of fluoropassivated polyester patches following carotid endarterectomy, Ann Vasc Surg, 2001, pp. 679-683.

[93] G. Laroche, Y. Marois, R. Guidoin, M.W. King, L. Martin, T. How, Y. Douville, Polyvinylidene fluoride (PVDF) as a biomaterial: From polymeric raw material to monofilament vascular suture, Journal of Biomedical Materials Research 29(12) (1995) 1525-1536.

[94] B.D. Ratner, The catastrophe revisited: Blood compatibility in the 21st Century, Biomaterials, 2007, pp. 5144-5147.

[95] B.D. Ratner, The blood Compatibility catastrophe, J Biomed Mater Res 27(3) (1993) 283-287.

[96] B.D. Ratner, Blood compatibility—a perspective, Journal of Biomaterials Science, 2000.

[97] J.M. Courtney, N.M. Lamba, S. Sundaram, C.D. Forbes, Biomaterials for blood-contacting applications., Biomaterials, 1994, pp. 737-744.

[98] I. Reviakine, S. Braune, Preface: In Focus Issue on Blood–Biomaterial Interactions, Biointerphases, 2016, p. 029501.

[99] S.L.J. Blok, G.E. Engels, W. van Oeveren, In vitro hemocompatibility testing: The importance of fresh blood, Biointerphases, 2016, p. 029802.

[100] B.D.B. Ratner, John W., M. Eden, Evaluation of the Blood Compatibility of Synthetic Polymers: Consensus and Significance, Contemporary Biomaterials: Material and Host Response, Clinical Applications, New Technology and Legal Aspects, William Andrew Publishing/Noyes.

[101] M.B. Gorbet, M.V. Sefton, Biomaterial-associated thrombosis: roles of coagulation factors, complement, platelets and leukocytes, Biomaterials, 2004, pp. 5681-5703.

[102] Y. Wu, F.I. Simonovsky, B.D. Ratner, T.A. Horbett, The role of adsorbed fibrinogen in platelet adhesion to polyurethane surfaces: A comparison of surface hydrophobicity, protein adsorption, monoclonal antibody binding, and platelet adhesion, J. Biomed. Mater. Res., 2005, pp. 722-738.

[103] C.J. Wilson, R.E. Clegg, D.I. Leavesley, Mediation of biomaterial-cell interactions by adsorbed proteins: a review, Tissue, 2005.

[104] J.M. Grunkemeier, W.B. Tsai, C.D. McFarland, T.A. Horbett, The effect of adsorbed fibrinogen, fibronectin, von Willebrand factor and vitronectin on the procoagulant state of adherent platelets, Biomaterials, 2000, pp. 2243-2252.

[105] C.C. Tsai, H.H. Huo, P. Kulkarni, R.C. Eberhart, Biocompatible coatings with high albumin affinity., ASAIO Trans, 1990, pp. M307-M310.

[106] W.-B. Tsai, J.M. Grunkemeier, T.A. Horbett, Variations in the ability of adsorbed fibrinogen to mediate platelet adhesion to polystyrene-based materials: a multivariate statistical analysis of antibody binding to the platelet binding sites of fibrinogen., J. Biomed. Mater. Res., 2003, pp. 1255-1268.

[107] W.B. Tsai, J.M. Grunkemeier, T.A. Horbett, Human plasma fibrinogen adsorption and platelet adhesion to polystyrene., J. Biomed. Mater. Res., 1999, pp. 130-139.

[108] B. Sivaraman, R.A. Latour, The Adherence of platelets to adsorbed albumin by receptor-mediated recognition of binding sites exposed by adsorption-induced unfolding, Biomaterials, Elsevier Ltd, 2010, pp. 1036-1044.

[109] A. Chiumiento, S. Lamponi, R. Barbucci, Role of Fibrinogen Conformation in Platelet Activation, Biomacromolecules, 2007, pp. 523-531.

[110] R.C. Eberhart, M.S. Munro, J.R. Frautschi, Influence of Endogenous Albumin Binding on Blood-Material Interactionsa, Annals of the New York Academy of Science, 1987.

[111] K. Kottke-Marchant, J.M. Anderson, Y. Umemura, Effect of albumin coating on the in vitro blood compatibility of Dacron® arterial prostheses, Biomaterials, 1989.

[112] U. Schöllkopf, W. Hartwig, U. Sprotte, Lactidkontraktion, eine Methode zur Synthese von α, α′-Dihydroxyketonen aus α-Hydroxycarbonsäuren, Angewandte Chemi, 1979.

[113] T. Trimaille, M. M ller, R. Gurny, Synthesis and ring-opening polymerization of new monoalkyl-substituted lactides, J. Polym. Sci. A Polym. Chem., 2004, pp. 4379-4391.

[114] X. Jiang, M.R. Smith, G.L. Baker, Water-Soluble Thermoresponsive Polylactides, Macromolecules, American Chemical Society 2008, pp. 318-324.

[115] A. Pedna, L. Rosi, M. Frediani, P. Frediani, High glass transition temperature polyester coatings for the protection of stones, J. Appl. Polym. Sci., 2015, pp. n/a-n/a.

[116] Y. Tanabe, R. Nagase, Y. Iida, M. Sugi, T. Misaki, Improved Robust Method for Preparing Optically Active 3-Alkyl-3-phenyl-1,4-dioxane-2,5-diones; A Promising New Chiral Template, Synthesis 2008(22) (2008) 3670-3674.

[117] M. Bueno, I. Molina, J.A. Galbis, 1,4-Dioxane-2,5-dione-type monomers derived from l-ascorbic and d-isoascorbic acids. Synthesis and polymerisation, Carbohydrate research 344(15) (2009) 2100-4.

[118] R. Nagase, Y. Iida, M. Sugi, T. Misaki, Y. Tanabe, Improved Robust Method for Preparing Optically Active 3-Alkyl-3-phenyl-1, 4-dioxane-2, 5-diones; A Promising New Chiral Template, Synthesis, 2008.

[119] S.M. Guillaume, E. Kirillov, Y. Sarazin, J.-F. Carpentier, Beyond Stereoselectivity, Switchable Catalysis: Some of the Last Frontier Challenges in Ring-Opening Polymerization of Cyclic Esters, Chem. Eur. J., 2015, pp. 7988-8003.

[120] Y. Hu, W. Daoud, K. Cheuk, C. Lin, Newly Developed Techniques on Polycondensation, Ring-Opening Polymerization and Polymer Modification: Focus on Poly(Lactic Acid), Materials, 2016, p. 133.

[121] O. Nuyken, S. Pask, Ring-Opening Polymerization—An Introductory Review, Polymers, 2013, pp. 361-403.

[122] Q. Yin, L. Yin, H. Wang, J. Cheng, Synthesis and Biomedical Applications of Functional Poly(α-hydroxy acids) via Ring-Opening Polymerization of O-Carboxyanhydrides, Acc. Chem. Res., 2015, pp. 1777-1787.

[123] O. Dechy-Cabaret, B. Martin-Vaca, Controlled ring-opening polymerization of lactide and glycolide, Chem. Rev., 2004.

[124] S. Kaihara, S. Matsumura, A.G. Mikos, J.P. Fisher, Synthesis of poly(L-lactide) and polyglycolide by ring-opening polymerization, Nature protocols 2(11) (2007) 2767-71.

[125] S.H. Hyon, K. Jamshidi, Y. Ikada, Synthesis of polylactides with different molecular weights, Biomaterials, 1997, pp. 1503-1508.

[126] H.R. Kricheldorf, A. Serra, Influence of various metal salts on the optical purity of poly(L-lactide), Polymer Bulletin 14(6) 497-502.

[127] S. Dutta, W.-C. Hung, B.-H. Huang, C.-C. Lin, Recent Developments in Metal-Catalyzed Ring-Opening Polymerization of Lactides and Glycolides: Preparation of Polylactides, Polyglycolide, and Poly(lactide-co-glycolide), 245 (2011) 219-283.

[128] S. Slomkowski, Overview of Synthesis of Functional Polyesters, Handbook of Polyester Drug Delivery Systems, Pan Stanford2016, pp. 1-31.

[129] R. Mazarro, L.I. Cabezas, A. De Lucas, I. Gracia, J.F. Rodríguez, Study of Different Catalysts and Initiators in Bulk Copolymerization of d,l-Lactide and Glycolide, Journal of Macromolecular Science, Part A 46(11) (2009) 1049-1059.

[130] H. Tavana, A.W. Neumann, Recent progress in the determination of solid surface tensions from contact angles, Advances in colloid and interface science, 2007, pp. 1-32.

[131] H. Tavana, Contact Angle Measurements, Applied Surface Thermodynamics, Second Edition, CRC Press2010, pp. 283-327.

[132] E. Atefi, J. Mann, J Adin, H. Tavana, A Robust Polynomial Fitting Approach for Contact Angle Measurements, Langmuir : the ACS journal of surfaces and colloids, 2013, pp. 5677-5688.

[133] D.Y. Kwok, A.W. Neumann, Contact angle measurement and contact angle interpretation, Advances in colloid and interface science, 1999.

[134] E.L. Decker, B. Frank, Y. Suo, S. Garoff, Physics of contact angle measurement, Colloids and Surfaces A, 1999.

[135] C. Urata, D.F. Cheng, B. Masheder, A. Hozumi, Smooth, transparent and nonperfluorinated surfaces exhibiting unusual contact angle behavior toward organic liquids, RSC Adv., 2012, p. 9805.

[136] H. Tavana, F. Simon, K. Grundke, D.Y. Kwok, M.L. Hair, A.W. Neumann, Interpretation of contact angle measurements on two different fluoropolymers for the determination of solid surface tension, Journal of colloid and interface science, 2005, pp. 497-506.

[137] R. David, M.K. Park, A. Kalantarian, A.W. Neumann, Drop size dependence of contact angles on two fluoropolymers, Colloid Polym Sci, 2009, pp. 1167-1173.

[138] H. Tavana, D. Jehnichen, K. Grundke, M.L. Hair, A.W. Neumann, Contact angle hysteresis on fluoropolymer surfaces, Advances in colloid and interface science 134–135 (2007) 236-248.

[139] E.F. Hare, E.G. Shafrin, W.A. Zisman, Properties of films of adsorbed fluorinated acids, The Journal of physical, 1954.

[140] D.F. Cheng, B. Masheder, C. Urata, A. Hozumi, Smooth Perfluorinated Surfaces with Different Chemical and Physical Natures: Their Unusual Dynamic Dewetting Behavior toward Polar and Nonpolar Liquids, Langmuir : the ACS journal of surfaces and colloids, 2013, pp. 11322-11329.

[141] E. Burunkaya, N. Kiraz, Ö. Kesmez, M. Asilturk, H. Erdem Çamurlu, E. Arpaç, Sol–gel synthesis of IPTES and D10H consisting fluorinated silane system for hydrophobic applications, J Sol-Gel Sci Technol, 2010, pp. 99-106.

[142] R.M. Cornelius, J. Macri, K.M. Cornelius, J.L. Brash, Lipoprotein interactions with a polyurethane and a polyethylene oxide-modified polyurethane at the plasma–material interface, Biointerphases, 2016, p. 029810.

[143] R.C. Eberhart, M.S. Munro, J.R. Frautschi, Influence of Endogenous Albumin Binding on Blood-Material Interactionsa, Annals of the New York Academy of Science, 1987, pp. 78-95.

[144] T.A. Horbett, J.L. Brash, Proteins at Interfaces II: Fundamentals and Applications, American Chemical Society: Washington, DC1995.

[145] S.-Y. Jung, S.-M. Lim, F. Albertorio, G. Kim, M.C. Gurau, R.D. Yang, M.A. Holden, P.S. Cremer, The Vroman Effect: A Molecular Level Description of Fibrinogen Displacement, Journal of the American Chemical Society 125(42) (2003) 12782-12786.

[146] S.L. Hirsh, D.R. McKenzie, N.J. Nosworthy, J.A. Denman, O.U. Sezerman, M.M.M. Bilek, The Vroman effect: Competitive protein exchange with dynamic multilayer protein aggregates, Colloids and Surfaces B: Biointerfaces 103 (2013) 395-404.

APPENDIX A

Stock iodine monochloride (ICl) solution.

ICl stock solution is consist of 0.02 M ICI, 2.0 M NaCl, 0.02 M KC1, and 1.0 M HC1. The following reaction was used to prepare it:

$$2KI + KIO_3 + 6HC1 \longrightarrow 3ICI + 3KC1 + 3H_2O$$

Materials:

Item	Qty
KI	0.5550 g
KIO_3	0.3567 g
NaCl	29.23 g
HCl	21 ml
DI water	250 ml
CCl_4	150 ml
Erlenmeyer flask	3-4
Sep Funnel	1

The ICl preparation should be carried out in the fume hood.

1. In an appropriate flask dissolve 0.5550 g KI (0.00334 mol), 0.3567g KIO_3 (0.00167 mole) and 29.23g NaCl in an approximately 150 ml of DI water.

2. Then add 21ml of concentrated HCl (sp.gr. 1.18, 11.8M HCl).

   Note: There should be no precipitate, and the resulting liquid should be a clear light yellow solution. Discard any preparation that is not a clear yellow solution.

3. Bring the solution up to 250 ml by adding enough DI water to the flask.

4. Place the solution in a clean separatory funnel.

5. Add 10 ml CCl_4 to the funnel and shake vigorously. Let the funnel sit for few minutes. Discard the lower pink (faint red) CCl_4 organic phase from the bottom of the funnel and repeat the extraction (4-5 times) until the organic phase is colorless.

Note: This step is required to remove the free iodine from the ICl solution. After the initial extraction, a biphasic solution forms: the top layer has a clear yellow color and contains ICl, whereas the bottom layer is pink or faint red CCl_4 layer. The number of extractions depends on the amount of the free iodine.
Caution: CCl_4 is a carcinogen: Avoid breathing vapors or skin contact.

6. Transfer the aqueous layer to a clean Erlenmeyer flask and aerate with saturated water vapor for 8-10h to remove any trace of CCl_4 (Fig.1).

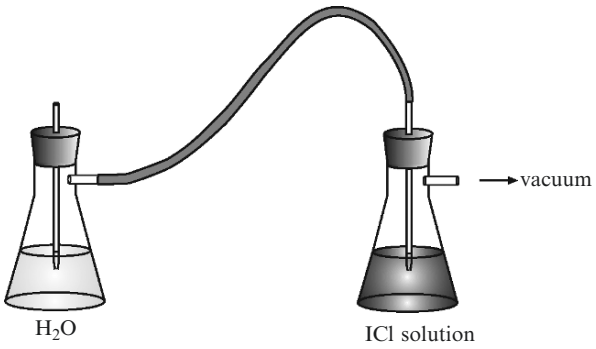

Fig.1A. Apparatus for removing the CCl_4 from the ICl solution with moist air. The first flask contains DI water. The vacuum draws moist air into the second flask that contains ICl solution.

References:

1. Ralph W. Helmkamp, Ruth L. Goodland, William F. Bale, Irving L. Spar, Letitia E. Mutschle., High Specific Activity Iodination of γ-Globulin with Iodine-131 Monochloride, CANCER RESEARCH. V20, p:1495-1500,1960
2. Lundblad Roger, Chemical Modification of Biological Polymers, Boca Raton, FL, CRC press, p119-120, 2012.

Albumin Iodination

Materials:

#	ITEM
2	Biorad Econo-Pac 10DG chromatography columns
5	Falcon 2054 tubes w/ caps
86	gamma tubes & racks (2x40 for columns, 6 for activity standards)
5	plastic transfer pipets
4	50 ml centrifuge tubes for buffers
1	50 ml centrifuge tube for biowaste
1	15 ml centrifuge tube for NaCl/ICl mixture
1	15 ml centrifuge tube for protein solution
80	2 oz. sample cups
	ice from 2nd floor chemistry
	latex and PP gloves
	lead pig
	0.02 M ICl solution (usually in Foege 351B)
	P20 & P1000 "hot" Pipetmans
	50 & 1000 µl "hot" pipet tips

Prep (day before):

a) 1L – 1X cPBSz

1L of 1x	
Chemical	**Amt. in grams**
NaCl	7.0
citric acid, monohydrate	2.1
Na phosphate, monobasic	1.3
pH to 6.93 using approx. 1.5 g solid NaOH Add azide to solution after pHing.	
Na azide	0.2
1X CPBSz at pH=7.4	

b) 50 ml – 2M NaCl

100 mL	
Chemical	**Amt. in grams**
NaCl	11.70

c) 50 mL– 2x Borate

100 mL	
Chemical	**Amt. in grams**
NaCl	1.87
H_3BO_3	2.47
pH to 7.75	

Make:

d) 50 ml – 2X Borate
e) 50 ml – 1X Borate
f) 50 ml – 2M NaCl
g) 1L – 1X cPBSz
h) 10ml – 10mg/mL Alb in 1X borate and store in a 15mL centrifuge tube

Prep: (day before)

- Make buffers.
- Collect all Materials.

Iodination:

1. Degas 1x cPBSz for ~1 h.
2. Place degassed 1X cPBSz over ice.
3. Place 1X Borate in 'cold' water bath.
4. Take cap off 1st column, pour off excess buffer and fill w/ cPBSz buffer to rinse. Fill at least 2X.
5. Make 10ml of 10mg/mL Alb w/ 1x Borate and store in 15ml centrifuge tube. Weigh out 100 mg Alb, place in 15ml centrifuge tube, fill to 10 mL with 1x Borate and place in water bath until dissolved.
6. Make ICl/NaCl mixture: 5ml 2M NaCl + 11.5 μl of 0.02M stock ICl (3:1 ratio).
7. Prepare following 3 – Falcon 2054 tubes and place on ice.

   Tube 1……. 0.5 ml of 2X Borate

   Tube 2……. 0.5 ml of ICl/NaCl mixture

Tube 3……. 0.5ml of 10mg/ml Alb in 1X Borate

8. Calculate volume of ^{125}I to give activity of 1mCi. Original solution is 100mCi/ml on reference date.

   decay factor = exp(-0.01153 x _____ days) = _____

   1mCi = 10 μl/decay factor = _____ μl ^{125}I to add.

9. Add ^{125}I to 0.5ml 2X borate.
10. Add ICl/NaCl mixture to 2X borate.
11. Add 0.5 ml of 10mg/ml Alb to 2X borate. Be careful not to create any bubbles as this can denature the protein.
12. Keep on ice for 20 min. to allow for protein labeling reaction. ^{125}I bind to the tyrosine amino acid in the protein.
13. Place 40 cups into rotating table.
14. Set up gamma tubes for 2 columns and activity standards.
15. Add 1.5 ml labeled protein to column along the side. Be careful to avoid creating bubbles. Let protein drip through advancing the table after 0.5ml has been collected in each cup (~10 drops). DO NOT add buffer until all protein solution has passed into the column.
16. Once drops stop, add 0.5ml cPBSz, collect 0.5 ml in cup, advance table, and repeat until 40 fractions have been collected.
17. Drain and rinse 2nd column.
18. Take 5μl samples from each cup and count for 0.1 min. to identify peak.
19. Pool samples from protein peak (3-4 cups) and run through the second column repeating fraction collection and peak identification.

20. Collect purified labeled protein (~3 cups) and run six 5 μl activity standards for 0.1 min. counts.

$$\text{Activity} = \frac{(\text{Ave \# counts for 0.1 min.}) \times 10}{(5\times10^{-3}\ \text{ml})} = \_\_\_\_\_\ \text{cpm/ml}$$

21. Aliquot (if necessary), place in lead pig, and freeze in -80ºC freezer.

22. Dispose of all radioactive waste in LSA box or liquid waste bucket.

23. Complete radiation survey of lab.

24. Get thyroid assay at Radiation Safety within 3 days!

Albumin Adsorption

Last Updated: 4/11/01

Materials:

#	Item
# samples	2oz. PS cups and racks
	buffer chemicals
# samples + 6	gamma tubes and racks
	250 mL PS bottle or 50 mL centrifuge tube
	human plasma
	iodinated Alb
	aluminum foil
	latex and PP gloves
	lead apron
	safety glasses
	lab coat
	P50 & P1000 "hot" Pipetman
	P1000 Pipetman
	timer
	50µl 1 1000µl pipet tips

Make:

- 4L 1X CPBSzI

Prep (day before):

a) 4L 1X cPBSzI

4L of 1x	
Chemical	**Amt. in grams**
NaCl	25.72
NaI	6.00
citric acid, monohydrate	8.41
Na phosphate, monobasic	5.52
pH to 7.4 using approx. 6.3 g solid NaOH. Add azide to solution after pHing.	
Na azide	0.80

Prep: (day before)
a) Make 4L 1X CPBSzI
b) Turn on water bath and check that it is at the correct temperature and has enough water to come ½ way up the PS cups in the racks.

Protein Adsorption: Note difference in size of activity standards due to higher [Alb] in plasma

1. Turn on water bath and set to 37ºC.

2. Rinse samples in DI.

3. Presoak samples for 2 h in 0.75ml degassed buffer. Cover samples with aluminum foil.

4. Thaw iodinated protein in hood.

5. Thaw human plasma.

6. Fill rinse system with 3L 1X CPBSzI and check it is working properly.

7. Prepare 2% plasma w/ degassed 1X CPBSzI in 250ml PS bottle. Shake gently to mix:

   (# of samples)(0.75ml/sample)(1.1) = ml of 2% plasma to make, round up to convenient number.

8. Calculate minimum protein to signal ratio:

   (ng protein/cm^2 to measure)(area/sample) = 100 cpm and **solve for 1ng protein = "x" cpm**.

9. Calculate protein concentration in dilute plasma.

10. Calculate the amount of iodinated protein to be added to the 2% plasma.

    (ng protein/mL 1% plasma)(min. protein/cpm ratio)(mL of 1% plasma)(1/specific activity of hot protein)(1000 μL/1mL) = **μL of hot protein to add.**

11. Place presoaked samples into water bath to bring up to 37ºC.

12. Add iodinated protein to 2% plasma.

13. Take six **5**μl activity standards of "hot" 2% plasma and count for 1 min.
    - if large variability, repeat
    - if not hot enough, calculated the necessary amount of iodinated protein to add, add it to the 2% plasma, and repeat the activity standards.
14. Start timer and add 0.75ml of "hot" 2% plasma to the first sample at 1 minute. Do subsequent samples at 30 second to 1 minute intervals until all samples complete.
15. Set up gamma tubes and racks.
16. Wait until 2 hours have expired since first sample was started.
17. Rinse each sample at the same time interval as the "hot" protein solution was added. Rinse in two steps into two different containers: 1st rinse of 3 seconds for hot rinse, and 2nd rinse of 4-5 seconds for cold rinse. 1st rinse goes into the radioactive liquid waste bucket. 2nd rinse is poured down the sink and flushed with lots of water.

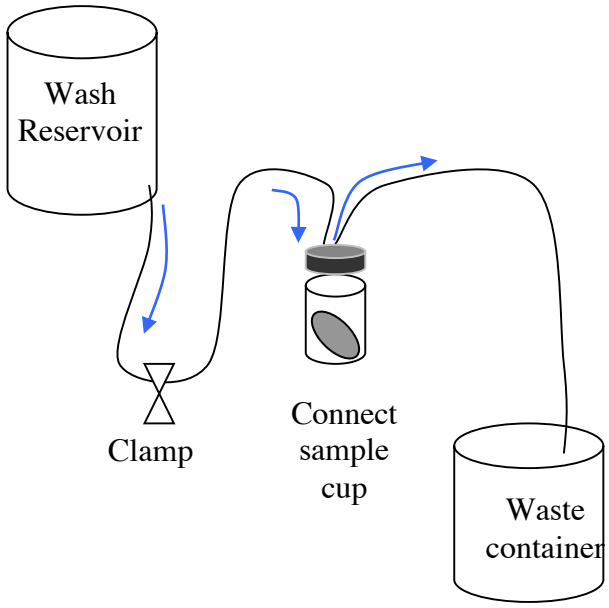

Fig.2A. Apparatus for washing samples.

18. Each sample is placed in an individual gamma counter tube and counted for 10 minutes each.

19. Dispose of all radioactive waste in LSA box or liquid waste bucket.

20. Turn off water bath.

21. Complete radiation survey of lab.

22. Get thyroid assay at Radiation Safety within 3 days!

Fibrinogen Iodination

Materials:

#	ITEM
2	Biorad Econo-Pac 10DG chromatography columns
5	Falcon 2054 tubes w/ caps
86	gamma tubes & racks (2x40 for columns, 6 for activity standards)
5	plastic transfer pipets
4	50 ml centrifuge tubes for buffers
1	50 ml centrifuge tube for biowaste
1	15 ml centrifuge tube for NaCl/ICl mixture
1	1.5 ml centrifuge tube for protein solution
80	2 oz. sample cups
	ice from 2nd floor chemistry
	latex and PP gloves
	lead pig
	0.02 M ICl solution (usually in B20)
	P20 & P1000 "hot" Pipetmans
	P200 & P1000 Pipetmans
	50 & 1000 µl "hot" pipet tips

Prep (day before):

a) 1L – 1X cPBSz

1L of 1x	
Chemical	**Amt. in grams**
NaCl	7.0
citric acid, monohydrate	2.1
Na phosphate, monobasic	1.3
pH to 6.93 using approx. 1.5 g solid NaOH Add azide to solution after pHing.	
Na azide	0.2
1X CPBSz at pH=7.4	

b) 50 ml – 2M NaCl

100 mL	
Chemical	**Amt. in grams**
NaCl	11.70

c) 50 mL– 2x Borate

100 mL	
Chemical	**Amt. in grams**
NaCl	1.87
H_3BO_3	2.47
pH to 7.75	

Make:

d) 50 ml – 2X Borate
e) 50 ml – 1X Borate
f) 50 ml – 2M NaCl
g) 1 L – 1X cPBSz
h) 1 ml – 10 mg/mL Fg in 1X cPBSz and store in a 1.5mL centrifuge tube

i) **Prep:** (day before)

- Make buffers.
- Collect all Materials.

Iodination:

1. Degas 1x cPBSz for ~ 1hr
2. Turn on water bath and set to 37 ºC.
3. Take cap off 1st column, pour off excess buffer and fill w/ CPBSZ buffer to rinse. Fill at least 2X.
4. Thaw Fg in 37ºC water bath.
5. Make 1ml of 10mg/ml Fg w/ 1X CPBSZ and store in 1.5ml centrifuge tube in water bath.

   (ml of Fg solution to use) = 10mg/(Fg solution concentration)

   - add CPBSZ to 1ml.
6. Make ICl/NaCl mixture: 10ml 2M NaCl + 29.1 μl 0.02M stock ICl (2:1 ratio).
7. Prepare following 3 – Falcon 2054 tubes and place on ice.

   Tube 1……. 0.5 ml of 2X Borate

   Tube 2……. 0.5 ml of ICl/NaCl mixture

Tube 3……. 0.5ml of 10mg/ml Fg in CBPSZ

8. Calculate volume of ^{125}I to give activity of 1mCi. Original solution is 100mCi/ml on reference date.

   decay factor = exp(-0.01153 x _____ days) = _____

   1mCi = 10 μl/decay factor = _____ μl ^{125}I to add.

9. Add ^{125}I to 0.5ml 2X borate.
10. Add ICl/NaCl mixture to 2X borate.
11. Add 0.5 ml of 10 mg/ml Fg to borate. Be careful not to create any bubbles as this can denature the protein.
12. Keep on ice for 20 min. to allow for protein labeling reaction. ^{125}I bind to the tyrosine amino acid in the protein.
13. Place 40 cups into rotating table.
14. Set up gamma tubes for 2 columns and activity standards.
15. Add 1.5ml labeled protein to column along the side. Be careful to avoid creating bubbles. Let protein drip through advancing the table after 0.5ml has been collected in each cup (~10 drops). DO NOT add buffer until all protein solution has passed into the column.
16. Once drops stop, add 0.5ml CPBSZ, collect 0.5ml in cup, advance table, and repeat until 40 fractions have been collected.
17. Drain and rinse 2nd column.
18. Take 5μl samples from each cup and count for 0.1 min. to identify peak.
19. Pool samples from protein peak (3-4 cups) and run through the second column repeating fraction collection and peak identification.

20. Collect purified labeled protein (~3 cups) and run six 5 μl activity standards for 0.1 min. counts.

$$\text{Activity} = \frac{(\text{Ave \# counts for 0.1 min.}) \times 10}{(5\times10^{-3}\ \text{ml})} = \_\_\_\_\_\ \text{cpm/ml}$$

21. Aliquot (if necessary), place in lead pig, and freeze in -80ºC freezer.

22. Dispose of all radioactive waste in LSA box or liquid waste bucket.

23. Complete radiation survey of lab and get thyroid assay at Radiation Safety within 3 days!

Fibrinogen Adsorption

Materials:

#	Item
# samples	2oz. PS cups and racks
	buffer chemicals
# samples + 6	gamma tubes and racks
	250 mL PS bottle or 50 mL centrifuge tube
	50 μl 1000 μl pipet tips
	iodinated protein
	aluminum foil
	latex and PP gloves
	lead apron
	safety glasses
	lab coat
	P50 & P1000 "hot" Pipetman
	P1000 Pipetman
	timer

Prep (day before):

a) 4L 1X cPBSzI

4L of 1x	
Chemical	**Amt. in grams**
NaCl	25.72
NaI	6.00
citric acid, monohydrate	8.41
Na phosphate, monobasic	5.52
pH to 7.4 using approx. 6.3 g solid NaOH. Add azide to solution after pHing.	
Na azide	0.80

Prep: (day before)
c) Make 4L 1X cPBSzI
d) Degas 1L of 1X cPBSzI for a minimum of 1 hours

Protein Adsorption:

1. Turn on water bath and set to 37ºC.
2. Rinse samples in DI.
3. Presoak samples for 2 hrs in 0.75ml degassed buffer. Cover samples with aluminum foil.
4. Thaw iodinated protein in hood.
5. Fill rinse system with 3L 1X CPBSzI and check that it is working properly.
6. Prepare 2% plasma concentration (2x) of protein w/ degassed 1X CPBSzI in 50ml centrifuge tube. Rock gently to mix:

   (# of samples)(0.75ml/sample) = ml of 2x protein to make, round up to convenient number, must account for 0.6 mL for two sets of activity standards.
7. Calculate minimum signal needed from standards:

   (CPM desired)/(ng protein)(2x protein concentration, mg/mL)(Standard volume, uL)(1000) = (**minimum CPM needed)** for adequate sample measurement. EXAMPLE:

   For a 1% Fg (0.03mg/mL) protein adsorption, we want 2x the background of the gamma-counter detection of 1 ng of protein:

   (50CPM/ng)(0.06mg/mL)(10uL)(1000) = **30,000 CPM** is the minimum standard counts needed.
8. Calculate protein concentration in dilute plasma.

   Calculate the amount of iodinated protein to add:

   (mL of 2x protein)(mg/mL of 2x protein)(CPM/ng desired)(10^6 ng/mg)/ (CPM/mL from iodination standards)= **mL of hot protein to add.**
9. Place presoaked samples into water bath to bring up to 37ºC.

10. Add iodinated protein to 2 x protein in buffer.

11. Take five 10 μl activity standards of "hot" 2x protein and count for 1 min.

    - if large variability, repeat
    - if not hot enough, based on calculations from step7, calculate the necessary amount of iodinated protein to add, add it to the 2x protein, and repeat the activity standards.

12. Start timer and add 0.75ml of "hot" 2x protein to the first sample. Reaspirate 3 times to insure adequate mixing. Do subsequent samples at 30 second to 1 minute intervals until all samples complete.

13. Set up gamma tubes and racks.

14. Wait until 1-2 hours have expired since first sample was started (based on experimental design).

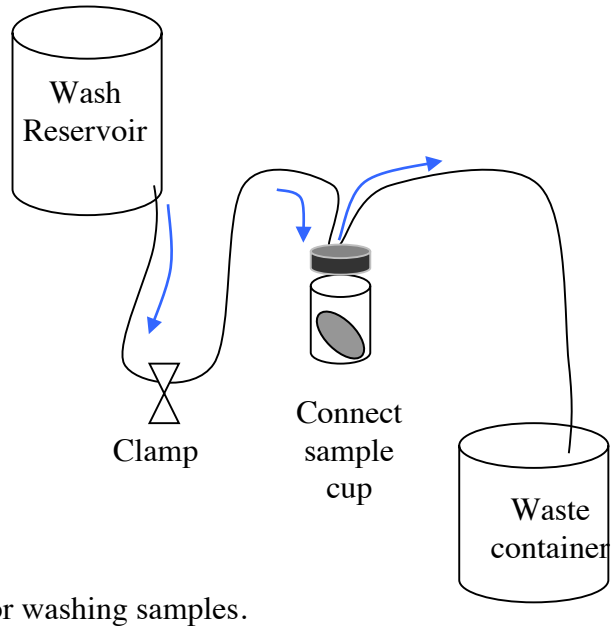

Fig.2A. Apparatus for washing samples.

15. Rinse each sample at the same time interval as the "hot" protein solution was added. Rinse in two steps into two different containers: 1st rinse of 3 seconds for hot rinse, and 2nd rinse of

4-5 seconds for cold rinse. 1st rinse goes into the radioactive liquid waste bucket. 2nd rinse is poured down the sink and flushed with lots of water.

16. Each sample is placed in an individual gamma counter tube and counted for 10 minutes each.
17. Dispose of all radioactive waste in LSA box or liquid waste bucket and record waste values on sheets.
18. Turn off water bath.
19. Complete radiation survey of lab and sign log-book.
20. Get thyroid assay at Radiation Safety within 3 days!

Platelet Adhesion

SOLUTIONS, REAGENTS

1X PSB, pH=7.4	1X PSB-complete	
(reagent diluent)	(platelet suspension)	1X DUBELCCO'S PBS
137mmNaCl	1X PSB	Lonza catalog # 17-513
5.5mM dextrose	2.5mM $CaCl_2$	
4mg/ml BSA	1.0mM $MgCl_2$	
2.7mM KCl	0.1U/ml apyrase	
1.4mM Na phosphate, mono		
10mM HEPES	Human plasma, 1ml tube	Apyrase, 200 μL

FOR PLATELET ASSAY (all solutions at room temperature)

50mls 1X PSB➔ use to make 50 mls 1% human plasma preincubation solution

50ml 1X PSB + 500uL pooled human plasma, block 1.5hr, 37'C

50mls 1X PSB➔use to block preincubated samples, RT, 1hr

40mls platelets @ 10^8 platelets per ml in 1XPSB-complete, in 50ml conical tube

40.0mls – X mls of 1X PSB

50uL 100X $CaCl_2$

50uL 100x $MgCl_2$

200 μL apyrase (0.025UN/uL)

invert tube several times to mix

Add X mls of platelets to equal 40 x 10^8 platelets

1X Dubelco's phosphate buffered saline for rinsing

PLATELETS

Blood drawn in ACD, handled at RT, plastic only

Spin 1—900rpm (180g) 20 minutes, harvest platelet rich plasma fraction

Spin 2—2800rpm (1500g) 15 minutes, draw off plasma and resuspend platelet pellet in 1XPSB to count
Count platelets at 1:400 dilution, calculate total final volume needed so that platelets are 10^8/ml
Using 1x PSB, adjust liquid volume so [final] = 1 x 10^8/ml platelets, + $CaCl_2$, $MgCl_2$, and 4uL/ml apyrase.

A dilution	B dilution
25μL platelets	25μL A dil
475μL 1X PSB/Tblu	475μL 1X PSB/Tblu
[final]=1:20	[final]=1:400

Samples:

1. Samples are rinsed 2x with 1X PSB
2. Preadsorb with 2.2ml 1% human plasma in 1X PSB, 1.5hr, 37'C. Aspirate.
3. Block samples with 2.2mls 1XPSB, 1.0hr, RT. Aspirate
4. Rinse 2x with 1X PBS to remove unbound proteins.
5. For cover slips, add 2.0ml platelets/1X PSB-complete.
6. Place cryotubes on their side in pipet reservoir and place in incubator along with cover slip plate. Gently rotate every 15 minutes. Platelets will settle via gravity and attach to surface. Total incubation time is 90 minutes.
7. Rinse 6x with 1X phosphate buffered saline to remove non-adherent platelets.
8. Process for SEM with all samples in 12 well plates

- Transfer samples to the same 12-well plate, add 1.0ml Karnovsky's solution in 0.1M NaCacodylate per well and fix 2 hrs (or overnight).
- 2 hour fixation—parafilm plate and leave in RT fume hood in labeled secondary container. Continue processing until sample is in 70% ethanol. Parafilm the plate, place in a labeled/dated secondary container, and leave in cold room overnight. The next day, allow the plate and contents to warm up to room temperature before continuing with next ethanol dehydration steps.
- Overnight fixation--Parafilm plates, place in a labeled/dated secondary container, and leave in the cold room overnight. Proceed with rinses, OsO_4 staining, h

FIXATION—All fixations solutions are toxic! Use only in working fume hood and work over absorbent pads. Make solutions fresh for each experiment. All leftover solutions, waste, and 50% ethanol rinses can be pooled in the same labeled waste bottle.

0.2M Sodium phosphate buffer —100ml media bottle

Solution X: 35.61g Na_2HPO_4 .$2H_2O$ in 100ml dH_2O

Solution Y: 27.6g $NaH_2PO4.H_2O$ in 100ml dH_2O

0.2M buffer: 40.5ml Sol X + 9.5ml Sol Y, pH = 7.4

Pipet following reagents into container in the given order.

Recipes given for processing 10-12 samples. Scale as necessary.

KARNOVSKY'S SOLUTION—50ml conical tube

5.0ml dH_2O

5.0ml 0.2M sodium phosphate buffer

15.0ml 0.2M sodium cacodylate

6.0ml Karnovsky's solution

mix by inverting, make fresh immediately before use

CaCo Rinse—100ml media bottle

25.0ml dH_20

25.0ml 0.2M sodium phosphate buffer

50.0ml 0.2M sodium cacodylate

Osmium tetroxide stain—50ml conical

2.0ml dH_2O

2.0ml 0.2M sodium phosphate buffer

8.0ml 0.2M sodium cacodylate

4.0ml 4% OsO_4

PROCESSING SAMPLES

Fix samples 2hrs RT or overnight 4 °C in 2ml Karnovsky's solution

All the following steps are done in a fume hood over an absorbent pad, collect all rinses in suction flask and dispose of as labeled hazardous waste

Rinse using 2.0ml CaCo rinse, 3 x 10 min RT

Stain using 1.5ml OsO_4 stain, 30min RT

Rinse using 2.0ml CaCo rinse, 3 x 10 min RT

Rinse in 50 % ethanol, 2 x 5min

The 1st and 2nd 50% ethanol rinse is collected as hazardous waste. Empty the waste flask, rinse 2X with 10mls 50% ethanol and collect that rinse as hazardous waste before collecting the 70% ethanol rinse. Beginning with the 70% ethanol rinse you will collect the washes as ethanol only waste ([final]=85%).

Rinse in 70% ethanol, 1 x 15 min (stop here if you're done for the day, leave at 4 °C O/N)

Rinse in 80% ethanol, 1 x 15 min

Rinse in 90% ethanol, 1 x 15 min

Rinse in 100% ethanol, 1 x 15 min

Change 100% ethanol rinse, parafilm the plate, and transport to MolES for CPD.

The sample must remain under 100% ethanol during transport and when transferred to ethanol-filled CPD chamber.

Allow 3-3.5 h total for CPD and sputter coating.

After sputter coating, store the samples in a sealed container with a desiccator packet.

PATENT APPLICATION PUBLICATION_US 2017/0342205 A1

HALOGENATED CYCLIC DIESTERS, RELATED POLYMERS, AND METHODS FOR THEIR PREPARATION AND USE

CROSS-REFERENCE TO RELATED APPLICATIONS

This application claims the benefit of U.S. Patent No. 62/259,514, filed November 24, 2015, and U.S. Patent No. 62/117,900, filed February 18, 2015, each expressly incorporated herein by reference in its entirety.

BACKGROUND OF THE INVENTION

Polymers derived from lactic acid and glycolic acid have been extensively used for various biomedical applications due to their biocompatibility and biodegradability. The ability to modify the physiochemical properties, such as degradability, hydrophobicity, and hydrophilicity, of these polymers is a key to expand the spectrum of their uses. Conventional approaches usually involve copolymerization and block copolymer preparations. In contrast, the use of lactic acid and glycolic acid derivatives as monomers for preparing polylactides and polyglycolides is less well known. Despites advances in the preparation of polylactides and polyglycolides, a need exists for the simple and versatile preparation of polylactides and polyglycolides having improved properties. The present invention seeks to fulfill these needs and provide further related advantages.

SUMMARY OF THE INVENTION

The present invention provides halogenated cyclic diesters, halogenated polymers derived from the cyclic diesters, and methods for making the halogenated cyclic esters and related halogenated polymers. In certain embodiments, the present invention provides fluorinated cyclic diesters, fluorinated polymers derived from these cyclic diesters, and methods for making the fluorinated cyclic diesters and related fluorinated polymers.

In one embodiment, the invention provides a cyclic diester having formula (I)

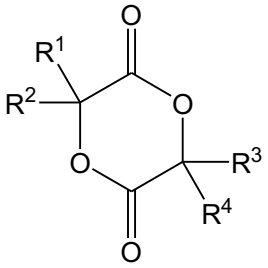

(I)

stereoisomers and racemates thereof,

wherein R^1, R^2, R^3, and R^4 are independently selected from hydrogen, C1-C24 alkyl, aryl, fluoro, chloro, and halocarbon, with the proviso that at least one of R^1, R^2, R^3, or R^4 is selected from fluoro, chloro, or halocarbon.

In another embodiment, the invention provides a cyclic diester having formula (I)

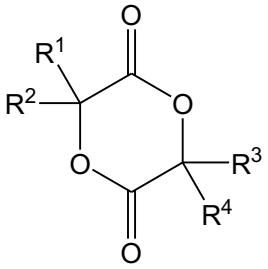

(I)

stereoisomers and racemates thereof,

wherein R^1, R^2, R^3, and R^4 are independently selected from hydrogen, C1-C24 alkyl, aryl, fluoro, and fluorocarbon (e.g., C1-C24 fluoroalkyl), with the proviso that at least one of R^1, R^2, R^3, or R^4 is selected from fluoro or fluorocarbon.

In certain embodiments, the fluorocarbon is a C1-C24 fluoroalkyl group. In other embodiments, the fluorocarbon is a C1-C12 fluoroalkyl group. In further embodiments, the fluorocarbon is a C1-C6 fluoroalkyl group.

In a further embodiment, the invention provides a cyclic diester having formula (II)

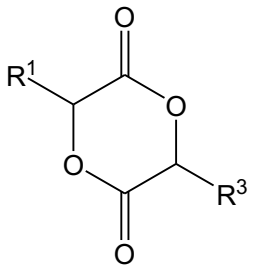

(II)

stereoisomers and racemates thereof,

wherein R^1 and R^3 are independently selected from C1-C24 alkyl and fluorocarbon (e.g., C1-C24 fluoroalkyl), with the proviso that at least on of R^1 or R^3 is fluorocarbon.

In another aspect, the invention provides polymers prepared from the cyclic diesters of the invention.

In one embodiment, the invention provides a halogenated polymer, comprising a repeating unit having formula (III)

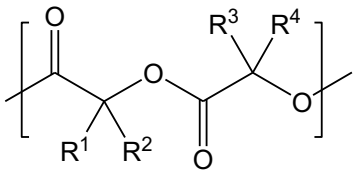

(III)

wherein

R^1, R^2, R^3, and R^4 are independently selected from hydrogen, C1-C24 alkyl, aryl, fluoro, chloro, and halocarbon, with the proviso that at least one of R^1, R^2, R^3, or R^4 is selected from fluoro, chloro, or halocarbon.

In another embodiment, the invention provides a fluorinated polymer, comprising a repeating unit having formula (III)

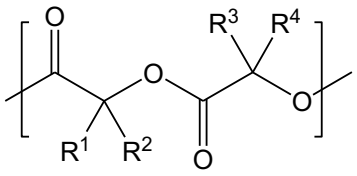

(III)

wherein

R^1, R^2, R^3, and R^4 are independently selected from hydrogen, C1-C24 alkyl, aryl, fluoro, and fluorocarbon (e.g., C1-C24 fluoroalkyl), with the proviso that at least one of R^1, R^2, R^3, or R^4 is selected from fluoro or fluorocarbon.

In one embodiment, the invention provides a halogenated polylactic acid, comprising a repeating unit having formula (IV)

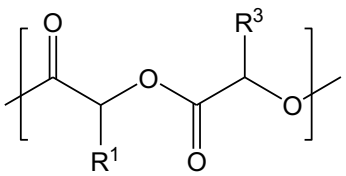

(IV)

wherein

R^1 and R^3 are independently selected from C1-C24 alkyl and halocarbon, with the proviso that at least one of R^1 or R^3 is halocarbon.

In another embodiment, the invention provides a fluorinated polylactic acid, comprising a repeating unit having formula (IV)

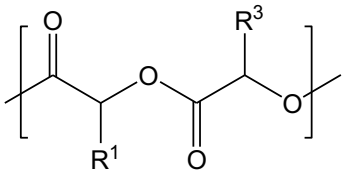

(IV)

wherein

R^1 and R^3 are independently selected from C1-C24 alkyl and fluorocarbon (e.g., C1-C24 fluoroalkyl), with the proviso that at least one of R^1 or R^3 is fluorocarbon.

In certain embodiments, the polymer of the invention further comprises one or more repeating units derived from comonomers suitable for polymerization with a halogenated cyclic diester.

In one embodiment, the invention provides a polymer having formula (V)

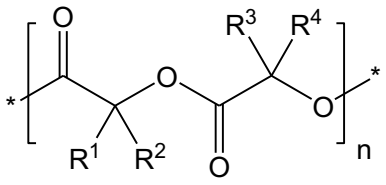

(V)

wherein

*represents the terminal groups of the polymer, and

n is an integer from about 10 to about 1000.

In another embodiment, the invention provides a polylactic acid having formula (VI)

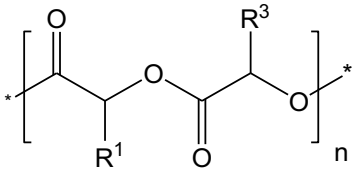

(VI)

wherein

*represents the terminal groups of the polymer, and

n is an integer from about 10 to about 1000.

In one embodiment, the invention provides a polymer having formula (VII)

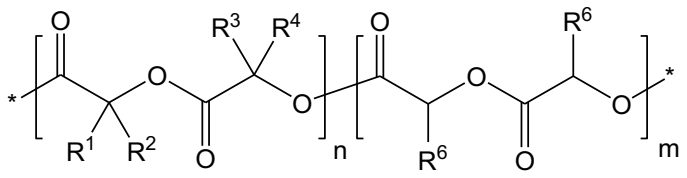

(VII)

wherein

R^6 is hydrogen or methyl,

n is an integer from about 10 to about 1000, and

m is an integer from about 10 to about 1000.

In another embodiment, the invention provides a polylactic acid having formula (VIII)

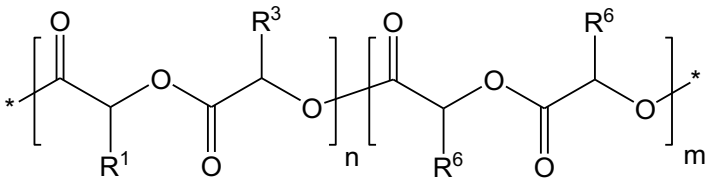

(VIII)

wherein

R^6 is hydrogen or methyl,

n is an integer from about 10 to about 1000, and

m is an integer from about 10 to about 1000.

In certain embodiments, the polymers of the invention are random copolymers. In other embodiments, the polymers of the invention are block copolymers.

In a further aspect of the invention, surfaces coated with a polymer of the invention are provided. In one embodiment, the invention provides a surface of a substrate, wherein at least a portion of the surface is coated with a polymer of the invention. Suitable substrates include drug delivery devices, devices having a degradation-inhibiting coating, devices having a hydrophobic surface with high contact angle, and devices that contact blood. In certain embodiments, the substrate is a medical device, such as a cardiovascular stent.

In another aspect, the invention provides methods for making halogenated polymers. In one embodiment, the method comprises:

subjecting a polymer with an ammonia plasma to provide a polymer functionalized with amino groups;

reacting the polymer functionalized with amino groups with a suitably reactive reagent comprising a halocarbon, wherein at least a portion of the amino groups react with the

reagent to provide a polymer having at least of portion of the amino groups converted to amine groups covalently coupled to the halocarbon.

In another embodiment, the method comprises:

subjecting a polymer with an ammonia plasma to provide a polymer functionalized with amino groups;

reacting the polymer functionalized with amino groups with a suitably reactive reagent comprising a fluorocarbon (e.g., fluoroalkyl group), wherein at least a portion of the amino groups react with the reagent to provide a polymer having at least of portion of the amino groups converted to amine groups covalently coupled to the fluorocarbon.

1.1 DESCRIPTION OF THE DRAWINGS

The foregoing aspects and many of the attendant advantages of this invention will become more readily appreciated as the same become better understood by reference to the following detailed description, when taken in conjunction with the accompanying drawings.

FIGURE 1 is a schematic illustration of a representative preparation of cyclic diesters of the invention from alpha-hydroxy acids and reactive alpha-bromo alkanoyl bromide compounds.

FIGURE 2 is a schematic illustration of a representative preparation of cyclic diesters of the invention starting from the alpha-hydroxy acid: $CF_3CH(OH)$-C(=O)OH.

FIGURE 3 is a schematic illustration of a representative preparation of cyclic diesters of the invention starting from the alpha-hydroxy acid: $CF_2(OH)$-C(=O)OH.

FIGURE 4 is a schematic illustration of a representative preparation of cyclic diesters of the invention starting from the alpha-hydroxy acid: $(CF_3)_2C(OH)$-C(=O)OH.

FIGURE 5 is a schematic illustration of a representative preparation of cyclic diesters of the invention starting from the alpha-hydroxy acid: $CF_3C(Ph)(OH)$-C(=O)OH.

FIGURE 6 is a schematic illustration of a representative preparation of fluorinated polymers of the invention from cyclic diesters.

FIGURE 7 is a schematic illustration of representative preparations of fluorinated polymers of the invention from cyclic diesters prepared from a representative alpha-hydroxy acid: $CF_3CH(OH)$-C(=O)OH.

FIGURE 8 is a ^1H NMR spectrum of trifluoromethyl-substituted lactic acid monomers in acetonitrile-d_3.

FIGURE 9 is a ^{13}C NMR spectrum of trifluoromethyl-substituted lactic acid monomers in acetonitrile-d_3.

FIGURE 10 is a ^{19}F NMR spectrum of trifluoromethyl-substituted lactic acid monomers in acetonitrile-d_3.

FIGURE 11 is a ^{1}H NMR spectrum of the trifluoromethyl-substituted polylactide in $CDCl_3$.

FIGURE 12 is a ^{19}F NMR spectrum of trifluoromethyl-substituted polylactide in $CDCl_3$.

FIGURE 13 is a schematic illustration of the preparation of fluorinated polymers of the invention prepared from reaction of suitably reactive fluoroalkyl reagents with amino-containing polymers prepared by treatment of suitable polymers with ammonia plasma.

DETAILED DESCRIPTION OF THE INVENTION

Fluorinated polymers demonstrate excellent inertness in various biological environments and good blood compatibility, and have been used in various biomedical applications, such as prosthetics and drug delivery.

In one aspect, the present invention provides halogenated polymers and methods for their preparation. In the halogenated polymers of the invention, the structure of polymer backbone remains unchanged and this in turn results in retention of their hydrolysis characteristics. However, due to the introduction of halogens (i.e., fluorine or chlorine) into these polymers the halogenated (e.g., fluorinated and or chlorinated) polymers of the invention hydrolyze at a divers rate due to their increased hydrophobicity associated with the replacement of hydrogen in the parent polymers with a halogen (e.g., fluorine or chlorine), thereby expanding their performance in biological environments.

As used herein, the term "halogenated" or "halogen" refers to a cyclic diester or polymer that includes one or more chlorine and/or fluorine atoms.

The present invention provides halogenated cyclic diester, halogenated polymers derived from the cyclic diesters, and methods for making the halogenated cyclic esters and related halogenated polymers. In certain embodiments, the present invention provides fluorinated cyclic diesters, fluorinated polymers derived from the cyclic diesters, and methods for making the fluorinated cyclic diesters and related fluorinated polymers.

Cyclic Diesters

In one aspect, the invention provides halogenated cyclic diesters (i.e., cyclic diesters that include one or more halogen substituents also referred to herein as halogen-containing cyclic diesters). The cyclic diesters of the invention can be prepared from alpha-hydroxy acids. See FIGURES 1-5 and 7. The cyclic diesters of the invention can be polymerized to provide polyesters that include fluorine and/or chlorine substituents. See FIGURES 6 and 7. The cyclic diesters of the invention are 6-membered ring compounds. In certain embodiments, the cyclic diester is a lactide or a lactide derivative. In other embodiments, the cyclic diester is a glycolide or a glycolide derivative. The cyclic diesters of the invention have the general structure shown in FIGURE 1 where R^1-R^4 are as described below. FIGURE 1 is a schematic illustration of a representative preparation of cyclic diesters of the invention from alpha-hydroxy acids and reactive alpha-bromo alkanoyl bromide compounds.

In one embodiment, the cyclic diester of the invention has formula (I)

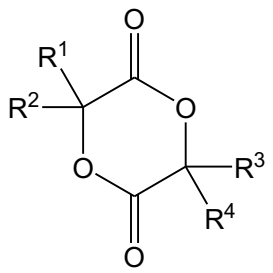

(I)

stereoisomers and racemates thereof, wherein R^1, R^2, R^3, and R^4 are independently selected from hydrogen, C1-C24 alkyl, aryl, fluoro, chloro, and halocarbon, with the proviso that at least one of R^1, R^2, R^3, or R^4 is selected from fluoro, chloro, or halocarbon.

As used herein, the term "halocarbon" refers to a substituent group that includes one or more carbons (e.g., C1-C24, C1-C12, or C1-C6) and one or more chlorine or fluorine atoms. The terms "halocarbon" and "halocarbon group" are used interchangeably. Suitable halocarbon groups include one or more chlorine atoms (chloro substituents), one or more fluorine atoms (fluoro substituents), or one or more chlorine atoms and one or more fluorine atoms (chloro and fluoro substituents). Representative halocarbon groups include $–CH_2Cl$, $-CH_2F$, and -CH(Cl)F groups, among others.

In another embodiment, the cyclic diester of the invention has formula (I)

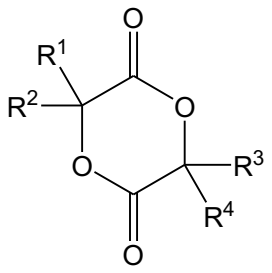

(I)

stereoisomers and racemates thereof, wherein R^1, R^2, R^3, and R^4 are independently selected from hydrogen, C1-C24 alkyl, aryl, fluoro, and fluorocarbon (e.g., C1-C24 fluoroalkyl), with the proviso that at least one of R^1, R^2, R^3, or R^4 is selected from fluoro or fluorocarbon.

As used herein, the term "fluoroocarbon" refers to a substituent group that includes one or more carbons (e.g., C1-C24, C1-C12, or C1-C6) and one or more fluorine atoms. The terms "fluorocarbon" and "fluorocarbon group" are used interchangeably. Suitable fluorocarbon groups include one or more fluorine atoms (fluoro substituents). Representative fluoroocarbon groups include $–CH_2F$, $-CHF_2$, and $–CF_3$ groups, among others. In certain embodiments, the fluorocarbon group is a C1-C24 fluoroalkyl group. In certain embodiments, C1-C24 alkyl is C1-C12 alkyl. In certain embodiments, C1-C24 alkyl is C1-C6 alkyl. Representative alkyl groups include straight chain (e.g., n-propyl), branched (e.g., isopropyl), and cyclo (e.g., C3-C7 cycloalkyl, such as cyclopentyl) groups. In certain embodiments, C1-C24 (or C1-C12 or C1-C6) alkyl is selected from methyl, ethyl, n-propyl, i-propyl, and n-butyl. In certain embodiments, C1-C24 (or C1-C12 or C1-C6) alkyl is methyl.

The alkyl and aryl groups of the cyclic diester may be substituted or unsubstituted. As used herein, the term "substituted C1-C24 alkyl" refers to a C1-C24 alkyl group in which one or more hydrogen atoms is replaced with a non-hydrogen atom. The term "substituted aryl" refers to an aryl group (e.g., phenyl group) in which one or more hydrogen atoms is replaced with a non-hydrogen atom. Representative non-hydrogen atoms include heteroatoms such oxygen, nitrogen, sulfur, and silicon atoms, as well as substituents that include these atoms (e.g., hydroxy, alkoxyl, amino, alkylamino, thiol, thioether).

In certain embodiments, the cyclic diesters of the invention include either a fluorine substituent or a fluoroalkyl substituent. As used herein the term "fluoroalkyl" or "fluoroalkyl group" refers to an alkyl group (i.e., a saturated hydrocarbon group) in which one or more hydrogen atoms is replaced with a fluorine atom (F). As used herein, the

terms "fluoro" and "fluorine" are used interchangeably and refer to the substituent F. Representative fluoroalkyl groups include -CF_3, -CH_2F, -CHF_2, -CF_2CF_3, -CH_2CF_3, -CF_2CH_3, -CH_2CHF_2, -CH_2CH_2F, among others.

In certain embodiments, C1-C24 fluoroalkyl is C1-C12 fluoroalkyl. In certain embodiments, C1-C24 fluoroalkyl is C1-C6 fluoroalkyl.

Representative fluoroalkyl groups include straight chain (e.g., n-propyl), branched (e.g., isopropyl), and cyclo (e.g., C3-C7 cycloalkyl, such as cyclopentyl) groups. In certain embodiments, C1-C24 (or C1-C12 or C1-C6) fluoroalkyl is selected from methyl, ethyl, n-propyl, i-propyl, and n-butyl in which one or more hydrogen atoms is replaced with a fluorine atom. In certain embodiments, the fluoroalkyl is perfluoroalkyl (e.g., trifluoromethyl, pentafluoroethyl, n-perfluoropropyl, n-perfluorobutyl, and n-perfluoropentyl). In certain embodiments, C1-C24 (or C1-C12 or C1-C6) alkyl is methyl (i.e., trifluoromethyl, difluoromethyl, and fluoromethyl).

In certain embodiments, the fluoroalkyl group(s) of the cyclic diester has a ratio of F:C from about 0.4 to about 3.0. In certain embodiments, the fluoroalkyl group(s) of the cyclic diester has a ratio of F:C of about 0.5. In other embodiments, the fluoroalkyl group(s) of the cyclic diester has a ratio of F:C of about 1.0. In further embodiments, the fluoroalkyl group(s) of the cyclic diester has a ratio of F:C of about 2.0.

In one embodiment of formula (I), R^1 and R^3 are hydrogen and R^2 and R^4 are trifluoromethyl.

In one embodiment of formula (I), R^1 and R^3 are hydrogen, R^2 is methyl, and R^4 is trifluoromethyl.

In one embodiment of formula (I), R^1 and R^2 are hydrogen and R^3 and R^4 are trifluoromethyl.

In one embodiment of formula (I), R^1, R^2, and R^3 are hydrogen and R^4 is trifluoromethyl.

In one embodiment of formula (I), R^1, R^2, R^3, and R^4 are trifluoromethyl.

In one embodiment of formula (I), R^1 and R^2 are hydrogen and R^3 and R^4 are fluoro.

In one embodiment of formula (I), R^1 is hydrogen, R^2 is methyl, and R^3 and R^4 are fluoro.

In one embodiment of formula (I), R^1, R^2, R^3, and R^4 are fluoro.

In another embodiment, the cyclic diester of formula (I) is a lactide having formula (II)

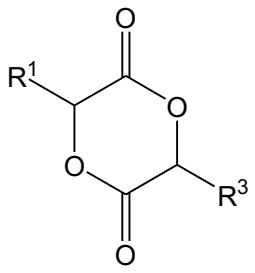

(II)

stereoisomers and racemates thereof, wherein R^1 and R^3 are independently selected from C1-C24 alkyl and fluorocarbon (e.g., C1-C24 fluoroalkyl), with the proviso that R^1 and R^3 at least one of R^1 and R^3 is fluorocarbon (e.g., C1-C24 fluoroalkyl). In this embodiment, R^1 and R^3 are as described above for formula (I).

In one embodiment of the lactide of formula (II), R^1 is methyl and R^3 is trifluoromethyl.

In one embodiment of the lactide of formula (II), R^1 is hydrogen and R^3 is trifluoromethyl.

In one embodiment of the lactide of formula (II), R^1 and R^3 are trifluoromethyl.

Representative cyclic diesters of the invention have the structures shown in FIGURES 2-5. FIGURE 2 is an illustration of the preparation a representative cyclic diester starting from $CF_3CH(OH)$-C(=O)OH. FIGURE 3 is an illustration of the preparation a representative cyclic diester starting from $CF_2(OH)$-C(=O)OH. FIGURE 4 is an illustration of the preparation a representative cyclic diester starting from $(CF_3)_2C(OH)$-C(=O)OH. FIGURE 5 is an illustration of the preparation a representative cyclic diester starting from $CF_3C(Ph)(OH)$-C(=O)OH.

Polymers

In another aspect, the invention provides halogenated polymers. As used herein the terms "halogenated polymer" refers to a polymer that includes one or more chlorine and/or one or more fluorine atoms, and particularly to a polymer that includes repeating units derived from monomers that include one or more halogen atoms (e.g., fluorine and/or chlorine atoms) or halogen-containing substituents (i.e., halocarbon groups, such as chlorocarbon, fluorocarbon, or chloro/fluorocarbon groups). In certain embodiments, the polymers of the invention are prepared from the halogenated cyclic diesters of the invention. In certain embodiments, the halogenated polymers are prepared by ring opening polymerization. In other embodiments, the halogenated polymers are prepared by condensation polymerization.

In one embodiment, the invention provides fluorinated polymers. As used herein the terms "fluorinated polymer" refers to a polymer that includes fluorine atoms, and

particularly to a polymer that includes repeating units derived from monomers that include one or more fluorine atoms or fluorine-containing substituents (e.g., fluorocarbon groups, such as fluoroalkyl groups). In one embodiment, the fluorinated polymers of the invention are prepared from the fluorinated cyclic diesters of the invention. In certain embodiments, the fluorinated polymers are prepared by ring opening polymerization. In other embodiments, the fluorinated polymers are prepared by condensation polymerization.

FIGURE 6 is a schematic illustration of a representative preparation of fluorinated polymers of the invention from cyclic diesters. FIGURE 7 is a schematic illustration of representative preparations of fluorinated polymers of the invention from cyclic diesters prepared from a representative alpha-hydroxy carboxylic acid: $CF_3CH(OH)$-C(=O)OH.

In certain embodiments, the halogenated polymer includes a repeating unit having formula (III)

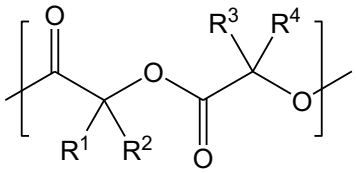

(III)

wherein R^1, R^2, R^3, and R^4 are independently selected from hydrogen, C1-C24 alkyl, aryl, fluoro, chloro, and halocarbon, with the proviso that at least one of R^1, R^2, R^3, or R^4 is selected from fluoro, chloro, or halocarbon.

In other embodiments, the fluorinated polymer includes a repeating unit having formula (III)

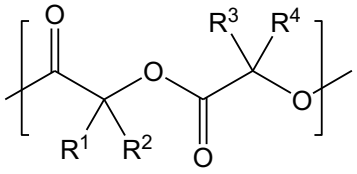

(III)

wherein R^1, R^2, R^3, and R^4 are independently selected from hydrogen, C1-C24 alkyl, aryl, fluoro, chloro, and halocarbon, with the proviso that at least one of R^1, R^2, R^3, or R^4 is selected from fluoro or fluorocarbon.

In certain embodiments, the halogenated polymer is a polylactic acid that includes a repeating unit having formula (IV)

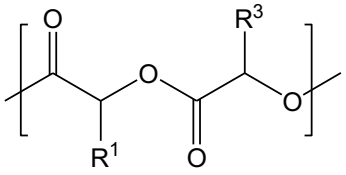

(IV)

wherein

R^1 and R^3 are independently selected from C1-C24 alkyl and halocarbon, with the proviso that at least one of R^1 or R^3 is halocarbon.

In other embodiments, the fluorinated polymer is a fluorinated polylactic acid that includes a repeating unit having formula (IV)

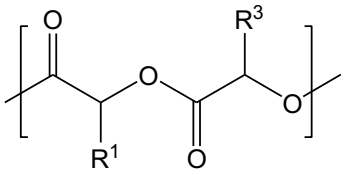

(IV)

wherein R^1 and R^3 are independently selected from C1-C24 alkyl and fluorocarbon (e.g., C1-C24 fluoroalkyl), with the proviso that at least one of R^1 and R^3 is fluorocarbon. R^1 and R^3 are as described above for the cyclic diesters.

In certain embodiments, the invention includes the polymers of formulae (III) and (IV) that further include one or more repeating units derived from comonomers suitable for polymerization with a halogenated (e.g., fluorinated) cyclic diester (e.g., ring opening polymerization or condensation polymerization). Suitable comonomers include cyclic diesters, such as lactides and lactide derivatives (e.g., non-halogenated lactides and non-halogenated lactide derivatives) and glycolides and glycolide derivatives (e.g., non-halogenated glycolides and non-halogenated glycolide derivatives), and other suitable polymerizable esters.

In certain embodiments, the halogenated (e.g., fluorinated) polymer has formula (V)

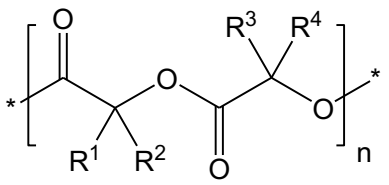

(V)

wherein *represents the terminal groups of the polymer, n is an integer from about 10 to about 1000, and R^1, R^2, R^3, and R^4 are as described above for the cyclic diesters.

The terminal groups of the polymer depend on the nature of the polymerization reaction used to form the polymer. For ring opening polymerizations, the terminal groups are

derived from the initiator used in the polymerization. Suitable initiators useful in polymerizing cyclic diesters are known and include water and alcohols. When the initiator is water, one terminal group is –OH and the other is –H. When the initiator is an alcohol (ROH), one terminal group is –OR and the other is –H. Representative alcohols useful as initiators include methanol, 2-propanol, 2-methyl-2-propanol, 1-butanol, 4-phenyl-2-butanol, 1-hexanol, 1-decanol, 1-dodecanol, 1-tetradecanol, 1-hexadecanol, 1-octadecanol, 1-eicosanol, 1-docosanol, 1-pyrene butanol, and benzyl alcohol. In certain embodiments, the R group of the alcohol includes a functional group that allows for further functionalization of the product polymer.

In certain embodiments, the halogenated (e.g., fluorinated) polymer has formula (VI)

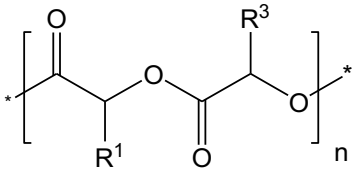

(VI)

wherein *represents the terminal groups of the polymer as defined above, n is an integer from about 10 to about 1000, and R^1 and R^3 are as described above for the cyclic diesters.

As noted above, in certain embodiments, n is an integer from about 10 to about 1000. In other embodiments, n is an integer from about 100 to about 10,000. In further embodiments, n is an integer from about 50 to about 500. In other embodiments, n is an integer from about 50 to about 2000.

In certain embodiments, the halogenated (e.g., fluorinated) polymer has formula (VII)

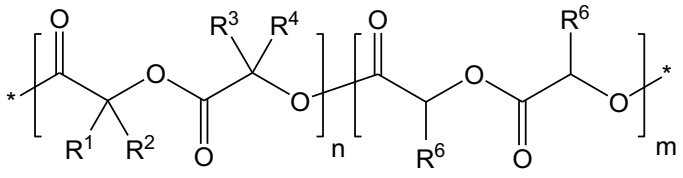

(VII)

wherein R^6 is hydrogen or methyl, n is an integer from about 10 to about 1000, m is an integer from about 10 to about 1000, and R^1, R^2, R^3, and R^4 are as described above for the cyclic diesters.

For the polymers of the invention, the ratio of n:m can vary depending on the desired degree of hydrophobicity and degradability (hydrolysis). In certain embodiments, n:m is about 1:100. In other embodiments, the ratio of n:m is about 100:1. In further

embodiments, the ratio of n:m is about 1:1. Other suitable n:m ratios include about 1:2, 1:3, 1:4, 1:5, 1:10, 1:20, 2:1, 3:1 4:1, 5:1, 10:1, and 20:1.

As used herein, the term "about" refers to +/- 5% of the specified value.

In certain embodiments, the fluorinated polymer is a halogenated (e.g., fluorinated) polylactic acid having formula (VIII)

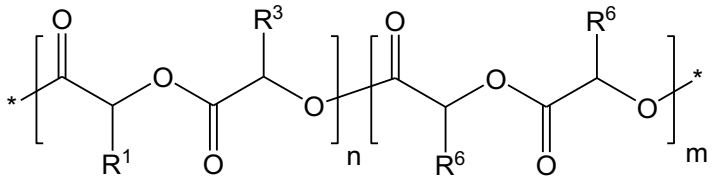

(VIII)

wherein R^6 is hydrogen or methyl, n is an integer from about 10 to about 1000, and m is an integer from about 10 to about 1000, the ratio of n:m is as described above for formula (VII), and R^1 and R^3 are as described above for the cyclic diesters.

As indicated above, certain of the polymers of the invention are homopolymers (i.e., include a single type of repeating unit). In certain embodiments, when the polymer includes two or more different types of repeating units, the polymer of the invention is a random copolymer. In other embodiments, when the polymer includes two or more different types of repeating units, the polymer of the invention is a block copolymer.

The polymers of the invention can be prepared from the cyclic diesters of the invention by polymerization methods. Suitable polymerization methods include polymerization methods known in the art for preparing polymers from cyclic diesters, and include ring opening polymerization methods and condensation polymerization methods. See, for example, U.S. Patent Nos. 6,469,133 and 8,927,682, each expressly incorporated herein by reference in its entirety.

In a representative polymerization method, a cyclic diester and a suitable catalyst are combined in a solvent to provide a reaction mixture, the reaction mixture is heated to polymerize the cyclic ester to form the polymer in the reaction mixture (preferably the mixture is heated to a temperature between about 20°C and 200°C), and the polymer is isolated from the reaction mixture.

Suitable catalysts include those known in the art. Representative catalysts useful for preparing the fluorinated polymers of the invention from cyclic diesters include tin reagents such as Sn(octanoate)$_2$, Sn(2-ethylhexanoate)$_2$, Sn(trifluoromethane sulfonate)$_2$,

dibutylSn(2-ethylhexanoate)$_2$, Sn(phenyl)$_4$, Sn(bromide)$_4$, Sn(bromide)$_2$, Sn(oxide).

Other suitable catalysts include 4-(dimethylamino)pyridine (DMAP).

A representative procedure for the polymerization of a cyclic diester to provide a polymer of the invention is described in Example 2.

Polymer-Coated Substrates

In a further aspect, the invention provides substrates and surfaces coated with a polymer of the invention.

In one embodiment, the invention provides a surface of a substrate, wherein at least a portion of the surface is coated with a polymer of the invention (i.e., polymer of formulae (III)-(VIII). In certain embodiments, the substrate is useful as a drug delivery device, a device having a degradation-inhibiting coating, a device having hydrophobic surfaces with high contact angle, and a device that contacts blood. In certain embodiments, the substrate is a medical device, such as a cardiovascular stent.

Ammonia Plasma Process

In another aspect of the invention, a method for making a halogenated polymer is provided. In the method, halocarbon groups are introduced into the polymer.

In one embodiment, the method includes:

subjecting a polymer with an ammonia plasma to provide a polymer functionalized with amino groups;

reacting the polymer functionalized with amino groups with a suitably reactive reagent comprising a halocarbon, wherein at least a portion of the amino groups react with the reagent to provide a polymer having at least of portion of the amino groups converted to amine groups covalently coupled to the halocarbon.

In another embodiment, the method includes:

subjecting a polymer with an ammonia plasma to provide a polymer functionalized with amino (-NH_2) groups;

reacting the polymer functionalized with amino groups with a suitably reactive reagent comprising a fluorocarbon (e.g., fluoroalkyl) group, wherein at least a portion of the amino groups react with the reagent to provide a polymer having at least of portion of the amino groups converted to amine groups covalently coupled to the fluorocarbon groups.

An embodiment of the method is illustrated schematically in FIGURE 13.

Methods for imparting amino groups to a polylactic acid film by ammonia plasma treatment are described in J. Biomedical Materials Research B: Applied Biomaterials,

February 2014, Vol. 102B, Issue 2, pages 345-355, expressly incorporated herein by reference in its entirety.

Suitable polymers useful in the method include polymers that can be modified by ammonia plasma to provide a polymer functionalized with amino groups. Polymers that are advantageously treated by the method of the invention include biocompatible, biodegradable polymers. Representative polymers include polylactic acids, polyglycolic acids, and poly(lactic-co-glycolic) acids.

Suitably reactive reagents comprising a halocarbon group have a reactive group capable of forming a covalent bond with the amino group imparted to the polymer by ammonia plasma. Representative reactive groups are selected from a carboxylic acid, carboxylic acid halide, carboxylic acid ester (NHS and fluorophenyl esters), isocyanate, isothiocyanate, acyl azide, aldehyde, epoxide, oxirane, carbonate, sulfonyl chloride, aryl halide, imidoester, glyoxal, carbodiimide, and anhydride. These reactive groups are covalently coupled to the amine groups by either alkylation or acylation.

Suitably reactive reagents comprising a fluorocarbon (e.g., fluoroalkyl) group have a reactive group capable of forming a covalent bond with the amino group imparted to the polymer by ammonia plasma. Representative reactive groups are selected from a carboxylic acid, carboxylic acid halide, carboxylic acid ester (NHS and fluorophenyl esters), isocyanate, isothiocyanate, acyl azide, aldehyde, epoxide, oxirane, carbonate, sulfonyl chloride, aryl halide, imidoester, glyoxal, carbodiimide, and anhydride. These reactive groups are covalently coupled to the amine groups by either alkylation or acylation.

In certain embodiments, the fluorocarbon is a fluoroalkyl group. In certan embodiments, the fluoroalkyl group is a C1-C24 fluoroalkyl group. In certain embodiments, the C1-C24 fluoroalkyl group is a C1-C12 fluoroalkyl group. In other embodiments, the C1-C24 fluoroalkyl group is a C1-C6 fluoroalkyl group. Representative fluoroalkyl groups include those described above for the cyclic diesters.

In certain embodiments of the method, the polymer subjected to ammonia plasma is a coating on at least a portion of a surface of a substrate. Suitable substrates include drug delivery devices, devices having a degradation-inhibiting coating, devices having a hydrophobic surface with high contact angle, and a device that contacts blood. In certain embodiments, the substrate is a medical device. In certain embodiments, the substrate is a cardiovascular stent.

In a further aspect, the invention provides a polymer prepared by the above ammonia plasma method. In one embodiment, the invention provides a surface of a substrate having at least a portion of the surface is coated with a polymer prepared by the above ammonia plasma method.

The following examples are provided for the purpose of illustrating, not limiting the invention.

EXAMPLES

Example 1

Preparation and Characterization of a Representative Cyclic Diester

In this example, preparations and characterization of representative cyclic diesters of the invention is described. The preparation is schematically illustrated in FIGURES 2 and 7.

Materials and Methods

^{1}H, ^{13}C NMR, and ^{19}F NMR spectra were recorded on a Bruker AV 300, 500, and DRX 499 spectrometer, respectively. Chemical shifts are reported in delta (δ) units, expressed in parts per million (ppm) downfield from tetramethylsilane using the residual protio-solvent as an internal standard ($CDCl_3$, ^{1}H: 7.26 ppm and ^{13}C: 77.16 ppm, CD_3CN, ^{1}H: 1.94 ppm and ^{13}C: 118.36 ppm). For ^{19}F NMR spectra, hexafluorobenzene (-164.9 ppm) was used as an internal standard in deuterated acetonitrile for monomer and deuterated chloroform for polymer.

Monomer synthesis

FIGURE 7 shows the synthetic rout for preparing trifluoromethyl-substituted lactic acid (**2**) monomer. Under nitrogen gas flow, trifluorolactic acid (6.2 g, 43 mmol) was added to a dry round bottom flask containing 70 ml dry acetonitrile and triethylamine (5.6 g, 7.8 mL, 56 mmol). The mixture was stirred and cooled in an ice bath. Then a solution of 2-bromopropionyl bromide (11.6 g, 5.7 mL, 54 mmol) in 10 mL of dry acetonitrile was added dropwise to the reaction mixture. After the addition was complete, the ice bath was removed and the mixture was stirred at room temperature for 3 h. The resulting white precipitate was filtered off through Celite, and the filtrate was concentrated under reduced pressure. The resulting product was then dissolved in ethyl acetate and filtered again to remove any remaining salts. The removal of the ethyl acetate by rotary evaporation gave product (**1**) as a brown oil, which was used without further purification for the next step.

For the synthesis of (**2**), sodium hydride (60 %, 2.6 g, 64.5 mmol) was stirred in dry acetonitrile (800 mL) in an ice bath under nitrogen gas flow. Next, solution of product (**1**) in dry acetonitrile (100 mL) was added dropwise to the sodium hydride mixture for 30 mins. The ice bath was then removed, and the reaction mixture was stirred at room temperature for 1 h. Afterward, the resulting mixture was heated to 70 °C, and stirred overnight under nitrogen gas atmosphere. Once the reaction was completed as shown by thin-layer chromatography (TLC), the resulting mixture was cooled to room temperature and white precipitate was filtered off through Celite and filtrate was concentrated. The product was then dissolved in dry ethyl acetate and filtered off through Celite to remove any residual salts. The filtrate was concentrated under reduced pressure, and purified by silica gel column chromatography using dry premium grade silica gel and a mixture of 30 % dry ethyl acetate/hexanes as an eluent under nitrogen gas flow. The resulting product was further purified by recrystallization in dry DCM/hexanes to give a white solid as a mixture of R,S (88 %, 7/8) and R,R/S,S (12 %, 1/8) diastereomers which was analyzed by NMR (2.27 g, 27 % yield). ^{1}H NMR (500 MHz, CD_3CN) δ 5.71 (q, J = 7.5 Hz, 1H × 1/8), 5.69 (q, J = 6.3 Hz, 1H × 7/8), 5.31 (q, J = 7.0 Hz, 1H × 1/8), 5.26 (q, J = 6.7 Hz, 1H × 7/8), 1.65 (d, J = 7.0 Hz, 3H × 1/8), 1.58 (d, J = 6.7 Hz, 3H × 7/8). ^{13}C NMR (126 MHz, CD_3CN) δ 165.8, 161.0, 121.4 (q, 1JCF = 278 Hz, CF_3), 73.7, 73.0 (q, 2JCF = 33 Hz, CF_3C-), 15.6. ^{19}F NMR (471 MHz, CD_3CN, C_6F_6) δ -75.3.

Results

The molecular structure of trifluotomethyl-substituted lactic acid (**2**) monomer was confirmed by ^{1}H, ^{13}C, and ^{19}F NMR spectroscopy. In ^{1}H NMR (FIGURE 9), the doublet from the methyl protons of R,S isomers is shown with coupling constant of J_{HH} = 6.7 Hz, and that from R,R or S,S isomers is shown with J_{HH} = 7.0 Hz. The methine protons next to the trifluoromethyl groups of the R,S isomers are deshielded due to the electron withdrawing trifluoromethyl groups, downfielded, and shown at 5.7 ppm, compared to the methine protons next to the methyl groups at 5.25 ppm. In addition, coupling constant (J_{HF} = 6.3 Hz) of the quartet from the methine protons next to the trifluoromethyl groups is distinct from that (J_{HH} = 6.7 Hz) next to the methyl groups. The equal integration from these methine groups confirms the presence of the monomer (**2**). The structure of the monomer (**2**) is further verified by ^{13}C NMR and ^{19}F NMR spectroscopy (FIGURES 10 and 11). ^{13}C NMR spectra (FIGURE 10) shows the quartet (at 121.4 ppm, $^{2}J_{CF}$ = 278 Hz)

from carbons of the trifluoromethyl groups due to carbon-fluorine couplings. In addition, it shows another quartet (at 73 ppm with $^1J_{CF}$ = 33 Hz) from carbons next to the trifluoromethyl groups, which is distinct from the singlet (at 73.7 ppm) from carbons next to the methyl groups.

Example 2

Representative Method for Polymerizing a Cyclic Diester

The solution polymerization was conducted in toluene at 110 °C using benzyl alcohol as an initiator and tin(II) 2-ethylhexanoate ($Sn(Oct)_2$) as a catalyst. The initiator and catalyst were purified by distillation prior to polymerization, and their stock solutions in dry benzene (0.1 M) were prepared. In a dry box, monomer (**2,** 198 mg, 1 mmol) were placed into a vial with dry toluene (4 mL, 0.25 M). Then stock solutions of $Sn(Oct)_2$ (**4**, 100 μL, 0.01 mmol) and benzyl alcohol (**3**, 100 μL, 0.01 mmol) were added to the monomer solution. The vial was sealed with a Teflon cap and heated to 110 °C. After 24 h, the mixture was cooled to room temperature and the product was dried under vacuum to remove solvent, catalyst and unreacted initiators. The crude polymer was dissolved in chloroform and filtered to selectively remove unreacted monomers. The chloroform was removed and the resulting solid product was stirred in methanol and dried under high vacuum to further remove any unreacted monomers. The resulting polymer was then dissolved in chloroform and precipitated in hexanes. The final product was obtained after removing hexanes and drying as a white powder (135 mg, 68 % yield).

Results

Polymerization was conducted by ring opening polymerization of the fluorine-substituted, cyclic diester monomers in solution using toluene as a solvent, benzyl alcohol as an initiator, and tin (II) 2-ethylhexanoate as a catalyst. The catalyst to initiator ratio was 1:1 for all polymerizations, and the monomer to initiator ratio was 100:1. The monomer was not very soluble in toluene at room temperature, but became soluble at 110 °C and reaction mixture remained homogeneous at 110 °C during polymerization. FIGURE 11 shows the ^{1}H NMR spectrum of the resulted trifluomethyl-substituted polylactide. The methine protons next to the trifluoromethyl groups are clearly shown from 5.47 to 5.7 ppm, and methine protons next to the methyl groups are from 5.2 to 5.45 ppm. The ratio of integration of the peaks from protons next to the trifluoromethyl groups to those next

to the methyl groups is 0.9, indicating approximately equal portions of trifluoromethyl and methyl groups in the backbones of polymer. This NMR analysis suggests the structure of alternating trifluoromethyl and methyl groups. In addition, ^{19}F NMR spectrum (FIGURE 12) of the trifluomethyl-substituted polylactide shows broad peaks compared to the ^{19}F NMR spectrum of monomer (FIGURE 10), indicating the distribution of polymer chains with different molecular weights.

CLAIMS

The embodiments of the invention in which an exclusive property or privilege is claimed are defined as follows:

1. A halogenated polymer, comprising a repeating unit having the formula

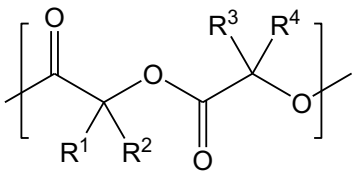

wherein

R^1, R^2, R^3, and R^4 are independently selected from hydrogen, C1-C24 alkyl, aryl, fluoro, chloro, and halocarbon, with the proviso that at least one of R^1, R^2, R^3, or R^4 is selected from fluoro, chloro, or halocarbon.

2. A fluorinated polymer, comprising a repeating unit having the formula

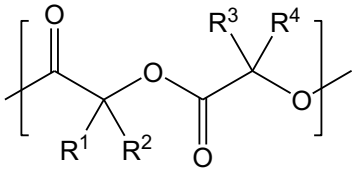

wherein

R^1, R^2, R^3, and R^4 are independently selected from hydrogen, C1-C24 alkyl, aryl, fluoro, and fluorocarbon (e.g., C1-C24 fluoroalkyl), with the proviso that at least one of R^1, R^2, R^3, or R^4 is selected from fluoro or fluorocarbon.

3. A halogenated polylactic acid, comprising a repeating unit having the formula

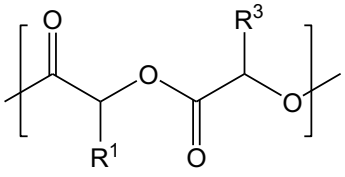

wherein

R^1 and R^3 are independently selected from C1-C24 alkyl and halocarbon, with the proviso that at least one of R^1 or R^3 is halocarbon.

4. A fluorinated polylactic acid, comprising a repeating unit having the formula

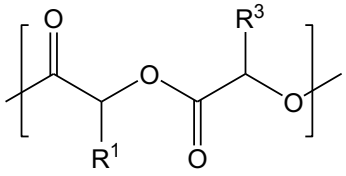

wherein

R^1 and R^3 are independently selected from C1-C24 alkyl and fluorocarbon (e.g., C1-C24 fluoroalkyl), with the proviso that at least one of R^1 or R^3 is fluorocarbon.

5. The polymer of any one of Claims 1-4 further comprising one or more repeating units derived from comonomers suitable for polymerization with a halogenated cyclic diester.

6. The polymer of Claims 1 or 2 having the formula

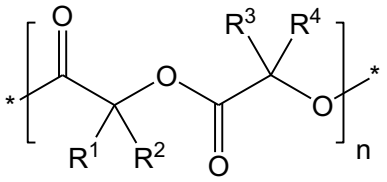

wherein

*represents the terminal groups of the polymer, and

n is an integer from about 10 to about 1000.

7. The polylactic acid of Claims 3 or 4 having the formula

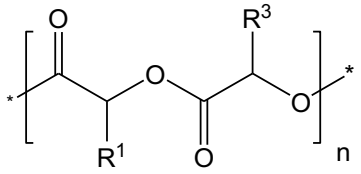

wherein

*represents the terminal groups of the polymer, and

n is an integer from about 10 to about 1000.

8. The polymer of Claims 1 or 2 having the formula

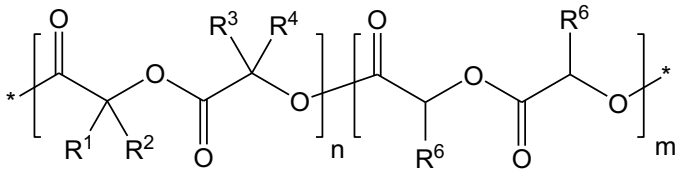

wherein

R^6 is hydrogen or methyl,

n is an integer from about 10 to about 1000, and

m is an integer from about 10 to about 1000.

9. The polylactic acid of Claims 3 or 4 having the formula

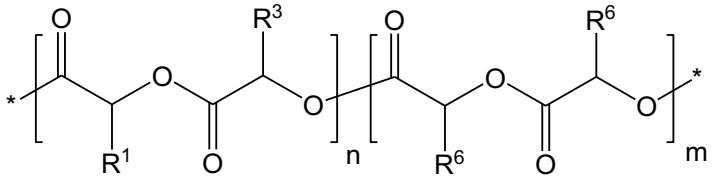

wherein

R^6 is hydrogen or methyl,

n is an integer from about 10 to about 1000, and

m is an integer from about 10 to about 1000.

10. The polymer of any one of Claims 1-5, 8, and 9, wherein the polymer is a random copolymer or a block copolymer.

11. A surface of a substrate, wherein at least a portion of the surface is coated with a polymer of any one of Claims 1-10.

12. The surface of Claim 11, wherein the substrate is a drug delivery device, a device having a degradation-inhibiting coating, a device having a hydrophobic surface with high contact angle, or a device that contacts blood.

13. The surface of Claim 11, wherein the substrate is a medical device.

14. The surface of Claim 11, wherein the substrate is a cardiovascular stent.

15. A method for making a halogenated polymer, comprising:

subjecting a polymer with an ammonia plasma to provide a polymer functionalized with amino groups;

reacting the polymer functionalized with amino groups with a suitably reactive reagent comprising a halocarbon, wherein at least a portion of the amino groups react with the reagent to provide a polymer having at least of portion of the amino groups converted to amine groups covalently coupled to the halocarbon.

16. A method for making a fluorinated polymer, comprising:

subjecting a polymer with an ammonia plasma to provide a polymer functionalized with amino groups;

reacting the polymer functionalized with amino groups with a suitably reactive reagent comprising a fluorocarbon (e.g., fluoroalkyl) group, wherein at least a portion of the amino groups react with the reagent to provide a polymer having at least of portion of the amino groups converted to amine groups covalently coupled to fluorocarbon (e.g., fluoroalkyl) groups.

17. The method of Claims 15 or 16 wherein the polymer is selected from the group consisting of a polylactic acid, a polyglycolic acid, and a poly(lactic-co-glycolic) acid.

18. The method of Claim 15, wherein suitably reactive reagent comprising a halocarbon has a reactive group selected from the group consisting of a carboxylic acid, carboxylic acid halide, carboxylic acid ester, isocyanate, isothiocyanate, acyl azide, aldehyde, epoxide, oxirane, carbonate, sulfonyl chloride, aryl halide, imidoester, glyoxal, carbodiimide, and anhydride.

19. The method of Claim 16, wherein suitably reactive reagent comprising a fluorocarbon group has a reactive group selected from the group consisting of a carboxylic acid, carboxylic acid halide, carboxylic acid ester, isocyanate, isothiocyanate, acyl azide, aldehyde, epoxide, oxirane, carbonate, sulfonyl chloride, aryl halide, imidoester, glyoxal, carbodiimide, and anhydride.

20. The method of Claim 16, wherein the fluoroalkyl group is a C1-C24 fluoroalkyl group.

21. The method of Claims 15 or 16, wherein the polymer is a coating on at least a portion of a surface of a substrate.

22. The method of Claim 21, wherein the substrate is a drug delivery device, a device having a degradation-inhibiting coating, a device having a hydrophobic surface with high contact angle, or a device that contacts blood.

23. The method of Claim 21, wherein the substrate is a medical device.

24. The surface of Claim 21, wherein the substrate is a cardiovascular stent.

25. A polymer obtainable by the process of any one of Claims 15-20.

26. A surface of a substrate having at least a portion of the surface is coated with a polymer obtainable by the process of any one of Claims 15-20.

27. A cyclic diester having the formula

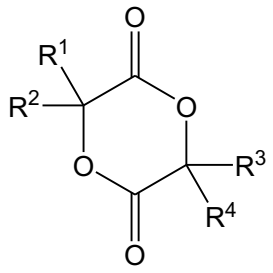

stereoisomers and racemates thereof,

wherein R^1, R^2, R^3, and R^4 are independently selected from hydrogen, C1-C24 alkyl, aryl, fluoro, chloro, and halocarbon, with the proviso that at least one of R^1, R^2, R^3, or R^4 is selected from fluoro, chloro, or halocarbon.

28. A cyclic diester having the formula

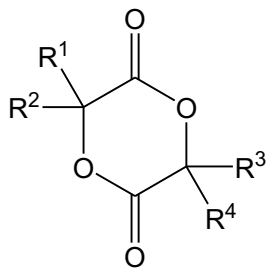

stereoisomers and racemates thereof,

wherein R^1, R^2, R^3, and R^4 are independently selected from hydrogen, C1-C24 alkyl, aryl, fluoro, and fluorocarbon (e.g., C1-C24 fluoroalkyl), with the proviso that at least one of R^1, R^2, R^3, or R^4 is selected from fluoro or fluorocarbon.

29. The cyclic diester of Claim 28, wherein the C1-C24 fluoroalkyl group is a C1-C12 fluoroalkyl group.

30. The cyclic diester of Claim 28, wherein the C1-C24 fluoroalkyl group is a C1-C6 fluoroalkyl group.

31. The cyclic diester of Claim 28, wherein R^1 and R^3 are hydrogen and R^2 and R^4 are trifluoromethyl.

32. The cyclic diester of Claim 28, wherein R^1 and R^3 are hydrogen, R^2 is methyl, and R^4 is trifluoromethyl.

33. The cyclic diester of Claim 28, wherein R^1 and R^2 are hydrogen and R^3 and R^4 are trifluoromethyl.

34. The cyclic diester of Claim 28, wherein R^1, R^2, and R^3 are hydrogen and R^4 is trifluoromethyl.

35. The cyclic diester of Claim 28, wherein R^1, R^2, R^3, and R^4 are trifluoromethyl.

36. The cyclic diester of Claim 28, wherein the C1-C24 alkyl is selected from the group consisting of straight chain, branched, and cyclo alkyl.

37. The cyclic diester of Claim 28, wherein the C1-C24 alkyl is selected from the group consisting of methyl, ethyl, n-propyl, i-propyl, and n-butyl.

38. The cyclic diester of Claim 28, wherein the C1-C24 alkyl is methyl.

39. The cyclic diester of Claim 28, wherein the C1-C24 fluoroalkyl is selected from the group consisting of straight chain, branched, and cyclo fluoroalkyl.

40. The cyclic diester of Claim 28, wherein the C1-C24 fluoroalkyl is a C1-C24 perfluoroalkyl.

41. The cyclic diester of Claim 28, wherein the C1-C24 fluoroalkyl has a ratio of F:C from 0.4 to 3.0.

42. The cyclic diester of Claim 28, wherein the C1-C24 fluoroalkyl is selected from the group consisting of trifluoromethyl, pentafluoroethyl, n-perfluoropropyl, n-perfluorobutyl, and n-perfluoropentyl.

43. The cyclic diester of Claim 28, wherein the C1-C24 fluoroalkyl is trifluoromethyl.

44. A cyclic diester having the formula

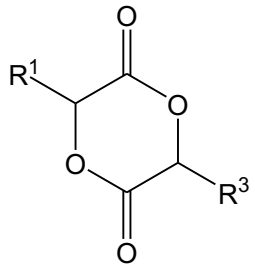

stereoisomers and racemates thereof,

wherein R^1 and R^3 are independently selected from C1-C24 alkyl and fluorocarbon (e.g., C1-C24 fluoroalkyl), with the proviso that at least on of R^1 or R^3 is fluorocarbon.

45. The cyclic diester of Claim 44, wherein R^1 is methyl and R^3 is trifluoromethyl.

46. The cyclic diester of Claim 44, wherein R^1 is hydrogen and R^3 is trifluoromethyl.

47. The cyclic diester of Claim 44, wherein R^1 and R^3 are trifluoromethyl.

48. A fluorinated polymer prepared from a cyclic diester of any one of Claims 28-46.

49. A halogenated polymer prepared from a cyclic diester of Claim 27.

ABSTRACT

Halogenated cyclic diesters, halogenated polymers derived from the cyclic diesters, and methods for making the halogenated cyclic diesters and related halogenated polymers.

VITA

Razieh Khalifehzadeh was born in Urmia, Iran. She graduated with B.S. degree in Materials Science and Engineering form Sharif University of Technology, Tehran, Iran and MS degree in Biomedical Engineering from AmirKabir University of Technology (AUT), Tehran, Iran. While at AUT, she worked on a synthesis of conducting polymers as a coating for load bearing Nitinol implants. This led toward an interest in biomaterials and particularly polymers and their applications for various medical devices. She earned a Doctor of Philosophy at the University of Washington in Chemical Engineering under the supervision of Prof. Buddy Ratner in 2018.

PUBLICATIONS

1. **R. Khalifehzadeh**, Winston Ciridon, Buddy D. Ratner., "Surface Fluorination of Polylactide as a Path to Improve Platelet Associated Hemocompatibility", In press, Acta Biomaterialia.
2. **R. Khalifehzadeh** and Buddy D. Ratner et al., "Trifluoromethyl-Functionalized Poly(lacic Acid): A Novel Biocompatible, Non-thrombogenic Fluoropolyester, In Preparation*
3. **R. Khalifehzadeh** and Buddy D. Ratner et al., "Calcium Phosphate Based Nanoparticles and Their Applications in Delivery of Therapeutic Agents", In Preparation*
4. **R. Khalifehzadeh** and Buddy D. Ratner et al., "DNA-controlled biomineralization of Strontium (Sr^{2+})-doped calcium phosphate nanoparticles: application for gene delivery in bone cells", In preparation *
5. **R. Khalifehzadeh** and Buddy D. Ratner et al., "One-step preparation of calcium phosphate nanoparticles (CaP NPs) by using nucleic acids as templates", In preparation*
6. CK. Lee, **R. Khalifehzadeh**, Buddy D. Ratner, AJ. Boydston," Facile Synthesis of Fluorine-Substituted Polylactides and Their Amphiphilic Block Copolymers" *Macromolecules*, 2018, 51 (4),1280–1289.
7. Buddy D. Ratner, **R. Khalifehzadeh**, Esmaeel Naeemi, Chang-Uk Lee, Andrew Boydston, "Halogenated Cyclic Diesters, Related Polymers, and Methods for Their Preparation and Use", US Patent 2017/0342205
8. R. **Khalifehzadeh**, "NextGenVoices", Science, Vol.343 No. 6166 (2014) pp25.

PRESENTATIONS

1. **R. Khalifehzadeh** et al., "Surface fluorination of polylactides for enhanced hemocompatibility", Society For Biomaterials (SFB) Annual Conference, April 2018, Atlanta, GA, US ((**oral**).

2. **R. Khalifehzadeh** et al., "Blood Compatibility Evaluation of Fluorinated Bioresorbable Polylactic Acid for Coronary Artery Stents", Pacific Rim Symposium on Surfaces, Coatings and Interfaces (PacSurf), December 2016, Hawaii, US ((**oral**).
3. **R. Khalifehzadeh** et al., "Perfluoro-Treated Bioresorbable Polylactic Acid for Coronary Artery Stents", American Institute of Chemical Engineering (AICHE) annual meeting, November 2016, San Francisco, CA, US (**poster).**
4. **R. Khalifehzadeh** et al., "Synthesis and characterization of fluorine-substituted polylactides/glycolides", World Biomaterials Congress (WBC), May 2016, Montreal, Canada (**oral).**
5. AM. Pinto, S. Creason, ZL. Wescoe, L. Zhen, **R. Khalifehzadeh**, M. Mecwan, C. Winston, FD. Magalhães, IC. Gonçalves, BD. Ratner, "Biocompatibility of silicone rubber/graphene-nanoplatelets composites with improved mechanical properties", European Graphene Forum 2017, Paris, France (**oral**)
6. **R. Khalifehzadeh** et al., "Blood Compatibility Evaluation of Fluorinated Bioresorbable Polylactic Acid for Coronary Artery Stents", Graduate Student Symposium (GSS), September 2016, University of Washington, Seattle, WA, US (**selected talk**)
7. T. Shikur, **R. Khalifehzadeh**, E. Naeemi, T.Mahary, BD. Ratner,"Synthesis of Substituted Polylactides for Drug Delivery Applications", B3-Program, August 2014, Seattle, WA, US (**poster**)
8. **R. Khalifehzadeh** et al., "Localized Gene Delivery from Polymer /Ceramic Scaffolds for Tissue Engineering", American Institute of Chemical Engineering (AICHE) annual meeting, November 19, 2014, Atlanta, GA, US (**poster).**
9. **R. Khalifehzadeh** et al., "Colloidal strontium doped calcium phosphate nanocomposites for gene therapy" American Institute of Chemical Engineering (AICHE) annual meeting, November 1, 2012, Pittsburg, PA, US (**oral**).
10. **R. Khalifehzadeh** et al., "One-step preparation of calcium phosphate nanoparticles by using nucleic acids as templates" American Institute of Chemical Engineering (AICHE) annual meeting, November 1, 2012, Pittsburg, PA, US (**oral**).